# New physics searches at LHCb and other highlights

Vincenzo Vagnoni
CERN and INFN Bologna

**MPP Munich, 25 July 2017**

# Setting the scene

- We know nowadays that the Standard Model (of particle physics) works beautifully up to an energy scale of a few hundred GeV
- However, there are compelling reason to state that it is incomplete, e.g.
  - Missing dark matter candidate
  - Standard Model *CP* violation for dynamical generation of the baryon asymmetry in the universe is largely insufficient
- As well as more fundamental reasons, such as
  - Why there are three families of quarks and leptons?
  - Why the masses of fundamental particles span several orders of magnitude?
  - How to accommodate gravity into the quantum picture?

# Precision measurements of *CP* violation and rare decays

- Instead of searching for new physics particles directly produced, look for their indirect quantum effects that the existence of such new particles bring down to low energy processes
  - e.g. *c*- and *b*-hadron mixing and decays

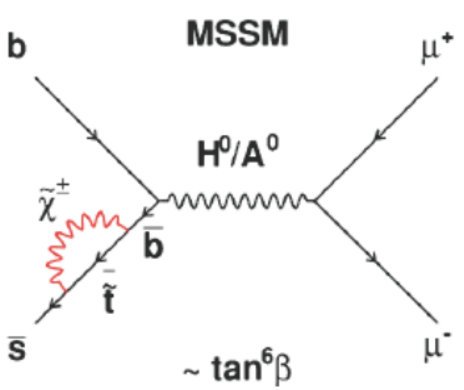


$B_s \rightarrow \mu\mu$

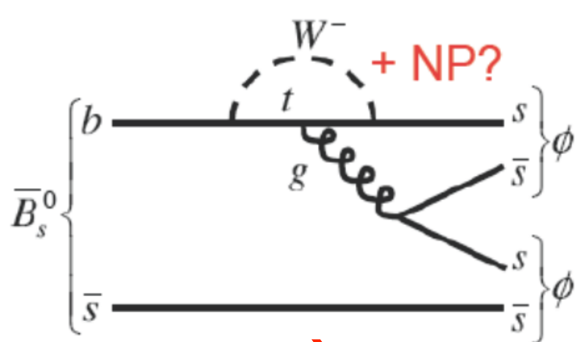


$B_s \rightarrow \phi\phi$

$B$-$\bar{B}$ mixing

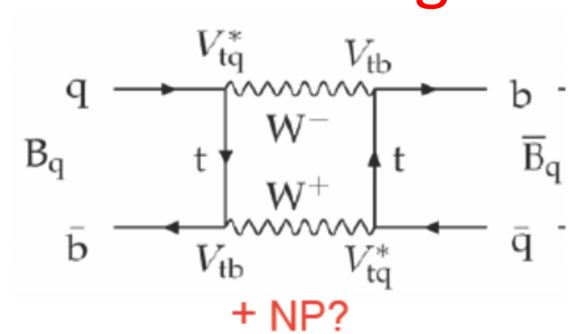

# Precision measurements of *CP* violation and rare decays

- General amplitude decomposition in terms of couplings and scales

$$A = A_0 \left[ c_{SM} \frac{1}{M_W{}^2} + c_{NP} \frac{1}{\Lambda^2} \right]$$

→ in presence of sizeable Standard Model contributions, new physics effects might be hidden
  - Need high precision measurements of theoretically clean observables, e.g. rare decays where the Standard Model amplitude is very small
- From present picture in the flavour sector, still room for new physics at the 10-20% level
- Studying *CP*-violating and flavour-changing processes → two fundamental tasks can be accomplished
  - Identify new symmetries (and their breaking) beyond the SM
  - Probe mass scales not accessible directly at nowadays colliders

# The LHCb collaboration today

- About 1200 members, from 72 Institutes in 16 Countries
  - Steadily growing through the years with new incoming Institutes
- About 800 authors

# LHCb physics paper statistics

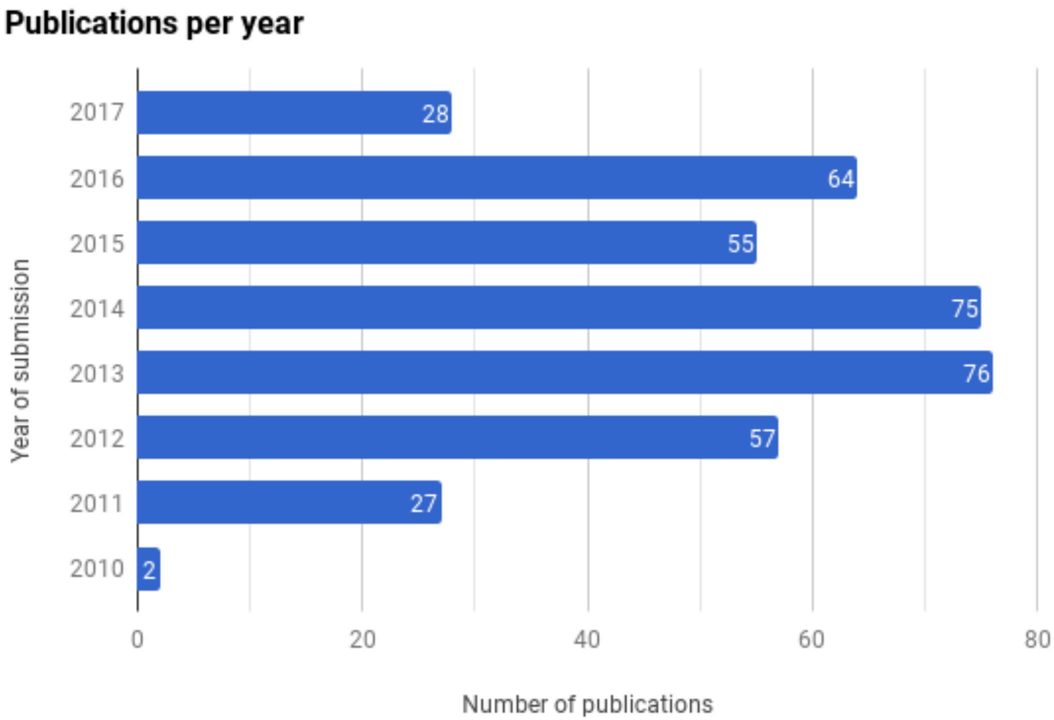


- 384 physics papers in total so far
- For a complete list of LHCb publications see

http://lhcbproject.web.cern.ch/lhcbproject/Publications/LHCbProjectPublic/Summary_all.html

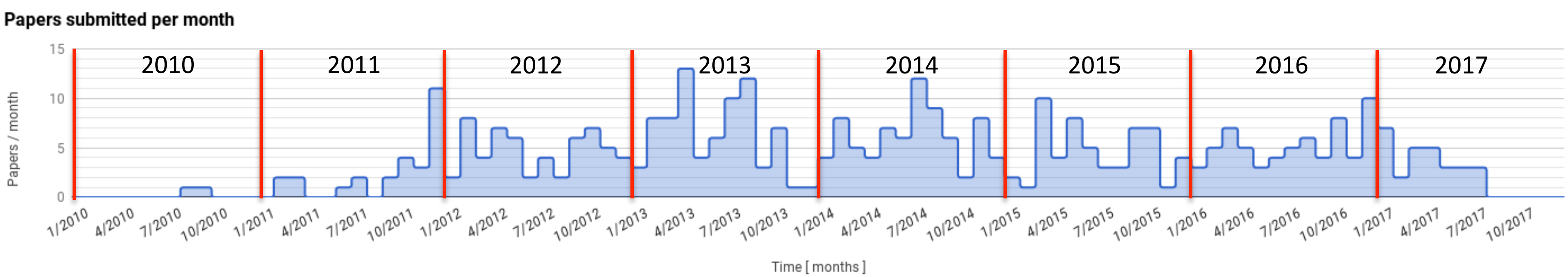

# LHCb detector layout

- LHCb is mainly (but not only) studying beauty (and charm)
  - At LHC, the production of heavy quark pairs is peaked forward/ backward
  - The detector is a single arm spectrometer
    - Both *b*-hadrons go together forward (or backward)
    - Acceptance $2 < \eta < 5$
  - A *b*-meson / baryon is boosted
    - It flies several millimetres before decaying
    - This is the main signature for selecting events

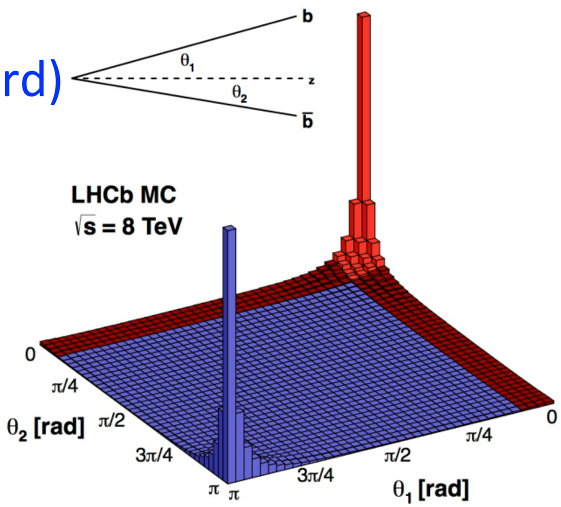


- General detector layout
  - The silicon vertex detector is a key component
  - Dipole magnet, and tracking stations after, to measure accurately the momentum
  - Particle identification by two RICH detectors, electromagnetic and hadronic calorimeters, and a muon system

# LHCb 3D sketch

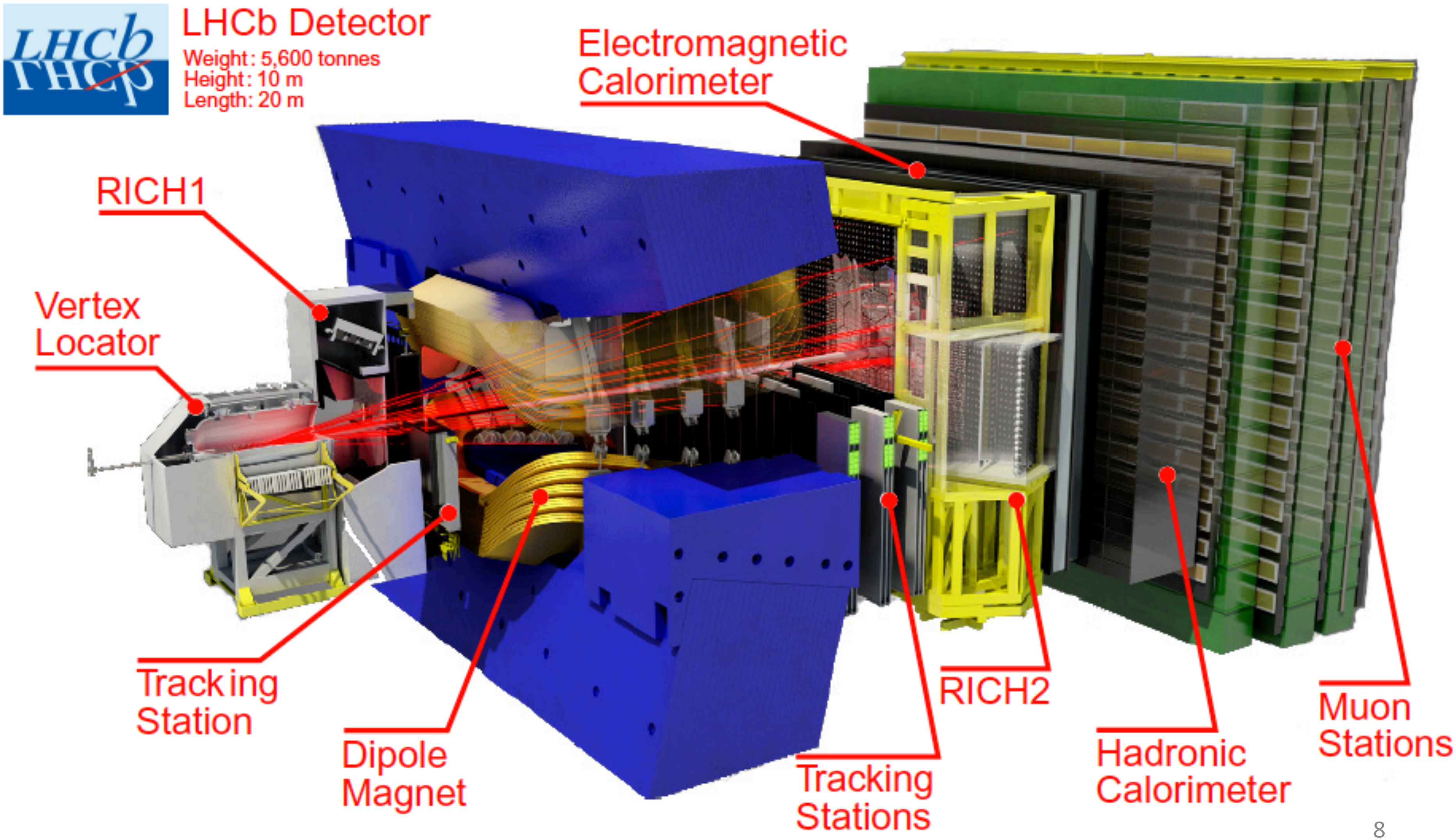

# Maybe easier to visualise it in 2D

- **Trigger**: Optimised for highest efficiency on heavy flavours
- **Tracking**: $\sigma_p/p$ 0.4%–0.6% (p from 5 to 100 GeV), $\sigma_{IP} < 20\ \mu m$
- **Calo**: $\sigma_E / E \sim 10\% / \sqrt{E} \oplus 1\%$
- **PID**: Excellent PID capabilities also for hadrons (RICH)

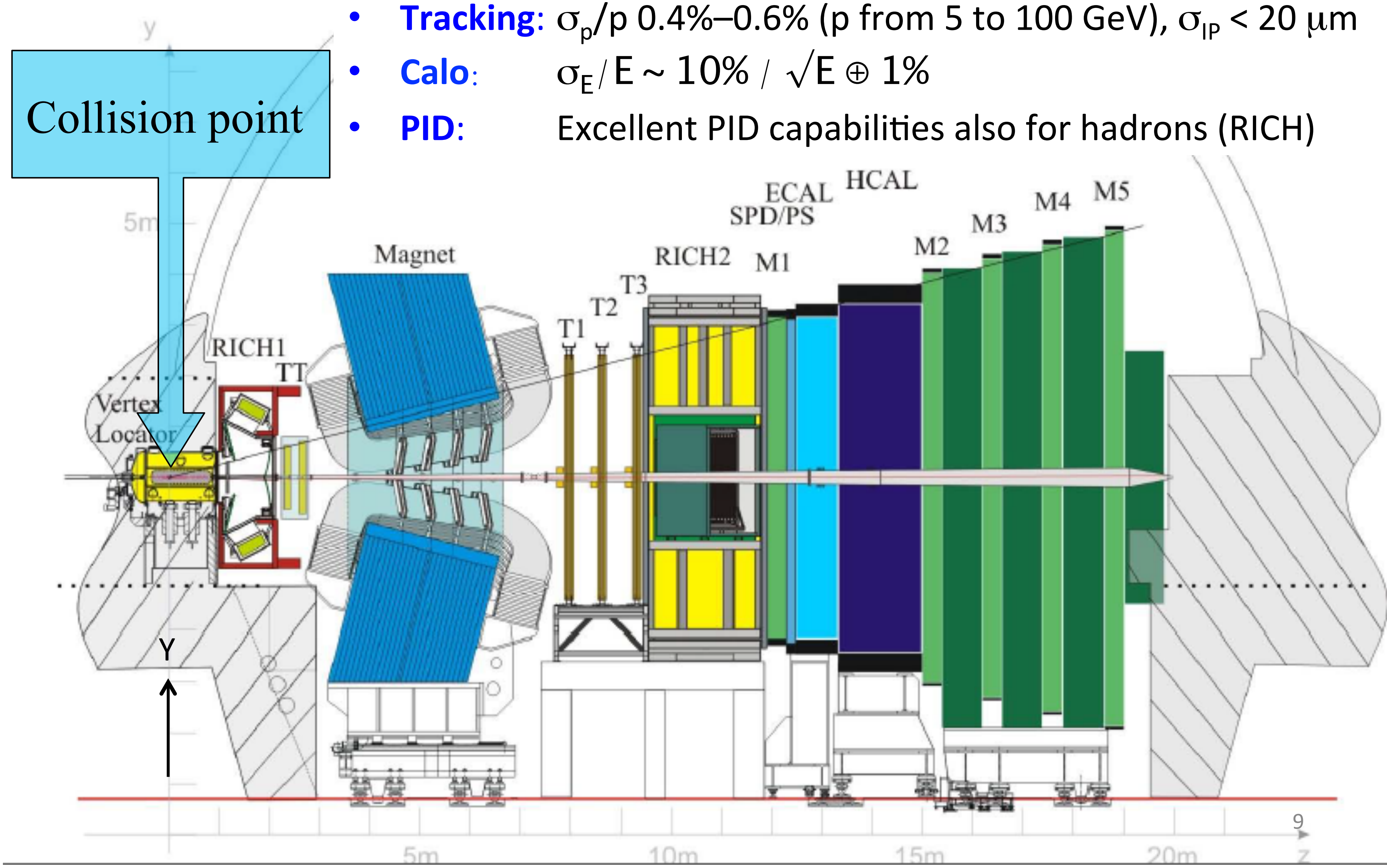

# Luminosity at LHCb

- Most of the results so far are based on the full Run 1 dataset

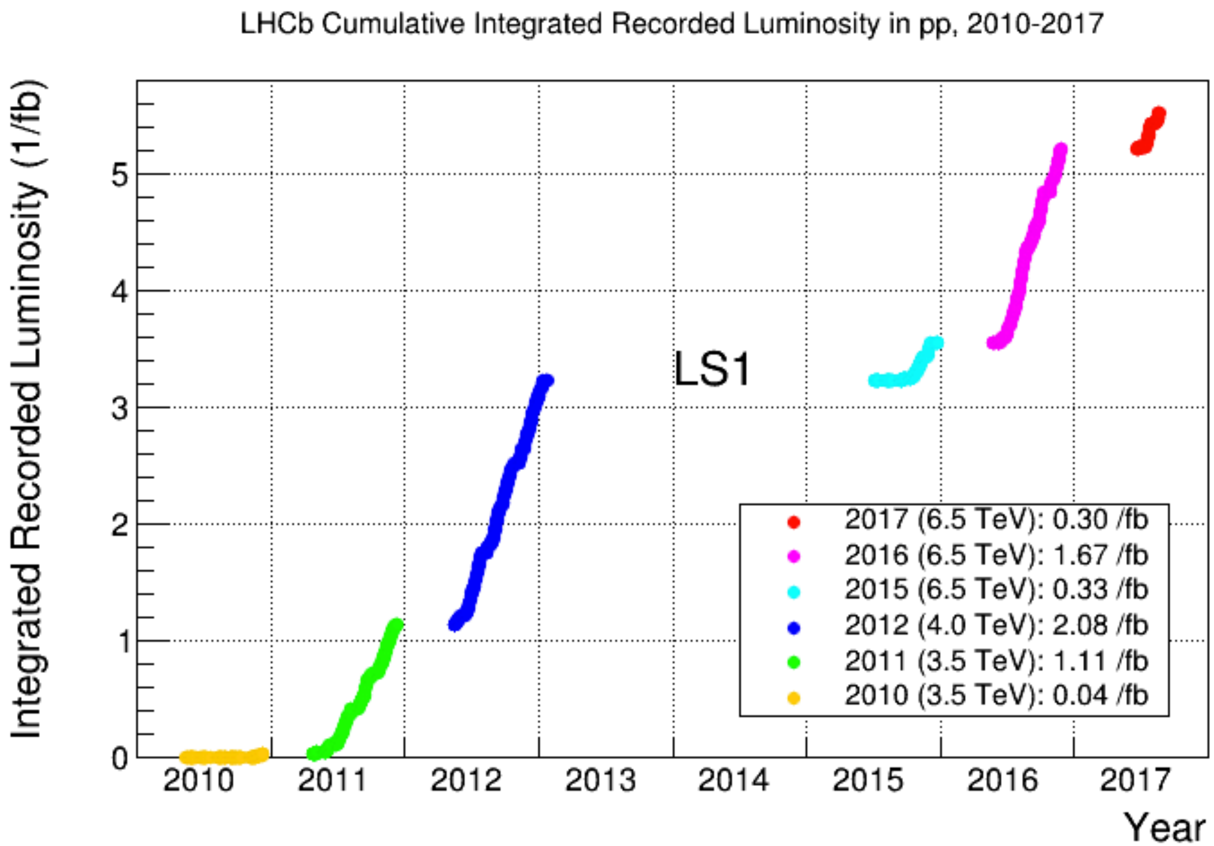


- Due to luminosity levelling, same running conditions throughout fills → $L = 4x10^{32}\ cm^{-2}s^{-1}$
  - to be raised to $2x10^{33}\ cm^{-2}s^{-1}$ in Run-3

# Anomalies in $b \to s l^+ l^-$ transitions

# b→sl⁺l⁻ transitions

- Quark-level transitions entering some of the most relevant decay amplitudes to search for new physics effects

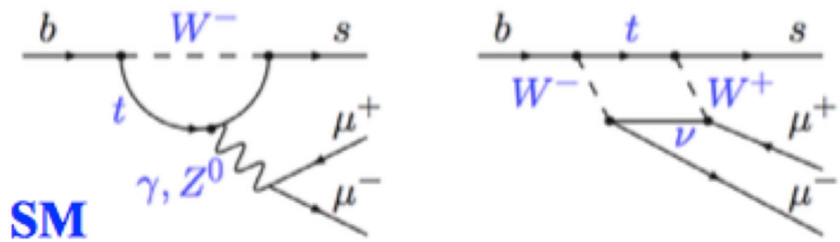


- The presence of new particles may lead to sizeable effects beyond the Standard Model

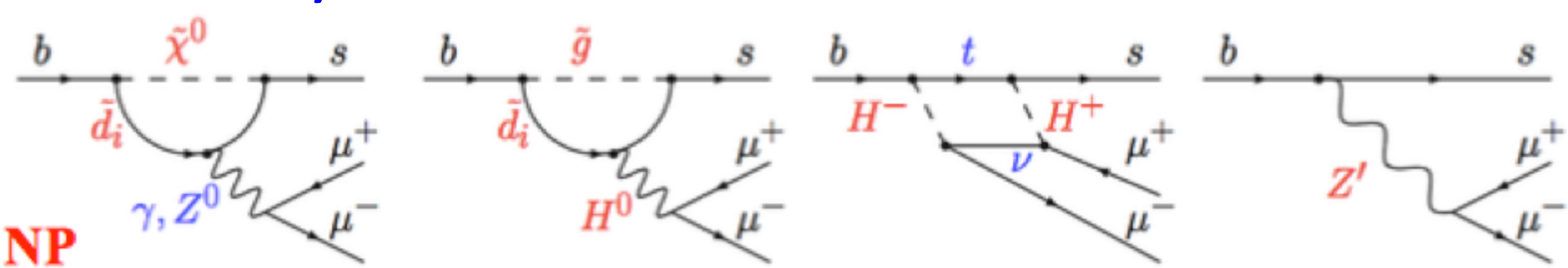

# Earlier lepton flavour universality test with b→sl⁺l⁻ transitions

- Ratio ($R_K$) of branching fractions of $B^+ \to K^+\mu^+\mu^-$ to $B^+ \to K^+e^+e^-$ expected to be equal to one in the Standard Model with excellent precision

$$\mathcal{R}_H = \frac{\int_{q^2_{\rm min}}^{q^2_{\rm max}} \frac{d\Gamma(B \to H\mu^+\mu^-)}{dq^2}\, dq^2}{\int_{q^2_{\rm min}}^{q^2_{\rm max}} \frac{d\Gamma(B \to He^+e^-)}{dq^2}\, dq^2}$$

$$\mathcal{R}_K = \frac{\mathcal{B}(B^+ \to K^+\mu^+\mu^-)}{\mathcal{B}(B^+ \to K^+J/\psi(\to \mu^+\mu^-))} \Big/ \frac{\mathcal{B}(B^+ \to K^+e^+e^-)}{\mathcal{B}(B^+ \to K^+J/\psi(\to e^+e^-))}$$

  – Observation of lepton flavour universality violation would be a clear sign of new physics
  – 2.6σ deviation from the Standard Model seen by LHCb

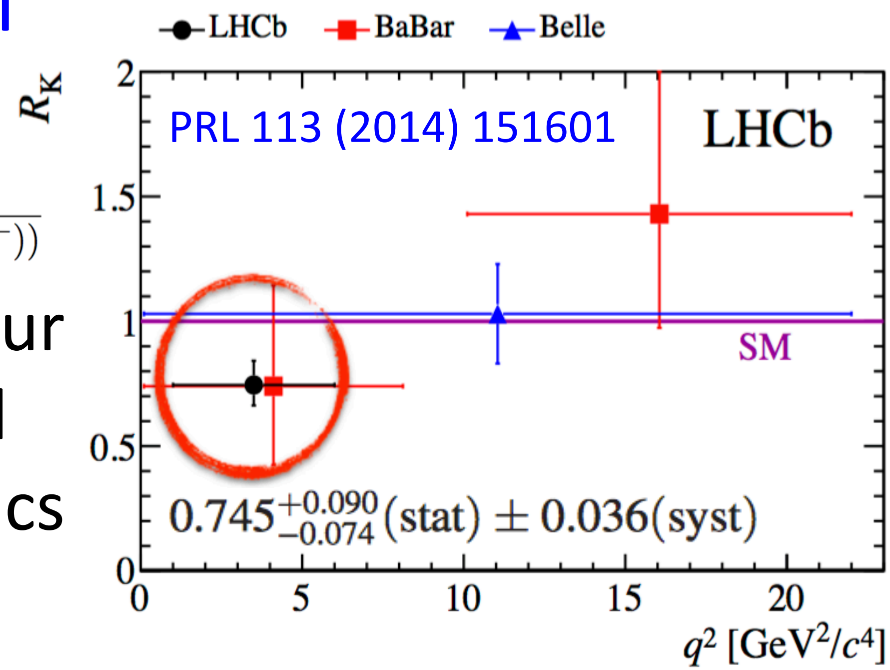

# Other anomalies in the sector: differential branching fractions

- Results consistently lower than SM predictions

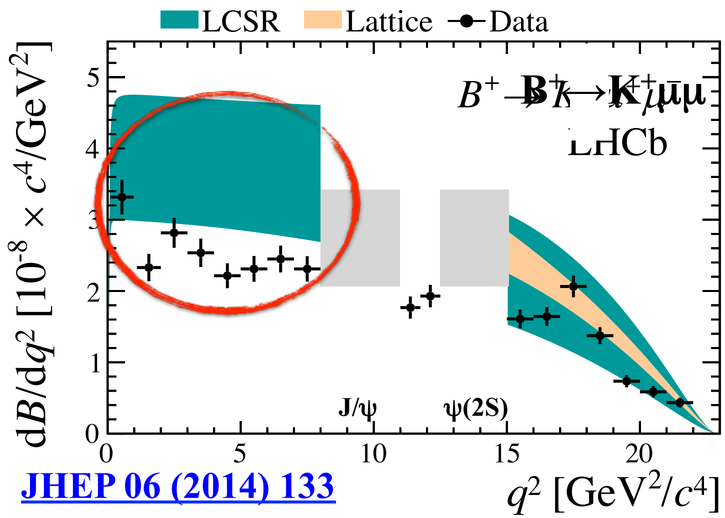


JHEP 06 (2014) 133

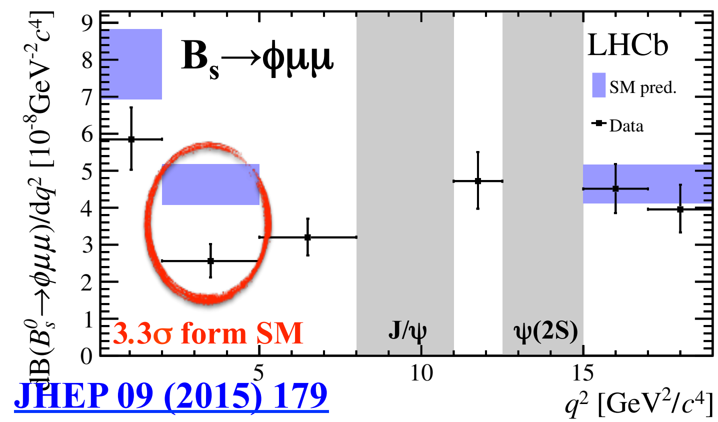


JHEP 09 (2015) 179

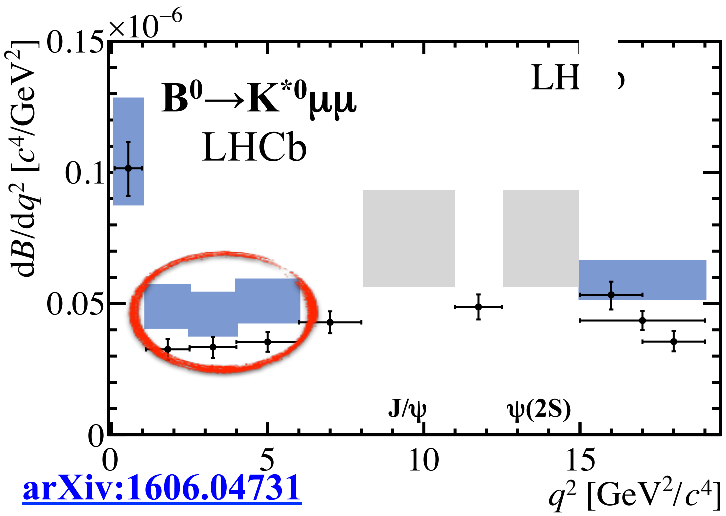


arXiv:1606.04731

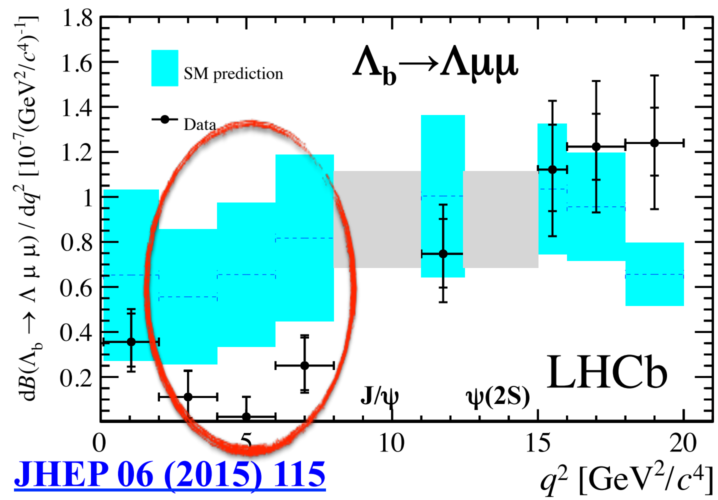


JHEP 06 (2015) 115

# Other anomalies in the sector: angular observables

- Complex angular distribution:

$$\frac{1}{\mathrm{d}(\Gamma+\bar{\Gamma})/\mathrm{d}q^2}\frac{\mathrm{d}^3(\Gamma+\bar{\Gamma})}{\mathrm{d}\vec{\Omega}}\bigg|_{\mathrm{P}} = \frac{9}{32\pi}\Big[\tfrac{3}{4}(1-F_{\mathrm{L}})\sin^2\theta_K + F_{\mathrm{L}}\cos^2\theta_K + \tfrac{1}{4}(1-F_{\mathrm{L}})\sin^2\theta_K\cos 2\theta_l - F_{\mathrm{L}}\cos^2\theta_K\cos 2\theta_l + S_3\sin^2\theta_K\sin^2\theta_l\cos 2\phi + S_4\sin 2\theta_K\sin 2\theta_l\cos\phi + S_5\sin 2\theta_K\sin\theta_l\cos\phi + \tfrac{4}{3}A_{\mathrm{FB}}\sin^2\theta_K\cos\theta_l + S_7\sin 2\theta_K\sin\theta_l\sin\phi + S_8\sin 2\theta_K\sin 2\theta_l\sin\phi + S_9\sin^2\theta_K\sin^2\theta_l\sin 2\phi\Big]$$

fraction of longitudinal polarisation of the K* ($F_{\mathrm{L}}$)

forward-backward asymmetry of the dilepton system ($A_{\mathrm{FB}}$)

The observables depend on form-factors for the $B \to K^*$ transition plus the underlying short distance physics (Wilson coefficients).

# Other anomalies in the sector: angular observables

- Full angular analysis of $B^0 \to K^{*0}\mu\mu$: measured all CP-averaged angular terms and CP-asymmetries
- Can construct less form-factor dependent ratios of observables

$$P'_{i=4,5,6,8} = \frac{S_{j=4,5,7,8}}{\sqrt{F_L(1-F_L)}}.$$

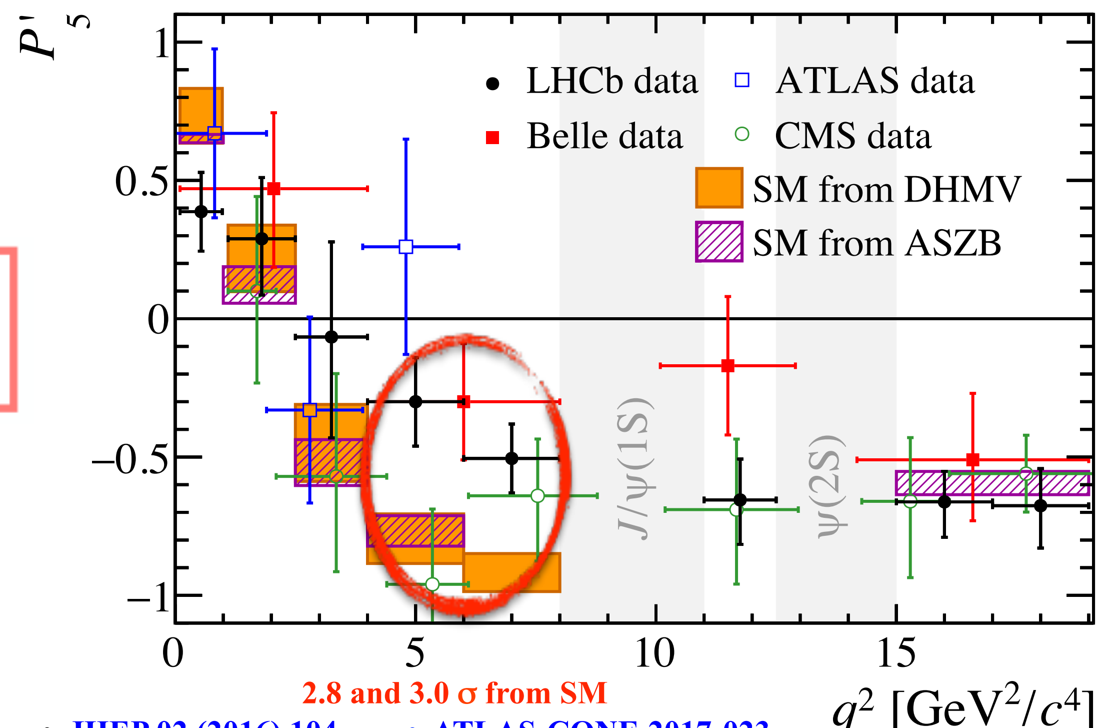


- JHEP 02 (2016) 104
- PRL 118 (2017)
- ATLAS-CONF-2017-023
- CMS-PAS-BPH-15-008

# Fits to all observables in the sector

- Several theory groups attempted to interpret results by performing global fits to data

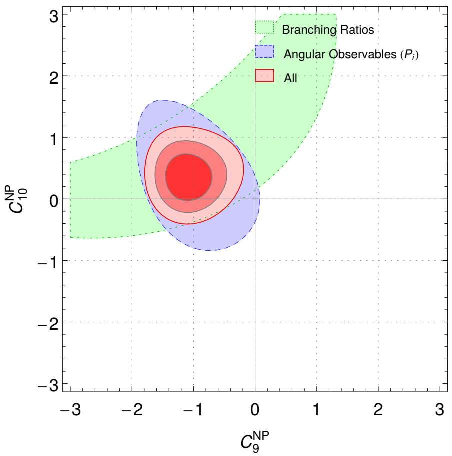


[arXiv:1510.04239](arXiv:1510.04239)

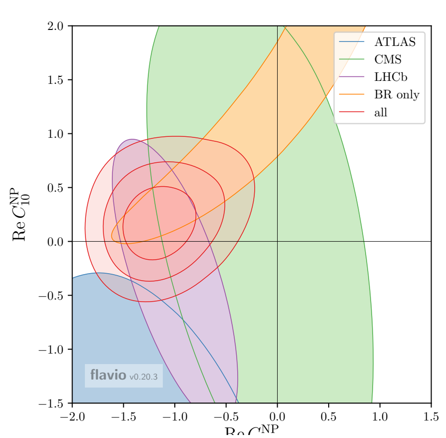


[arXiv:1703.09189](arXiv:1703.09189)

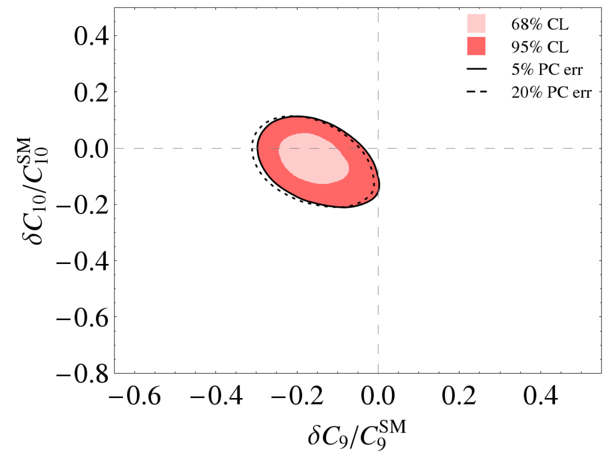


[arXiv:1611.05060](arXiv:1611.05060)

- Take into account ~90 observables from different experiments, including B→μμ and b→sll transitions
- Global fits require additional contributions with respect to the SM to accommodate the data at about 5σ
- But other theory groups are more skeptical on control of QCD effects in branching fractions and angular observables
  - e.g. correctly estimating the contribution from charm loops

# Measurement of $R_{K*}$

- Test of LFU with $B^0 \to K^{*0}\mu\mu$ and $B^0 \to K^{*0}ee$, $R_{K*}$

- Two regions of $q^2$
  - Low [0.045-1.1] $GeV^2/c^4$
  - Central [1.1-6.0] $GeV^2/c^4$

- Measured relative to $B^0 \to K^{*0}J/\psi(ll)$ in order to reduce systematics

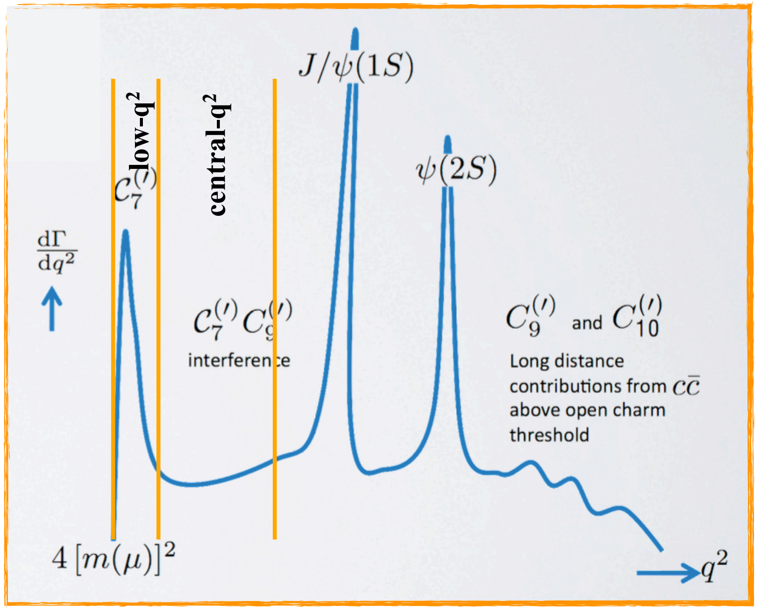


- $K^{*0}$ reconstructed as $K^+\pi^-$ within 100 MeV from the $K^*(892)^0$
- Blind analysis to avoid experimental biases
- Very challenging due to significant differences in the way $\mu$ and e "interact" with the detector
  - Bremsstrahlung
  - Trigger

**LHCb-PAPER-2017-013 (JHEP)**
**arXiv:1705.05802**

# Bremsstrahlung recovery

- Electrons emit a large amount of bremsstrahlung that results in degraded momentum and mass resolutions

- Two types of bremsstrahlung

**Downstream of the magnet**

Photon energy in the same calorimeter cell as the electron and momentum correctly measured

**Upstream of the magnet**

Photon energy in different calorimeter cells than electron and momentum evaluated after bremsstrahlung

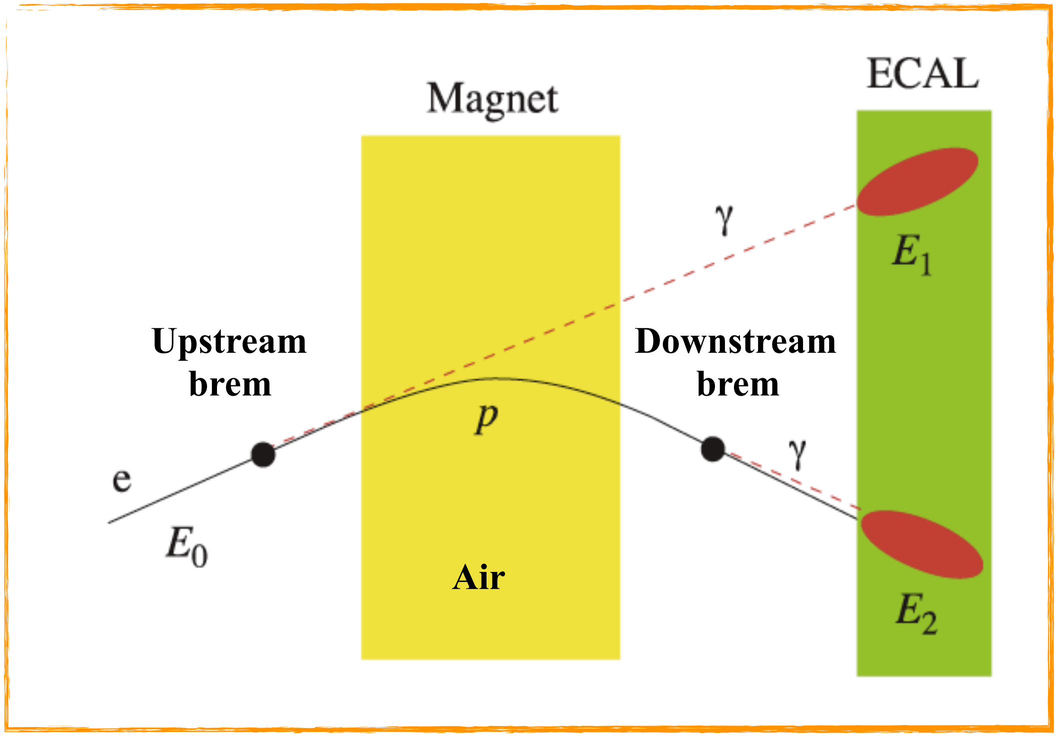

# Trigger categories

- Trigger system split in hardware (L0) and software (HLT) stages
- Due to higher occupancy of the calorimeters compared to the muon stations, hardware thresholds on the electron $E_T$ are higher than those for muons $p_T$
- To partially mitigate this effect, 3 exclusive trigger categories are defined

**L0 Electron (L0E):** electron hardware trigger fired by clusters associated to at least one of the two electrons ($E_T > 2.5$ GeV)

**L0 Hadron (L0H):** hadron hardware trigger fired by clusters associated to at least one of the $K^{*0}$ decay products ($E_T > 3.5$ GeV)

**L0 TIS (L0I):** any hardware trigger fired by particles in the event not associated to the signal candidate

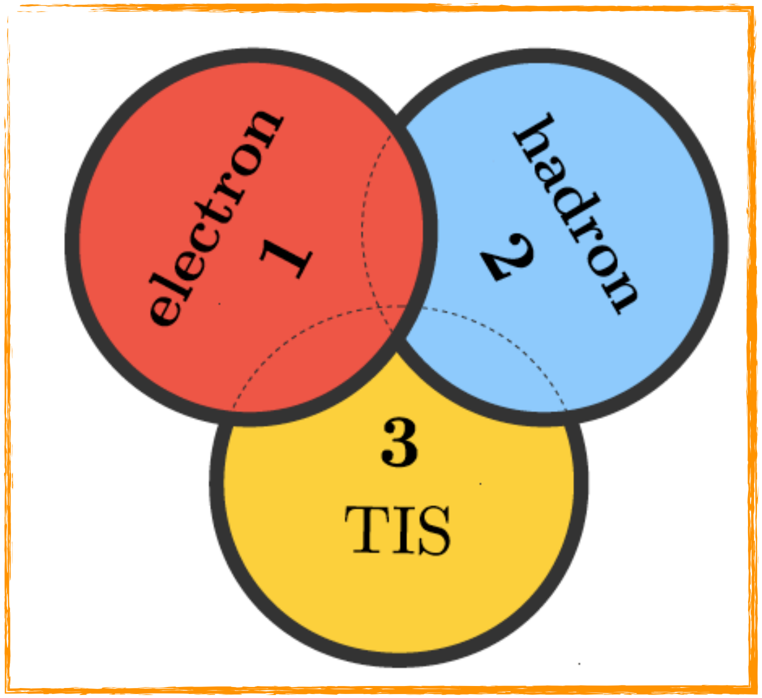

# Measure as a double ratio

- $R_{K*}$ determined as double ratio to reduce systematic effects

$$\mathcal{R}_{K^{*0}} = \frac{\mathcal{B}(B^0 \to K^{*0}\mu^+\mu^-)}{\mathcal{B}(B^0 \to K^{*0}J/\psi(\to \mu^+\mu^-))} \Bigg/ \frac{\mathcal{B}(B^0 \to K^{*0}e^+e^-)}{\mathcal{B}(B^0 \to K^{*0}J/\psi(\to e^+e^-))}$$

- Selection as similar as possible between $\mu\mu$ and ee
  - Pre-selection requirements on trigger and quality of the candidates
  - Cuts to remove peaking backgrounds
  - Particle identification to further reduce the background
  - Multivariate classifier to reject the combinatorial background
  - Kinematic requirements to reduce the partially-reconstructed backgrounds
  - Multiple candidates per event randomly rejected (1-2%)

- Efficiencies
  - Determined using simulation, but tuned using data

# Fit results for muonic channel

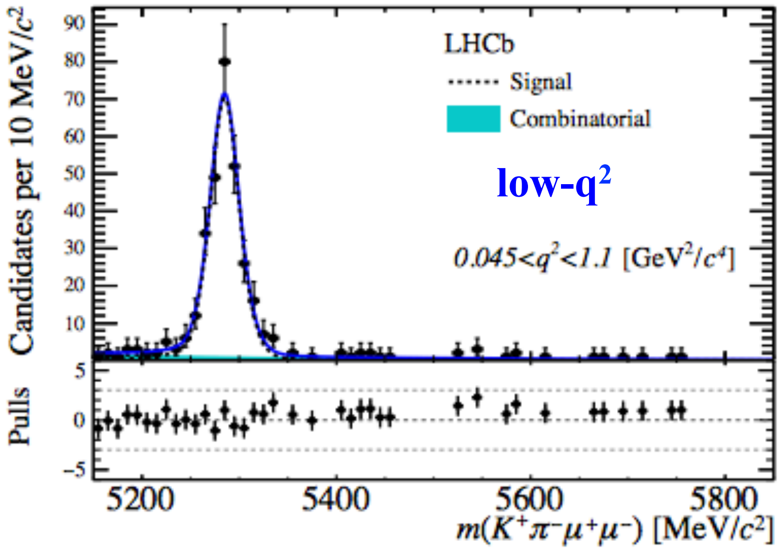


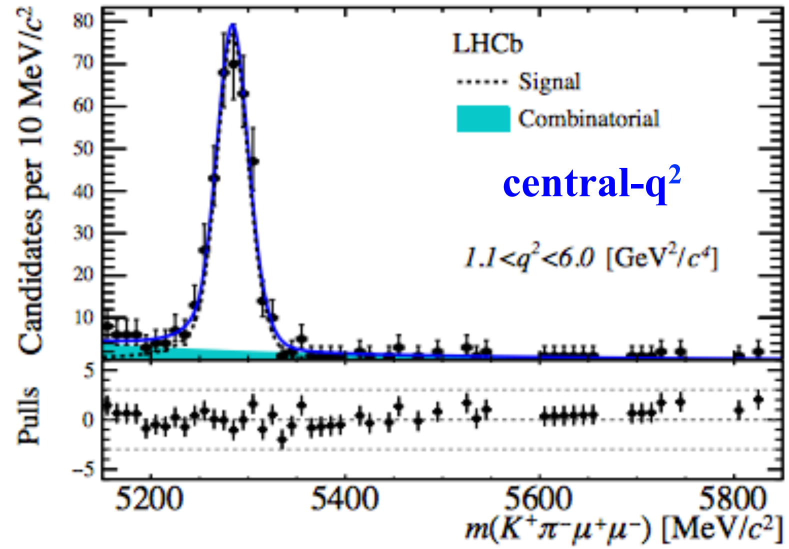


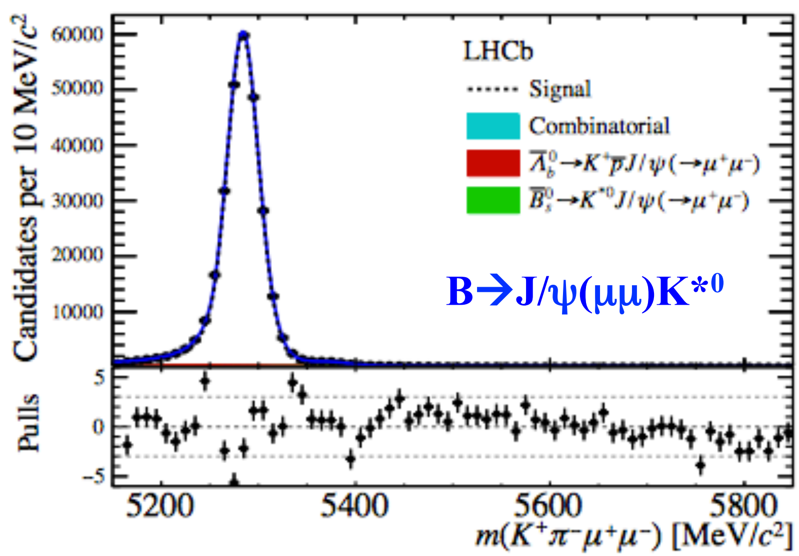

# Fit results for electron channel

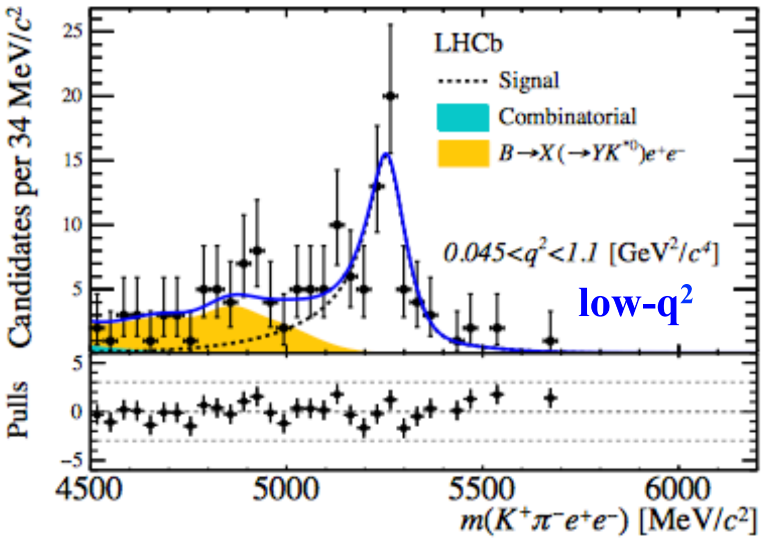


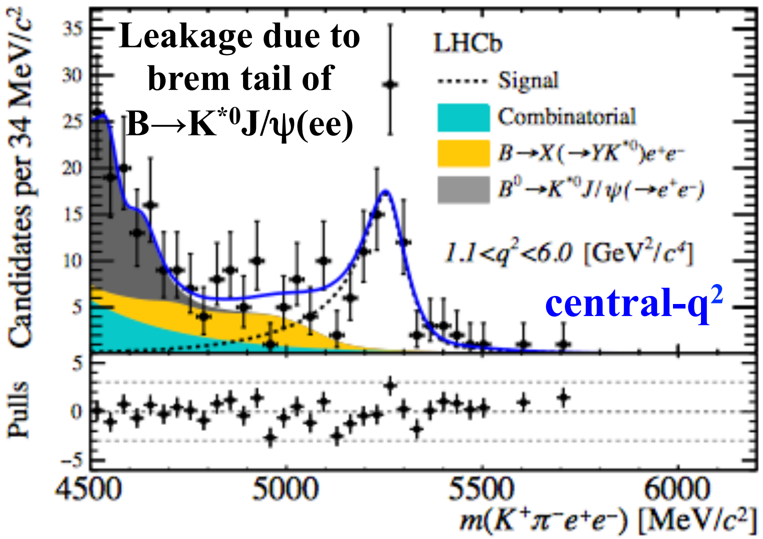


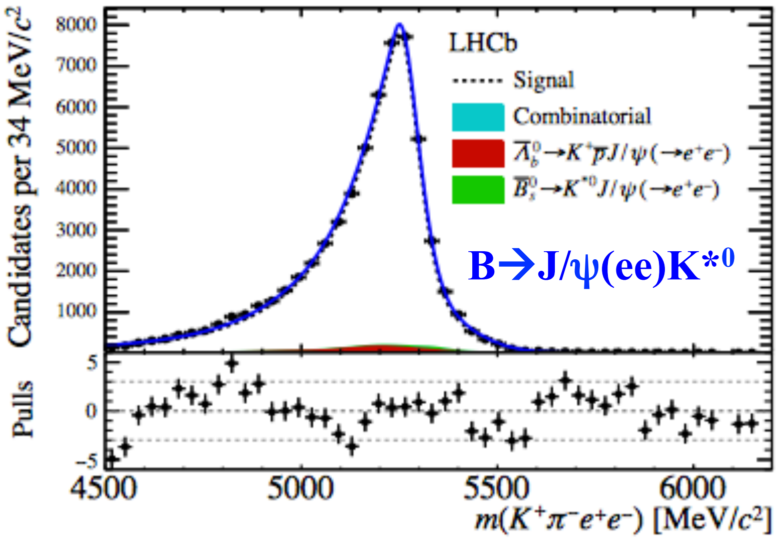

# Signal yields

- Precision of the measurement driven by the statistics of the electron samples

| | $B^0 \to K^{*0}\ell^+\ell^-$ | | $B^0 \to K^{*0} J/\psi (\to \ell^+\ell^-)$ |
|---|---|---|---|
| | low-$q^2$ | central-$q^2$ | |
| $\mu^+\mu^-$ | $285\ ^{+\ 18}_{-\ 18}$ | $353\ ^{+\ 21}_{-\ 21}$ | $274416\ ^{+\ 602}_{-\ 654}$ |
| $e^+e^-$ (L0E) | $55\ ^{+\ 9}_{-\ 8}$ | $67\ ^{+\ 10}_{-\ 10}$ | $43468\ ^{+\ 222}_{-\ 221}$ |
| $e^+e^-$ (L0H) | $13\ ^{+\ 5}_{-\ 5}$ | $19\ ^{+\ 6}_{-\ 5}$ | $3388\ ^{+\ 62}_{-\ 61}$ |
| $e^+e^-$ (L0I) | $21\ ^{+\ 5}_{-\ 4}$ | $25\ ^{+\ 7}_{-\ 6}$ | $11505\ ^{+\ 115}_{-\ 114}$ |

- In total, about 90 and 110 $B^0 \to K^{*0}ee$ candidates at low- and central-$q^2$, respectively

# Stringent cross check: $r_{J/\psi}$

- Control of the absolute scale of the efficiencies via the ratio

$$r_{J/\psi} = \frac{\mathcal{B}(B^0 \to K^{*0} J/\psi\,(\to \mu^+\mu^-))}{\mathcal{B}(B^0 \to K^{*0} J/\psi\,(\to e^+e^-))}$$

which is expected to be unity and measured to be

$$1.043 \pm 0.006\,(\mathrm{stat}) \pm 0.045\,(\mathrm{syst})$$

- Result observed to be independent of the decay kinematics and event multiplicity

- Very stringent test, which does not benefit from the cancellation of the experimental systematics provided by the double ratio

# Final results

| | low-$q^2$ | central-$q^2$ |
|---|---|---|
| $R_{K^{*0}}$ | $0.66\,^{+\,0.11}_{-\,0.07} \pm 0.03$ | $0.69\,^{+\,0.11}_{-\,0.07} \pm 0.05$ |
| 95.4% CL | [0.52, 0.89] | [0.53, 0.94] |
| 99.7% CL | [0.45, 1.04] | [0.46, 1.10] |

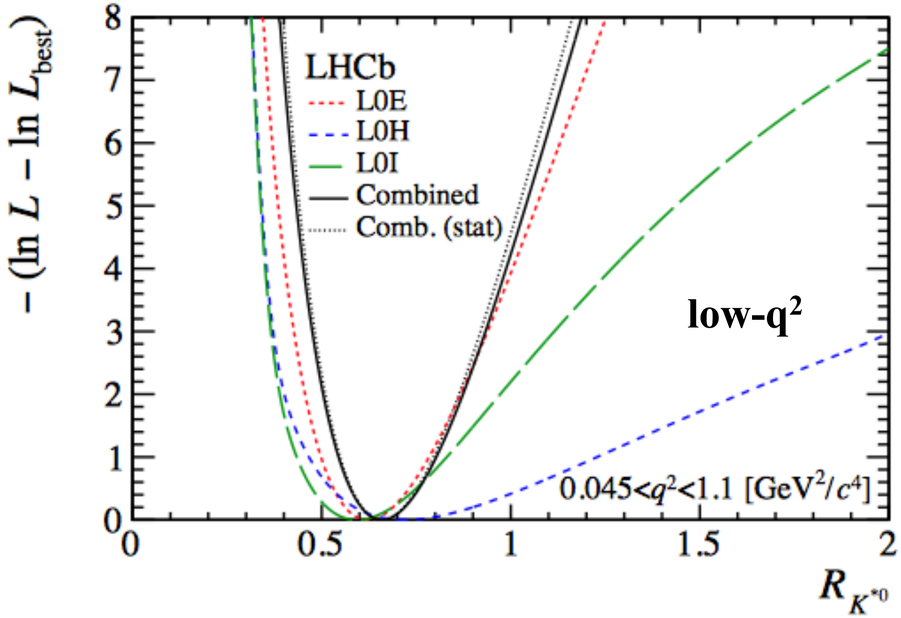


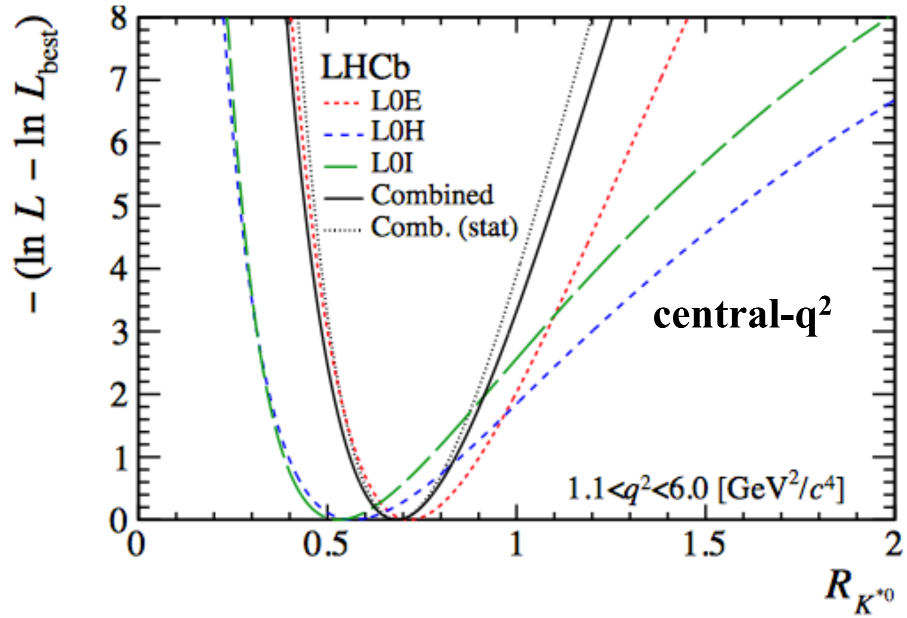


- The measured values of $R_{K*}$ are found to be in good agreement among the three trigger categories in both $q^2$ regions

# Comparison with SM expectation

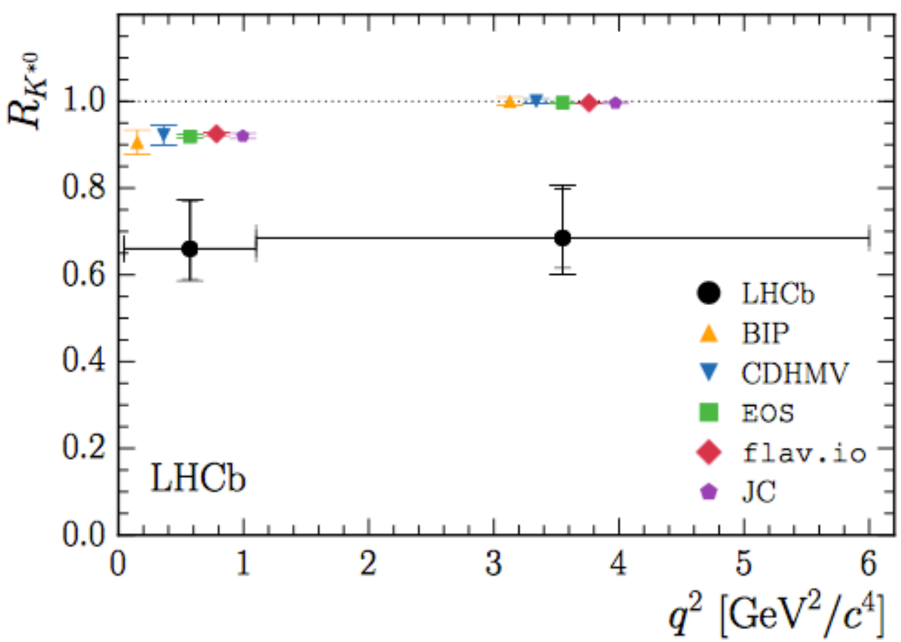


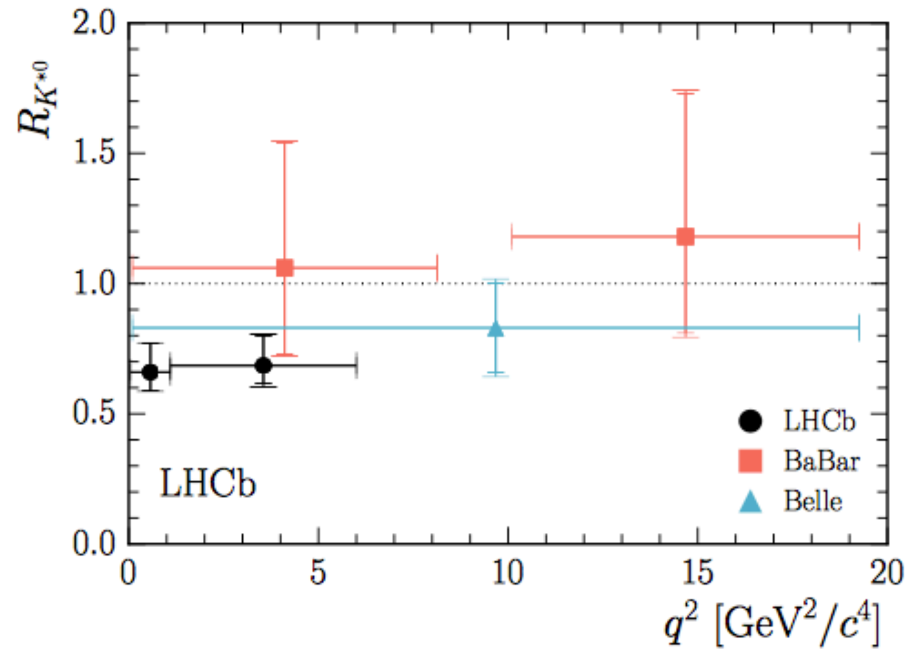


2.1 – 2.3 standard deviations from the Standard Model

$$0.66\ {}^{+\ 0.11}_{-\ 0.07}\,(\text{stat}) \pm 0.03\,(\text{syst}) \quad \text{for } 0.045 < q^2 < 1.1\ \ \text{GeV}^2/c^4$$

$$0.69\ {}^{+\ 0.11}_{-\ 0.07}\,(\text{stat}) \pm 0.05\,(\text{syst}) \quad \text{for } 1.1 \quad < q^2 < 6.0\ \ \text{GeV}^2/c^4$$

2.4 – 2.5 standard deviations from the Standard Model

# Theory at work…

- A plethora of theory preprints appeared right after the CERN seminar on April 18, and we lost count
  - This is just an example from Capdevilla *et al.* arXiv:1704.05340
- Some possible interpretations include a Z’ boson or a leptoquark coupling to quarks and leptons with competing amplitudes to the SM
- However more data are needed before toasting

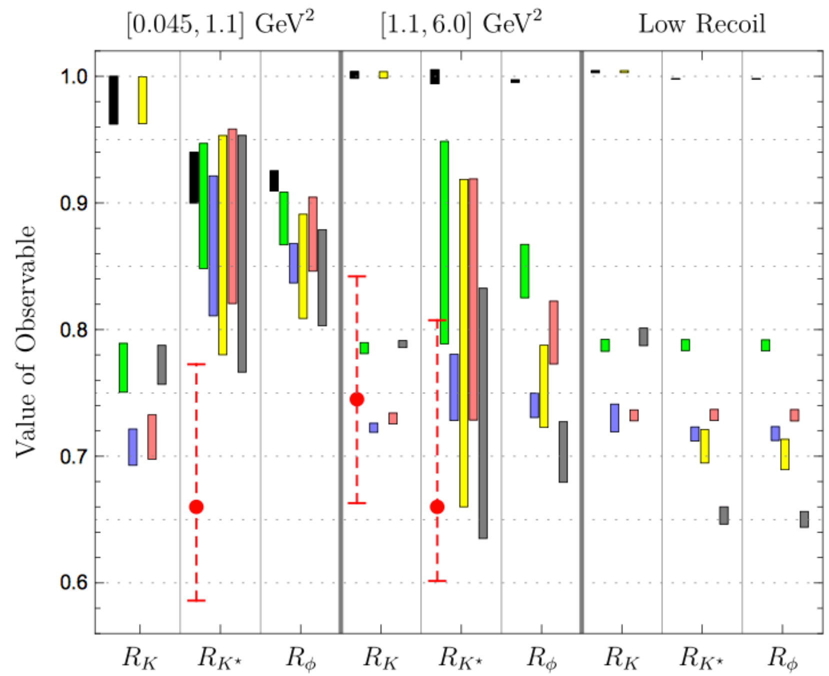


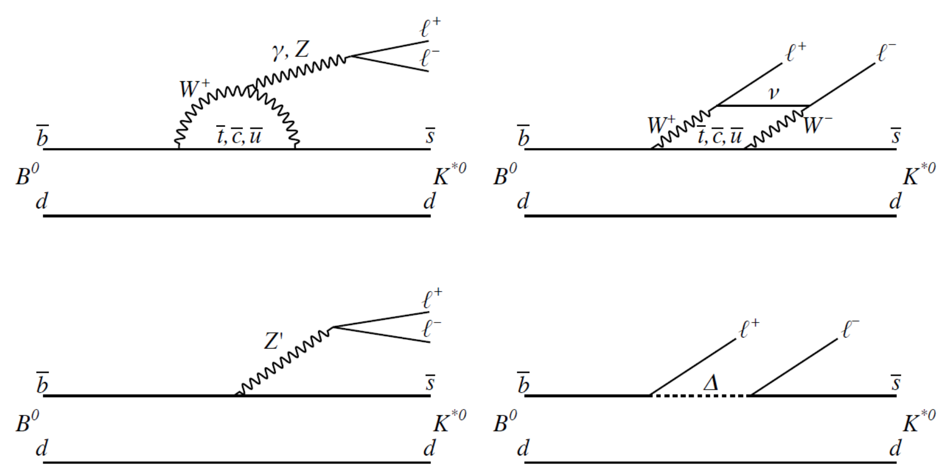

# Further Lepton Flavour non-universality hints with semitauonic decays: related to $b \to s l^+ l^-$?

# Status with R(D) and R(D*)

- $R_D{}^{(*)} = \dfrac{BR(B \to D^{(*)}\tau\nu)}{BR(B \to D^{(*)}\mu\nu)}$

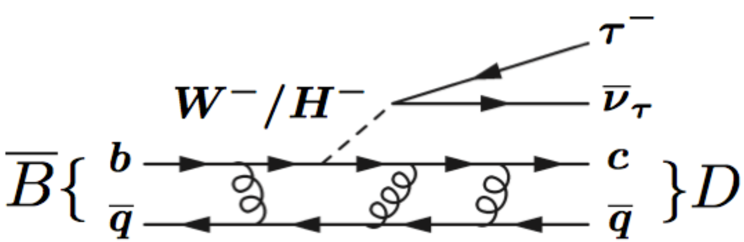


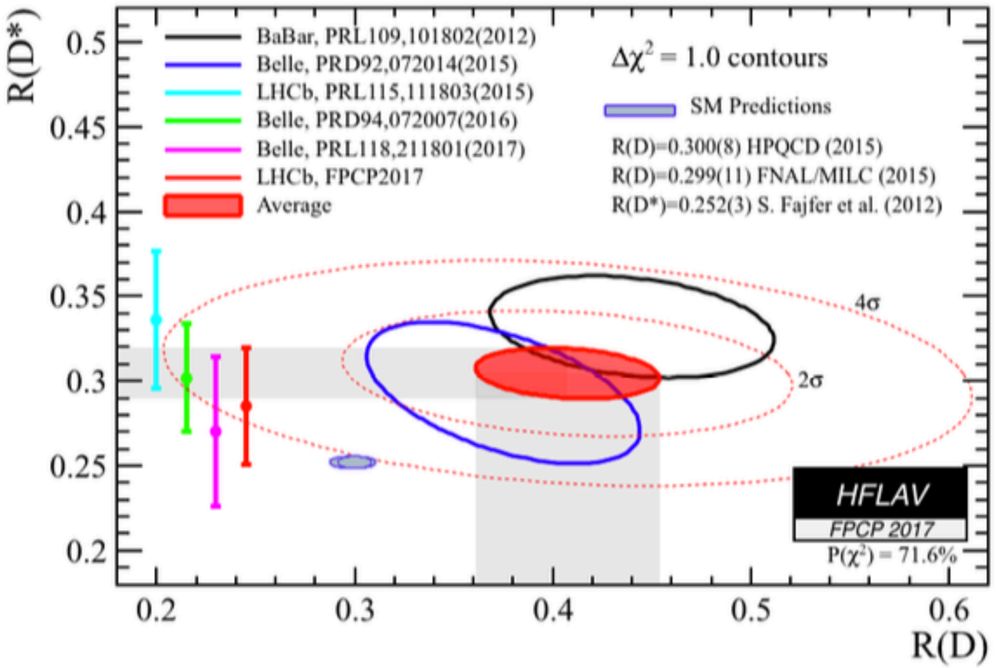


- Measurements of $R(D)$ and $R(D^*)$ by BaBar, Belle and LHCb
  - Overall average shows a 4σ discrepancy from the SM
- LHCb can also perform measurements with other *b* hadrons
  - e.g. $B_s$, $B_c$ and $\Lambda_b$ decays will help to better understand the global picture → very soon with news on this!

# R(D*) with 3-prong τ decay

Latest measurement from LHCb look at $\tau \rightarrow \pi^+\pi^-\pi^+\nu$ final states

Normalisation done though a very similar known final state

$$R(D^*) = K_{had}(D^*) \times \frac{BR(B^0 \to D^{*-}\pi^+\pi^-\pi^+)}{BR(B^0 \to D^{*-}\mu^+\nu_\mu)}$$

$$K_{had}(D^*) = \frac{BR(B^0 \to D^{*-}\tau^+\nu_\tau)}{BR(B^0 \to D^{*-}\pi^+\pi^-\pi^+)}$$

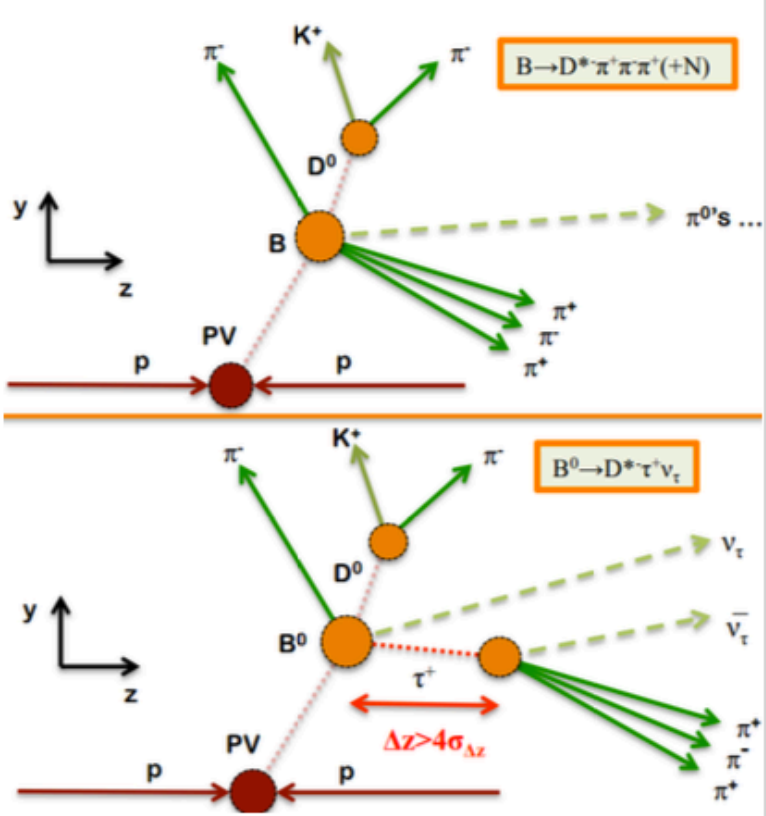

# R(D*) with 3-prong τ decay

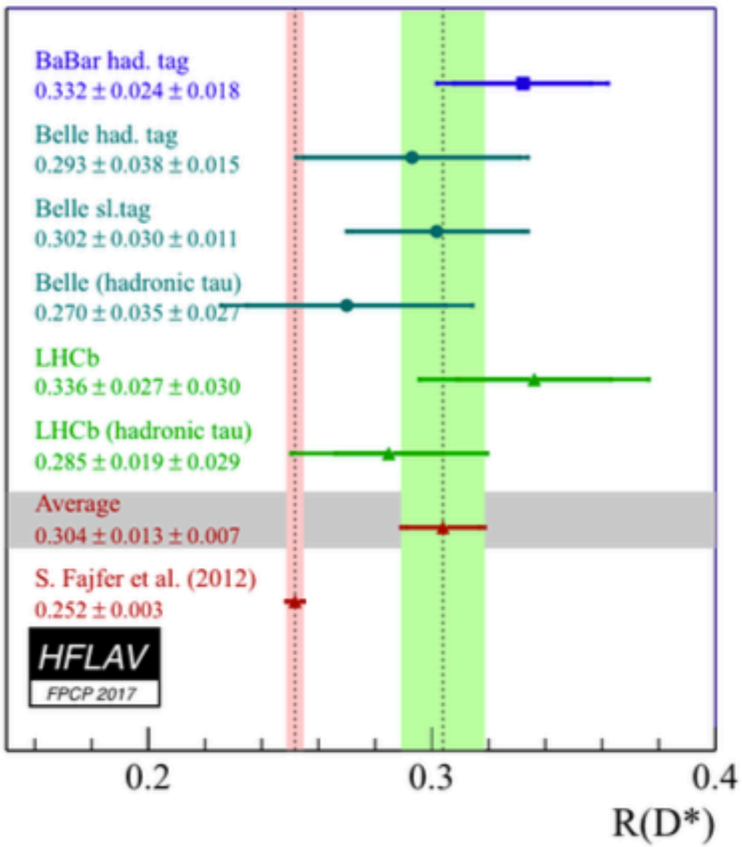


New LHCb measurement gives

R(D*)=0.285±0.019(stat)±0.025(syst)

LHCb-PAPER-2017-027

Compatible with SM expectation

but also fully supporting previous measurements of high value

# Some CKM metrology

# Measurement of $\phi_s = -2\lambda^2\bar{\eta}$

- *CP* violation arising from the interference of mixing and decay with $B_s \to J/\psi\phi$

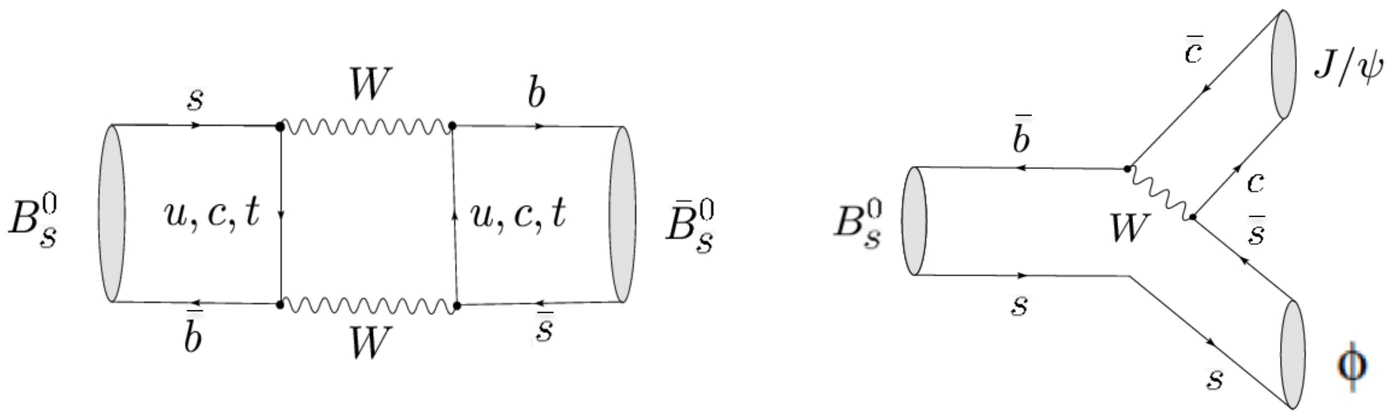


- Measures the phase-difference $\phi_s$ between the two diagrams, precisely predicted in the SM to be $\phi_s$=–37.4 ± 0.7 mrad → can be altered by new physics effects
- Conceptually similar to measuring sin(2β), but a pseudoscalar to vector-vector decay
  – Angular analysis of decay products is needed

# Legacy $\phi_s$ result from Run-1

LHCb-PAPER-2017-008

- LHCb measured $\phi_s$ from Run-1 with $B_s \to J/\psi KK$ (and $B_s \to J/\psi\pi\pi$) already some time ago
  - but the measurement only included the $KK$ system around the $\phi(1020)$ mass
- There is non negligible statistics for $m_{KK}$>1.05 GeV/$c^2$

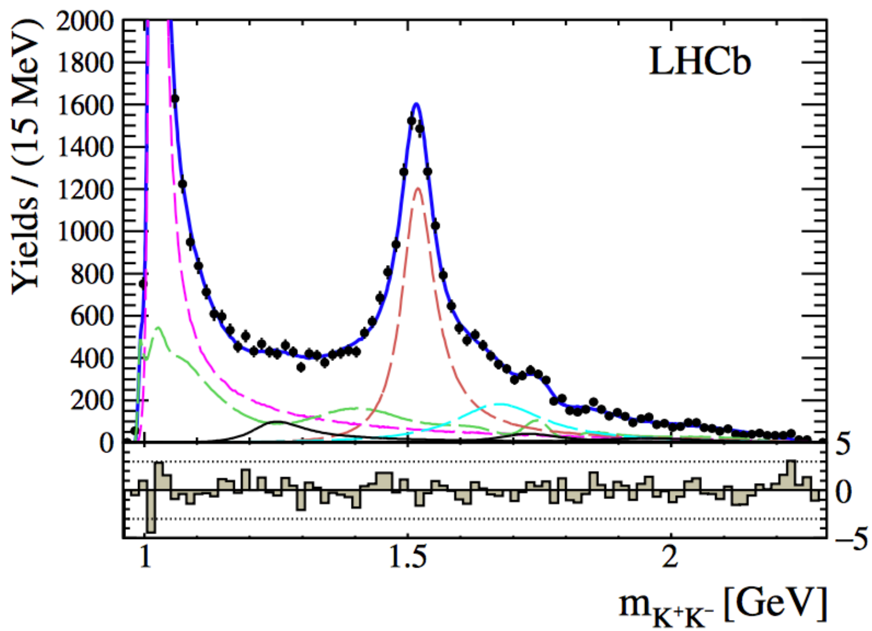


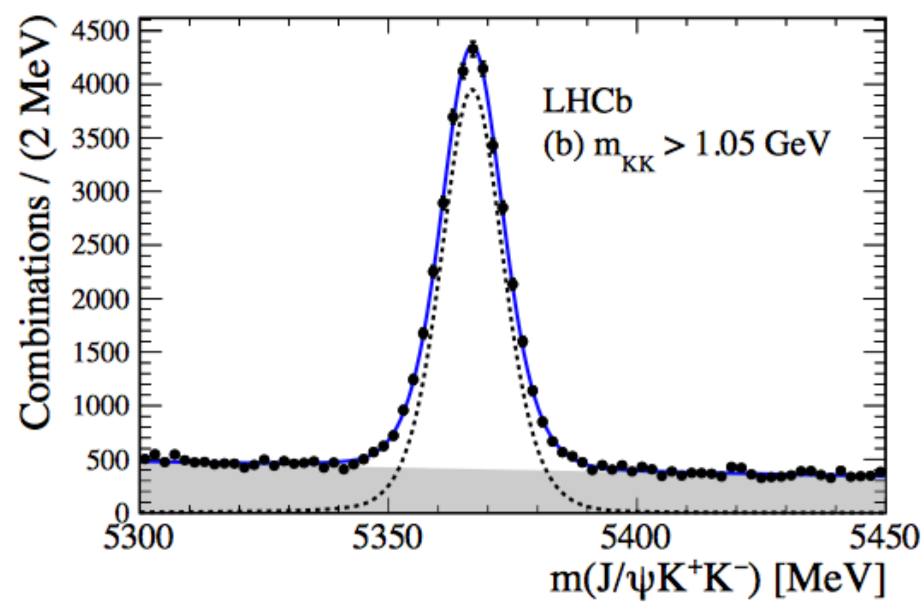

# Legacy $\phi_s$ result from Run-1

LHCb-PAPER-2017-008

- Quite challenging, as a decay-time dependent amplitude analysis is involved
- Results for $m_{KK}$>1.05 GeV/$c^2$

$$\begin{aligned} \phi_s &= 119 \pm 107 \pm 34\,\text{mrad}, \\ |\lambda| &= 0.994 \pm 0.018 \pm 0.006, \\ \Gamma_s &= 0.650 \pm 0.006 \pm 0.004\,\text{ps}^{-1}, \\ \Delta\Gamma_s &= 0.066 \pm 0.018 \pm 0.010\,\text{ps}^{-1}. \end{aligned}$$

- And averaging with low *KK* mass

$$\begin{aligned} \phi_s &= -25 \pm 45 \pm 8\,\text{mrad}, \\ |\lambda| &= 0.978 \pm 0.013 \pm 0.003, \\ \Gamma_s &= 0.6588 \pm 0.0022 \pm 0.0015\,\text{ps}^{-1}, \\ \Delta\Gamma_s &= 0.0813 \pm 0.0073 \pm 0.0036\,\text{ps}^{-1}. \end{aligned}$$

- Finally, including also $B_s \to J/\psi\pi\pi$

$$\phi_s = 1 \pm 37\,\text{mrad and } |\lambda| = 0.973 \pm 0.013$$

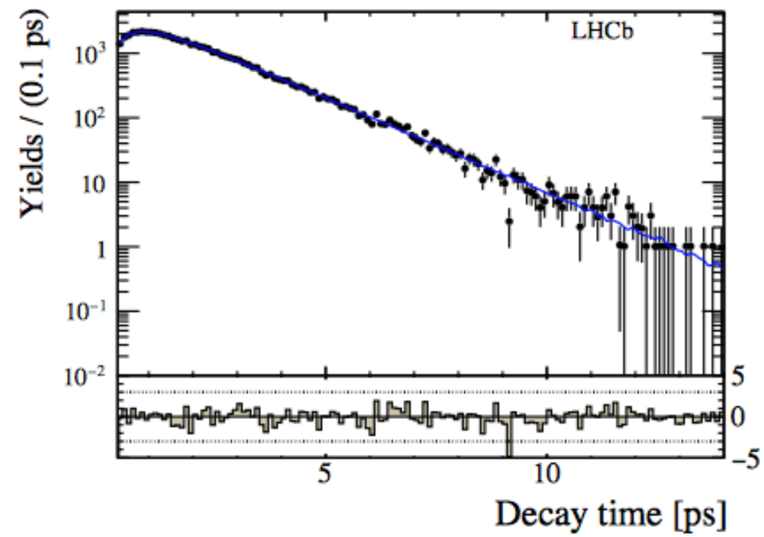


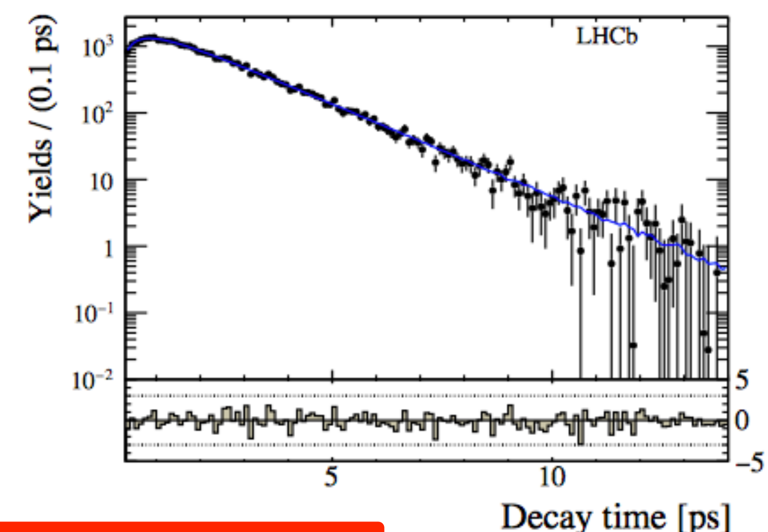

# World average of $\phi_s$

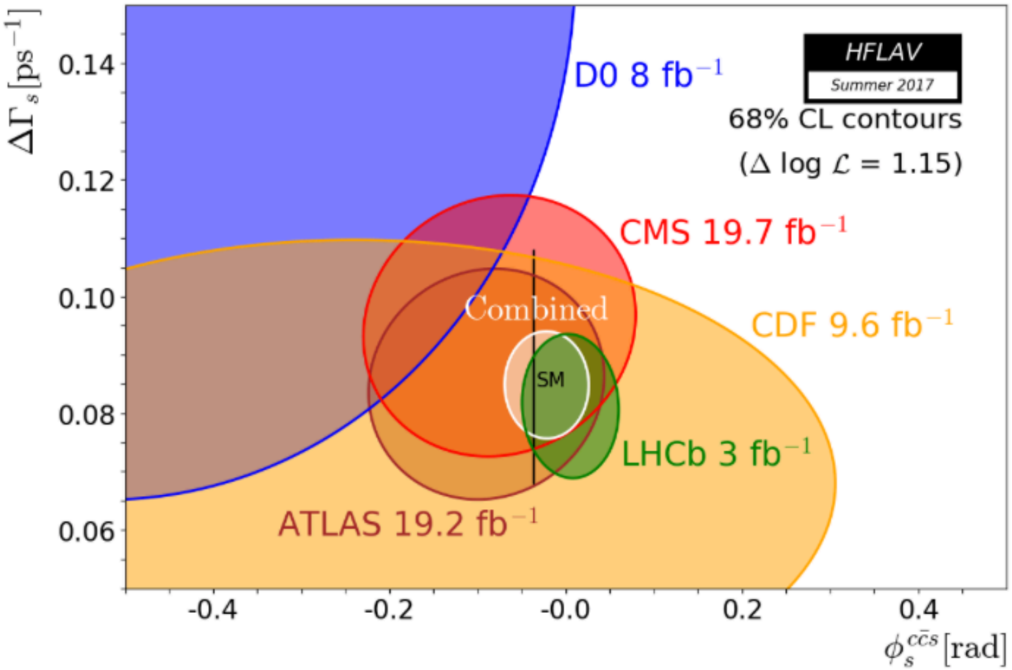


- Several measurements at the Tevatron and the LHC
- World average
  - $\phi_s$ = –21 ± 31 mrad
- Still compatible with the Standard Model at the present level of precision

| Exp. | Mode | Dataset | $\phi_s^{c\bar{c}s}$ | $\Delta\Gamma_s$ (ps$^{-1}$) | Ref. |
|---|---|---|---|---|---|
| CDF | $J/\psi\phi$ | 9.6 fb$^{-1}$ | $[-0.60, +0.12]$, 68% CL | $+0.068 \pm 0.026 \pm 0.009$ | [2] |
| D0 | $J/\psi\phi$ | 8.0 fb$^{-1}$ | $-0.55^{+0.38}_{-0.36}$ | $+0.163^{+0.065}_{-0.064}$ | [3] |
| ATLAS | $J/\psi\phi$ | 4.9 fb$^{-1}$ | $+0.12 \pm 0.25 \pm 0.05$ | $+0.053 \pm 0.021 \pm 0.010$ | [4] |
| ATLAS | $J/\psi\phi$ | 14.3 fb$^{-1}$ | $-0.110 \pm 0.082 \pm 0.042$ | $+0.101 \pm 0.013 \pm 0.007$ | [5] |
| ATLAS | above 2 combined | | $-0.090 \pm 0.078 \pm 0.041$ | $+0.085 \pm 0.011 \pm 0.007$ | [5] |
| CMS | $J/\psi\phi$ | 19.7 fb$^{-1}$ | $-0.075 \pm 0.097 \pm 0.031$ | $+0.095 \pm 0.013 \pm 0.007$ | [6] |
| LHCb | $J/\psi K^+K^-$ | 3.0 fb$^{-1}$ | $-0.058 \pm 0.049 \pm 0.006$ | $+0.0805 \pm 0.0091 \pm 0.0032$ | [7] |
| LHCb | $J/\psi\pi^+\pi^-$ | 3.0 fb$^{-1}$ | $+0.070 \pm 0.068 \pm 0.008$ | — | [8] |
| LHCb | $J/\psi K^+K^{-a}$ | 3.0 fb$^{-1}$ | $+0.119 \pm 0.107 \pm 0.034$ | $+0.066 \pm 0.018 \pm 0.010$ | [9] |
| LHCb | above 3 combined | | $+0.001 \pm 0.037$(tot) | $+0.0813 \pm 0.0073 \pm 0.0036$ | [9] |
| LHCb | $\psi(2S)\phi$ | 3.0 fb$^{-1}$ | $+0.23^{+0.29}_{-0.28} \pm 0.02$ | $+0.066^{+0.41}_{-0.44} \pm 0.007$ | [10] |
| LHCb | $D_s^+D_s^-$ | 3.0 fb$^{-1}$ | $+0.02 \pm 0.17 \pm 0.02$ | — | [11] |
| All combined | | | $-0.021 \pm 0.031$ | $+0.085 \pm 0.006$ | |

[a] $m(K^+K^-) > 1.05$ GeV/$c^2$.

See HFLAV page for the list of references

http://www.slac.stanford.edu/xorg/hflav/

# Measurement of $\gamma$

- $\gamma$ is the least known angle of the UT, measured via interference between b→u and b→c transitions

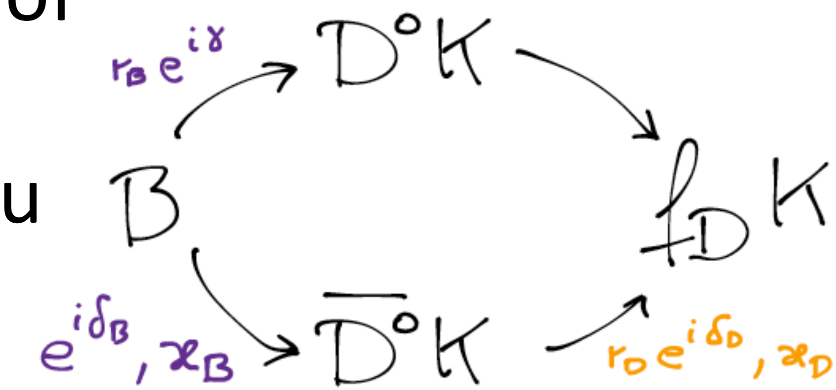


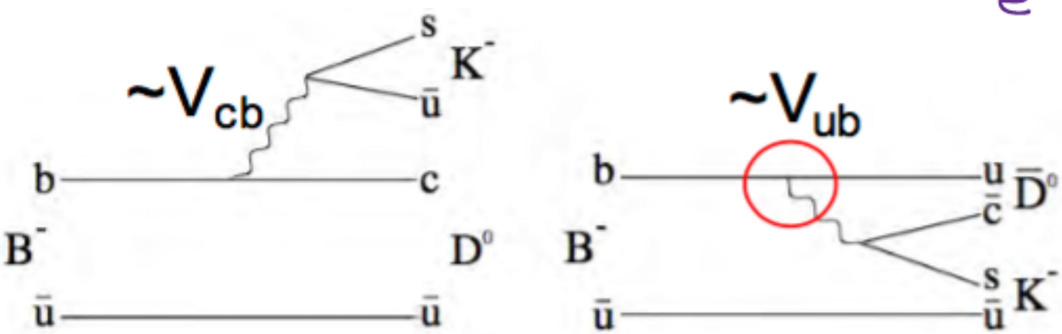


- Simple and clean theoretical interpretation, but experimentally very challenging

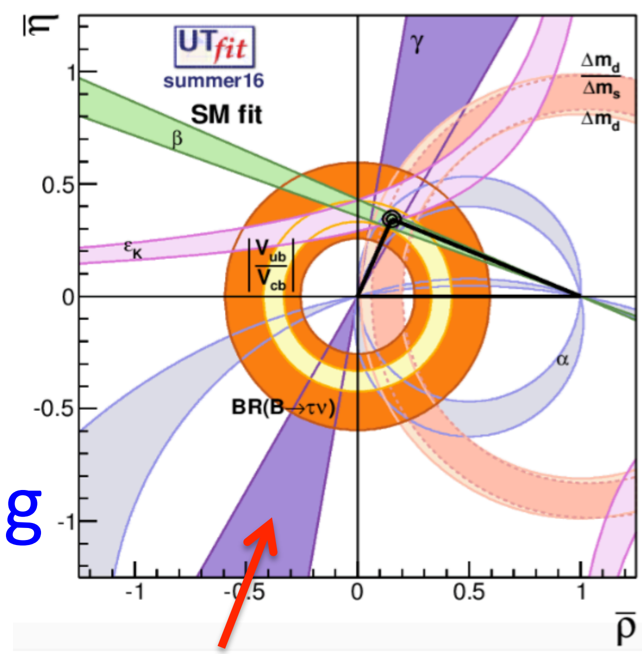

# Latest addition on γ from LHCb

From all Run-1 and 2 data a new measurement with $B^{\pm} \to (D^{*} \to D\pi^{0}/\gamma)K^{\pm}$

Partial reconstruction of $D^{*0}$ used

Sensitivity to $\gamma$ from $D^{0} \to K^{+}K^{-}$ and $D^{0} \to \pi^{+}\pi^{-}$ decay CP eigenstates

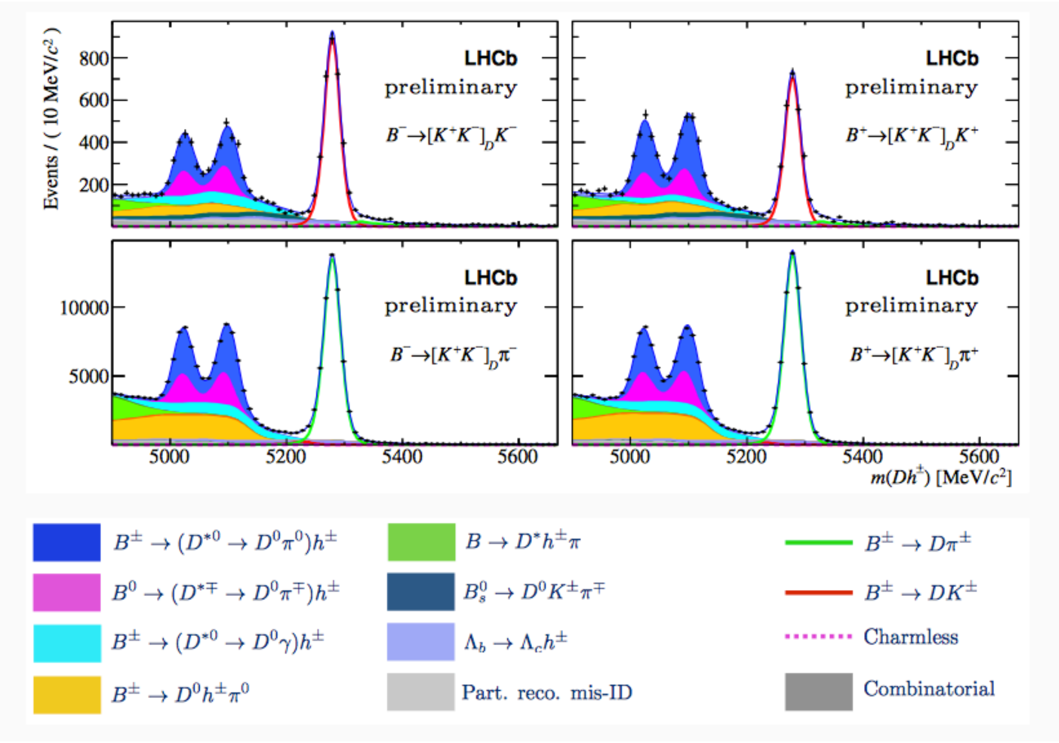


**LHCb-PAPER-2017-021**
(including Run-2 data)

# LHCb combination for $\gamma$

- A plethora of independent measurements exploiting different methods and decays
- Recent additions to the LHCb combination
  - $B^{\pm} \to D^0 K^{*\pm}$ ADS/GLW [LHCb-CONF-2016-014] NEW
  - $B^{\pm} \to D^{*0} K^{*\pm}$ GLW [LHCb-PAPER-2017-021] NEW
  - $B_s^0 \to D_s^{\mp} K^{\pm}$ TD [LHCb-CONF-2016-015] $1\ \text{fb}^{-1} \to 3\ \text{fb}^{-1}$
  - $B^{\pm} \to D^0 K^{\pm}$ GLW [LHCb-PAPER-2017-021] $3\ \text{fb}^{-1} \to 5\ \text{fb}^{-1}$
- Significantly more precise than previous results from the *B*-factories and undergoing continuous improvements

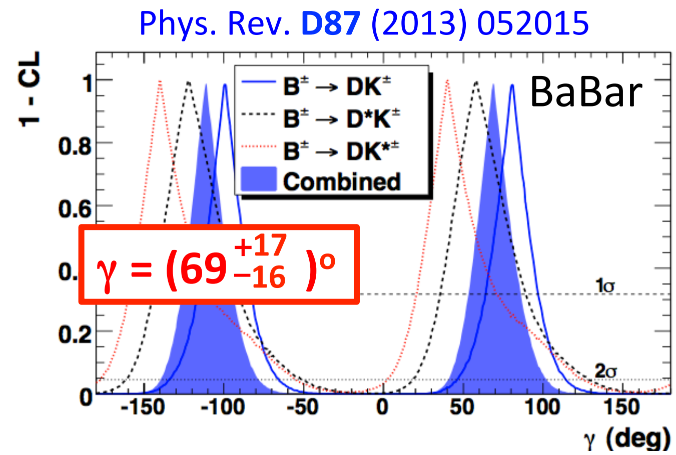


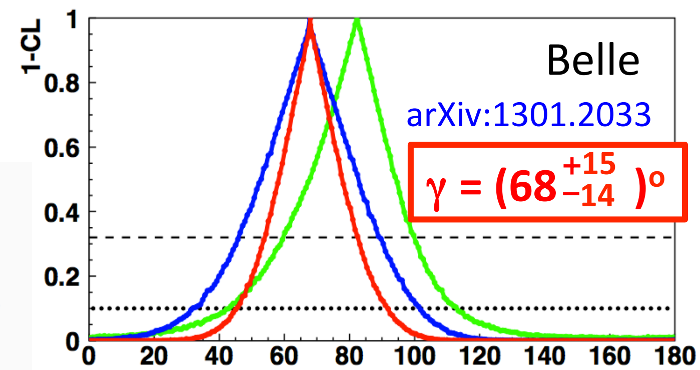


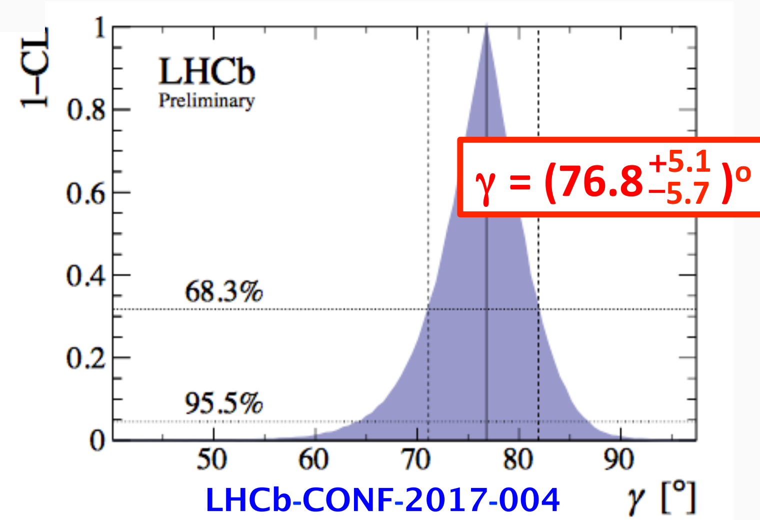

# A taste of very rare decays

# Very rare decays as another avenue to new physics: $B_s \to \mu^+\mu^-$

- The rarest B decay ever observed
- Branching fraction still compatible with the Standard Model expectation at the current level of precision
  - no sign of new physics yet

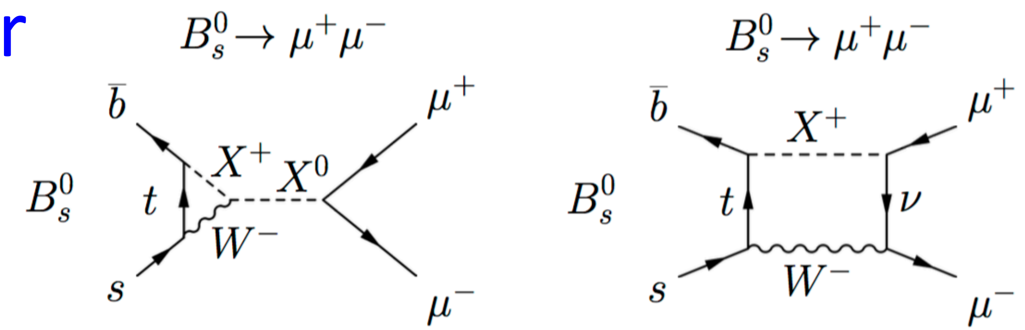


Phys. Rev. Lett. 118, 191801 (2017)

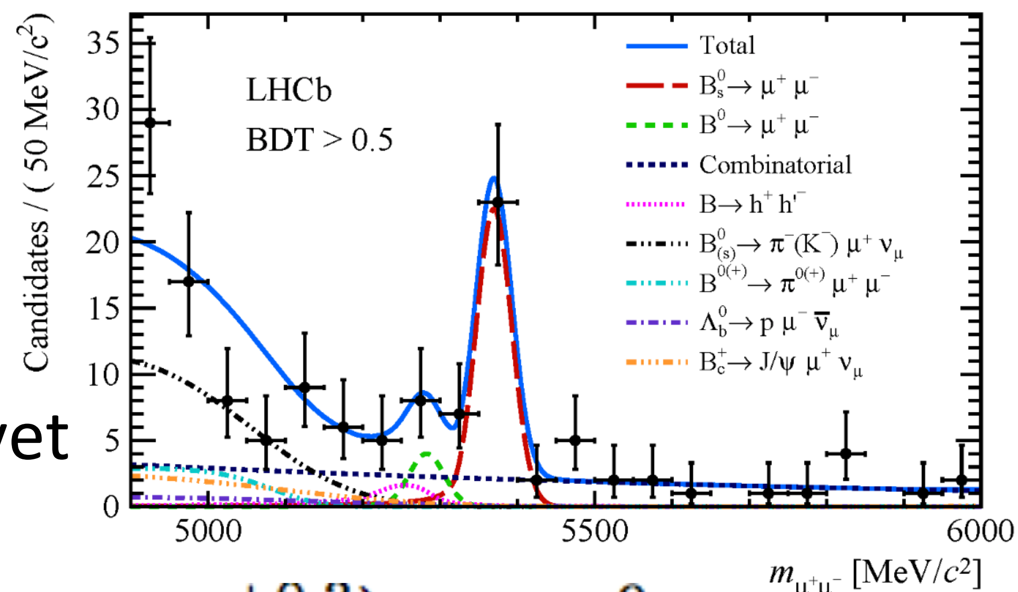


$$\mathcal{B}(B_s^0 \to \mu^+\mu^-) = (3.0 \pm 0.6^{+0.3}_{-0.2}) \times 10^{-9}$$

# $B^0$ and $B_s \to \mu^+\mu^-$ history

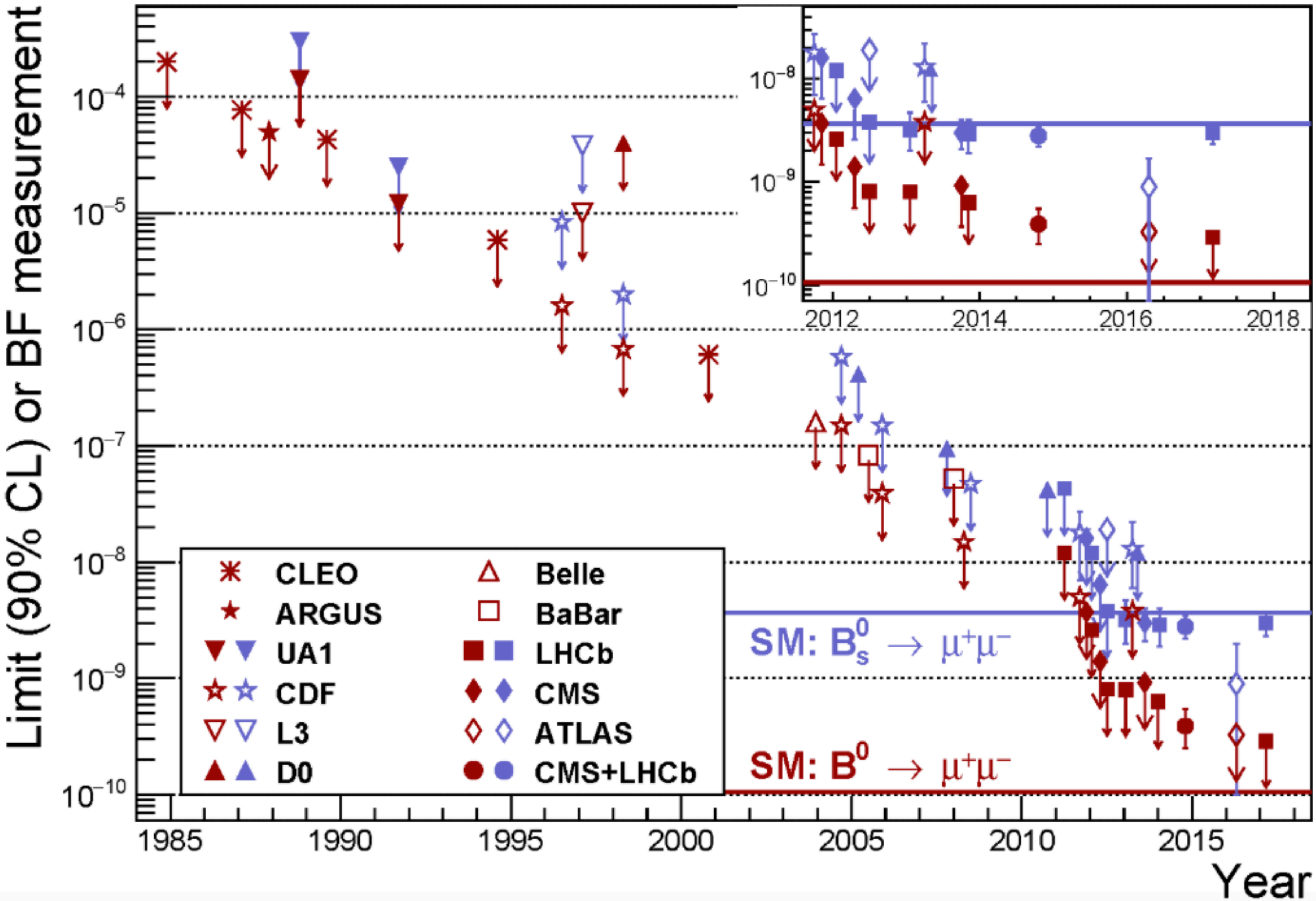

# Effective $B_s \rightarrow \mu\mu$ lifetime

- Moreover, it starts to be possible to measure other properties of the $B_s \rightarrow \mu\mu$ decay, such as the effective lifetime, and in the further future we will have *CP* asymmetries
  - These observables will be particularly relevant for discriminating between NP models in the event that (or better say when?) effects beyond the SM will be observed

$$\tau(B_s^0 \rightarrow \mu^+\mu^-) = 2.04 \pm 0.44 \pm 0.05\,\text{ps}$$

- Experimental precision not yet in the interesting range, but important proof of concept that allows for reliable scaling to larger luminosity

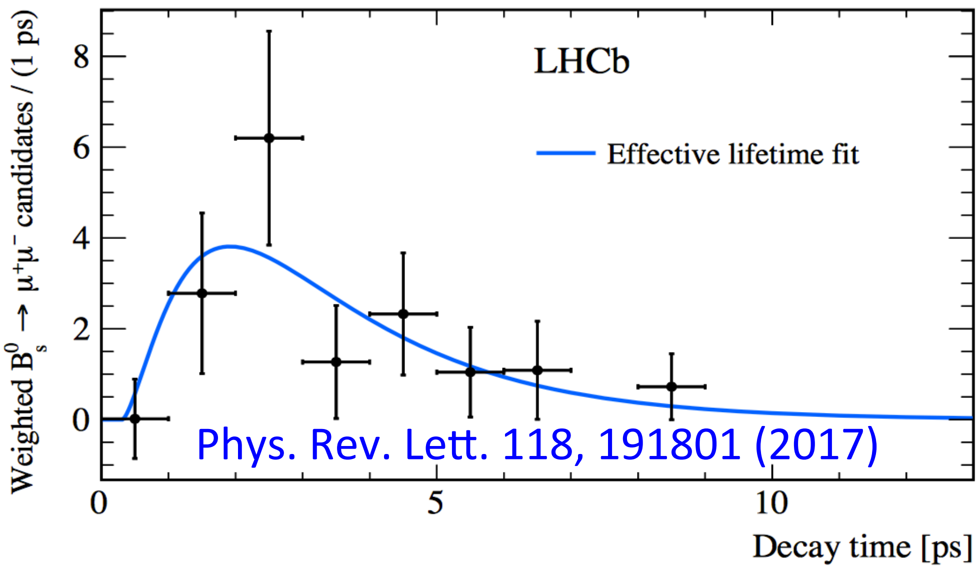

# Heavy Flavour Spectroscopy

# The pentaquark

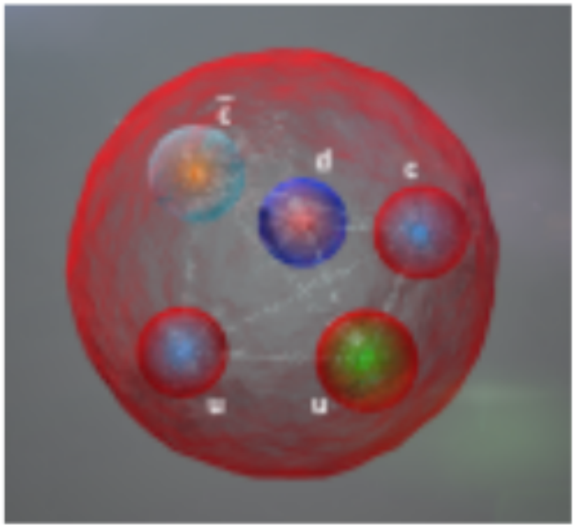

Phys. Rev. Lett. 115 072001 (2015)

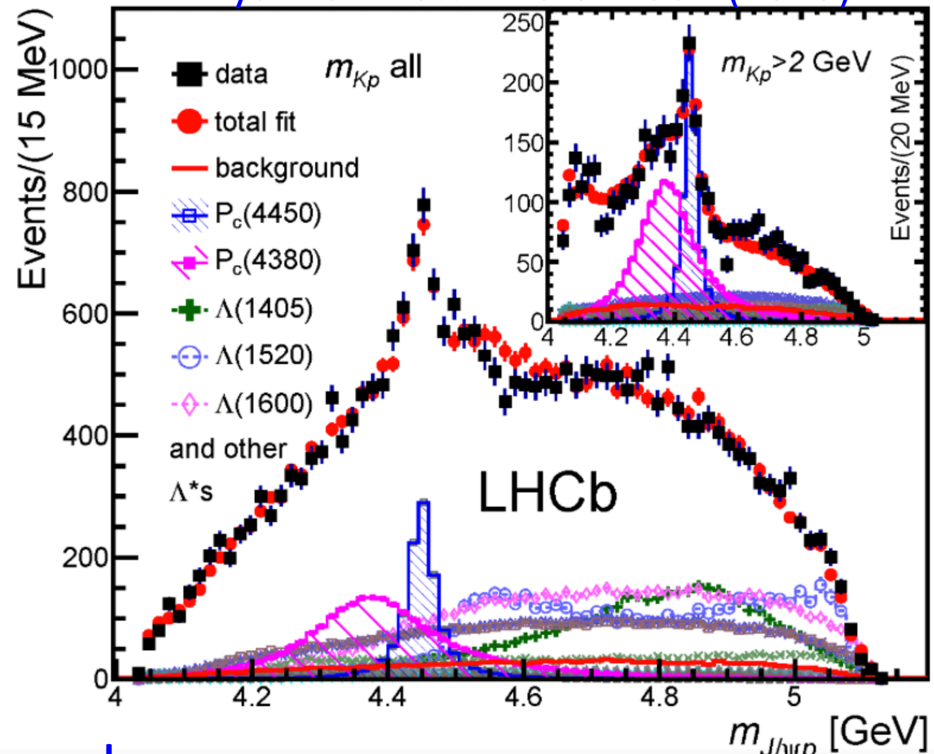


- For the first time, LHCb observed two states composed of five quarks decaying into a J/ψ meson and a proton
- Since the quark model was proposed, 50 years were needed to demonstrate unambiguously the existence of such states
- Significant efforts undergoing to strengthen the first observation improving models and looking for signals in other modes

# Observation of $\Lambda_b \to \chi_{cJ} pK$ decays

- Similar $\Lambda_b \to \chi_{cJ} pK$ decays can provide another avenue for pentaquark studies
  - First step is observation
- Two new decay modes observed with overwhelming statistical significance
  - $\Lambda_b \to \chi_{c1} pK$ and $\Lambda_b \to \chi_{c2} pK$

LHCb-PAPER-2017-011

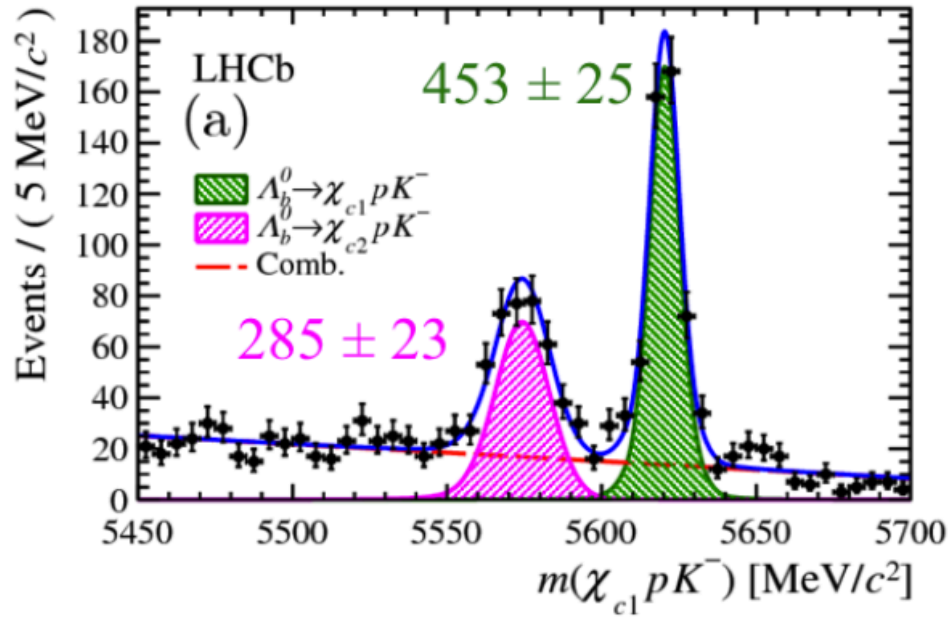


$$\frac{\mathcal{B}(\Lambda_b^0 \to \chi_{c1} pK^-)}{\mathcal{B}(\Lambda_b^0 \to J/\psi pK^-)} = 0.242 \pm 0.014 \pm 0.013 \pm 0.009$$

$$\frac{\mathcal{B}(\Lambda_b^0 \to \chi_{c2} pK^-)}{\mathcal{B}(\Lambda_b^0 \to J/\psi pK^-)} = 0.248 \pm 0.020 \pm 0.014 \pm 0.009$$

$$\frac{\mathcal{B}(\Lambda_b^0 \to \chi_{c2} pK^-)}{\mathcal{B}(\Lambda_b^0 \to \chi_{c1} pK^-)} = 1.02 \pm 0.10 \pm 0.02 \pm 0.05$$

# Tetraquark states in J/ψφ

- Looking at the J/ψφ spectrum, a narrow state $X(4140)^0$ reported by CDF, D0, CMS but not seen by Belle. Hints of X(4274) also seen by CDF and CMS
- LHCb amplitude analysis of B →J/ψφK ⇒ confirmed these 2 + 2 new states

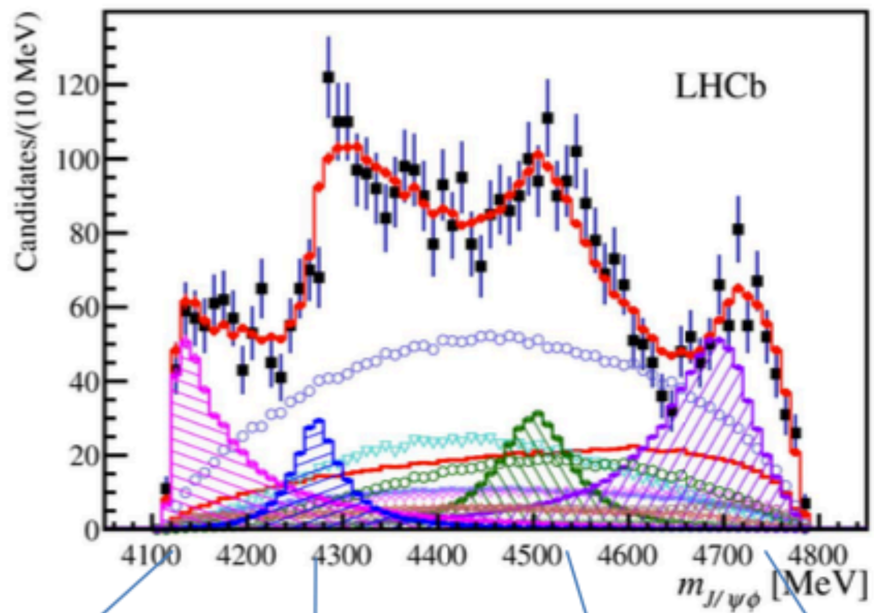


PRL 118 (2017) 022003

| X(4140) | X(4274) | X(4500) | X(4700) |
|---|---|---|---|
| 8.4 σ | 5.8 σ | 6.1 σ | 5.6 σ |
| $J^{PC}= 1^{++}$ | $J^{PC}= 1^{++}$ | $J^{PC}= 0^{++}$ | $J^{PC}= 0^{++}$ |

# Excited $\Omega_c$ states (?)

Phys. Rev. Lett. 118, 182001 (2017)

- This is an example of a very recent analysis that lead to the discovery of five new states, attributed to be excited states of the $\Omega_c$ baryon decaying to a $\Xi_c$ baryon and a kaon
- Now working to precisely pinpoint the quantum numbers
  – No theory consensus on the subject
  – Why all five so narrow? Some theorists speculating on charmed exotics...

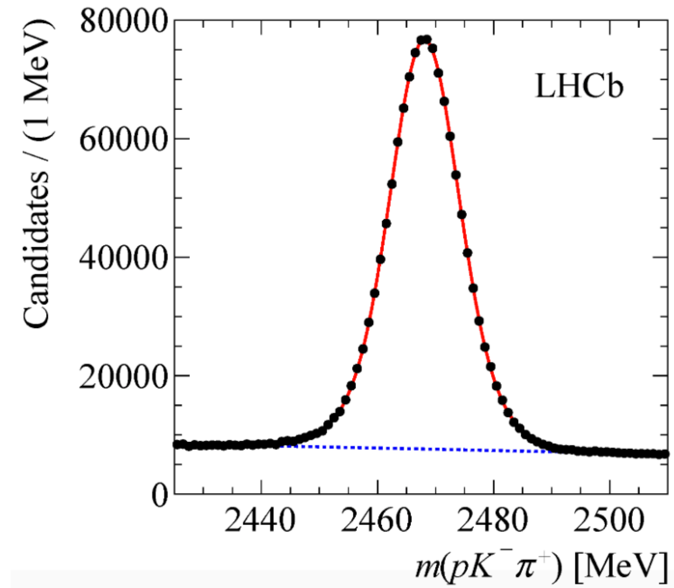


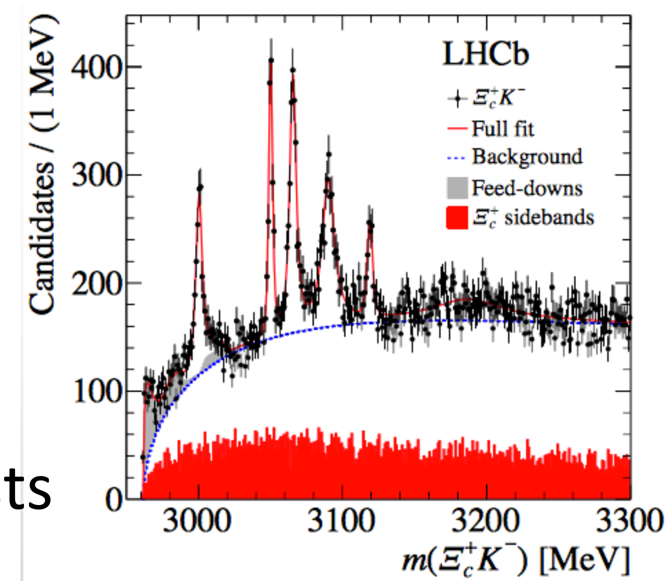

# Doubly charmed baryons

3 states expected from quark model:

$\Xi_{cc}^{++}$= ccu, $\Xi_{cc}^{+}$= ccd, $\Omega_{cc}^{+}$= ccs

$\Xi_{cc}^{+}$ observation reported by the SELEX experiment (*PRL89(2002)112001, PRB628(2005)18*)

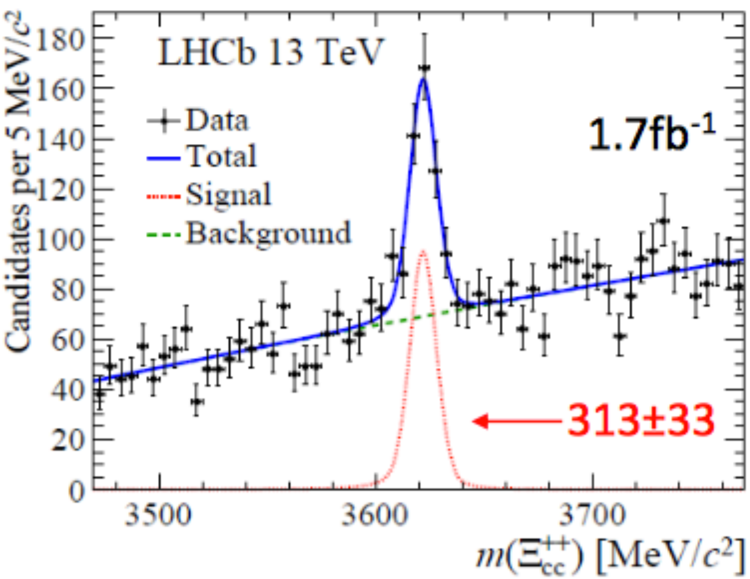


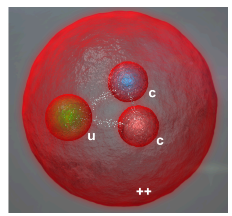


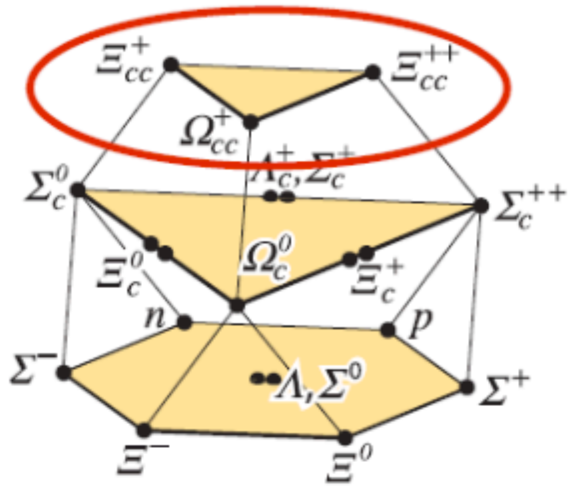


SU(4) flavor multiplets, PDG Review of Particle Physics, Phys.Rev. D86, 010001.

arXiv:1707.01621

**First observation of $\Xi_{cc}^{++}$**

Mass ~100 MeV larger than the one reported by SELEX for $\Xi_{cc}^{+}$, disfavouring the $\Xi_{cc}^{+}$ hypothesis of SELEX

**First observation of a baryon containing two heavy quarks**

- Now at work to measure properties: lifetime, production mechanisms, decay modes, ...
- ... as well as to observe singly charged and strange partners

# What else to make LHCb a general purpose forward detector?

# $Z \to b\bar{b}$ decays

Looking at $pp \to (Z \to b\bar{b})j$ events

Events with 3 jets, where two are b-tagged

$$\sigma(pp \to Z)\mathcal{B}(Z \to b\bar{b})$$
$$= 332 \pm 46(\text{stat.}) \pm 59(\text{syst.})\ \text{pb}$$

Important measurement for future searches of heavy particles decaying to b-jets

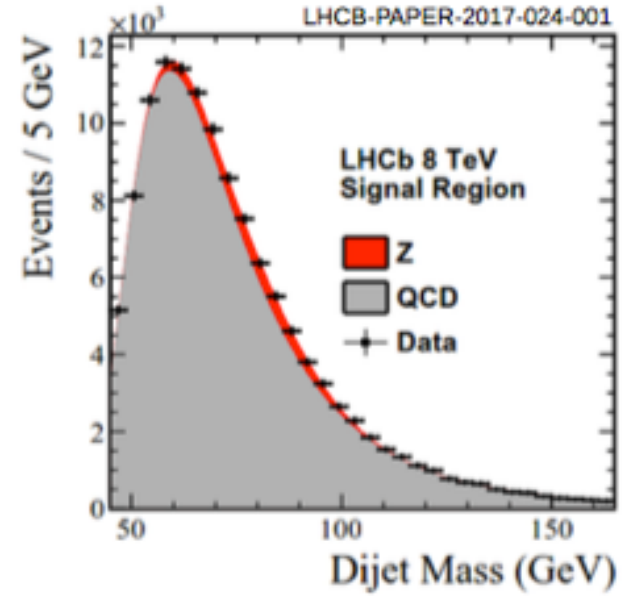


Background subtracted

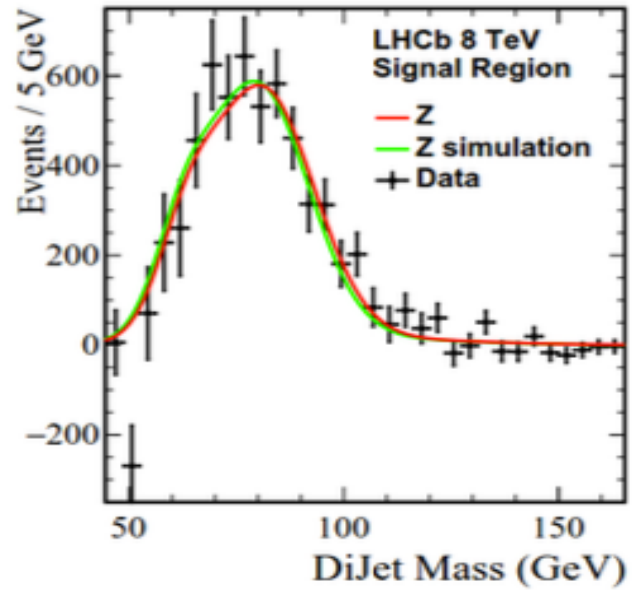

# Heavy ion collisions

Data taken during 2016 p-Pb and Pb-p runs @ $\sqrt{s_{NN}} = 8.16$ TeV

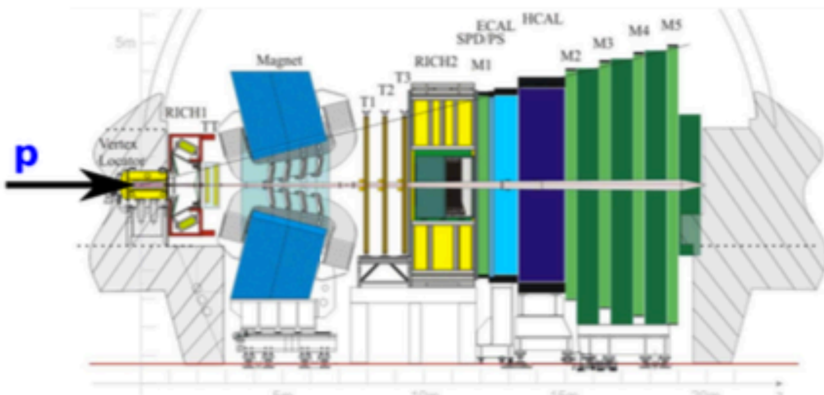


Forward

$1.5 < y^* < 4.5$

$y^* = y_{lab} - 0.465$

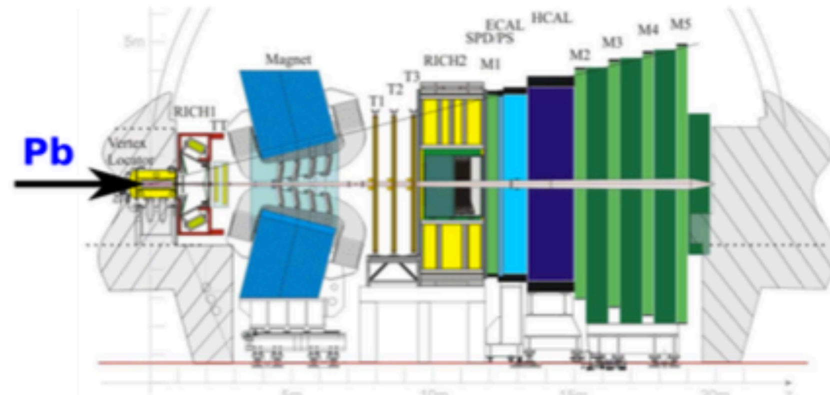


Backward

$-5.5 < y^* < -2.5$

$y^* = -(y_{lab} + 0.465)$

# Prompt and non-prompt J/ψ production in *p*Pb collisions

J/ψ **prompt** and non-prompt (from b-hadrons) cross section

Measure production relative to pp collisions (scaled by factor 208)

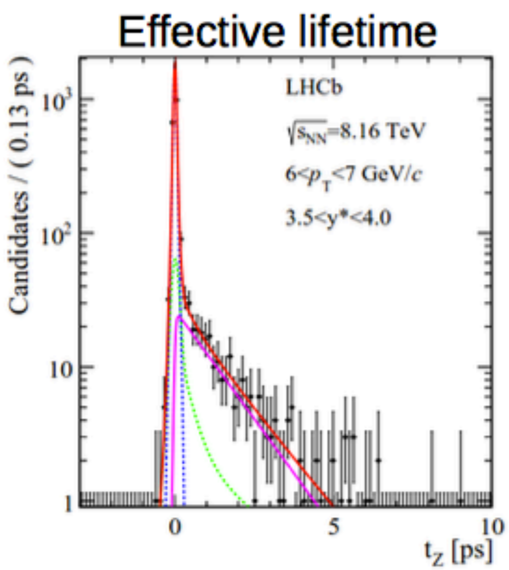


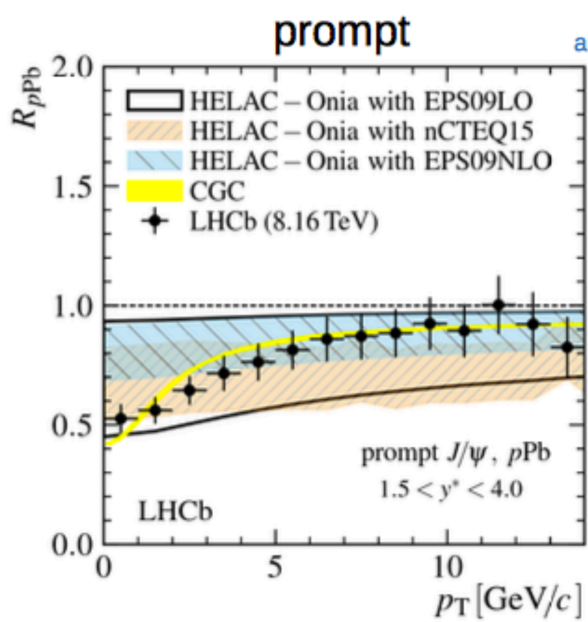


arXiv:1706.07122

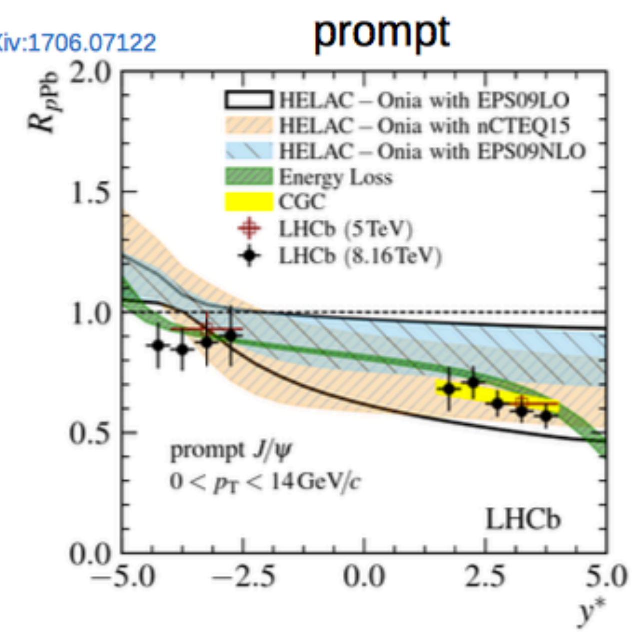

# Prompt and non-prompt J/ψ production in *p*Pb collisions

J/ψ **prompt** and non-prompt (from b-hadrons) cross section

Measure production relative to pp collisions (scaled by factor 208)

Effective lifetime

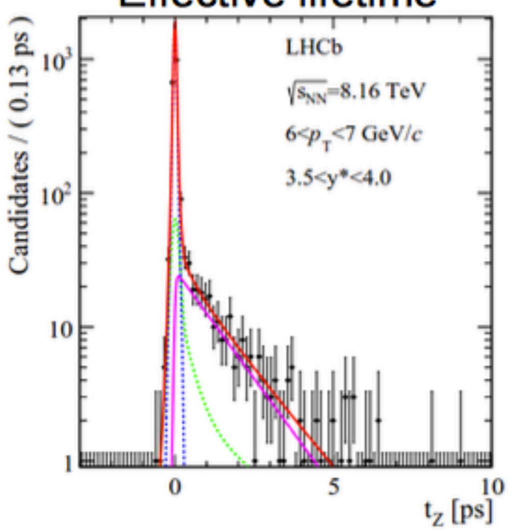


non-prompt

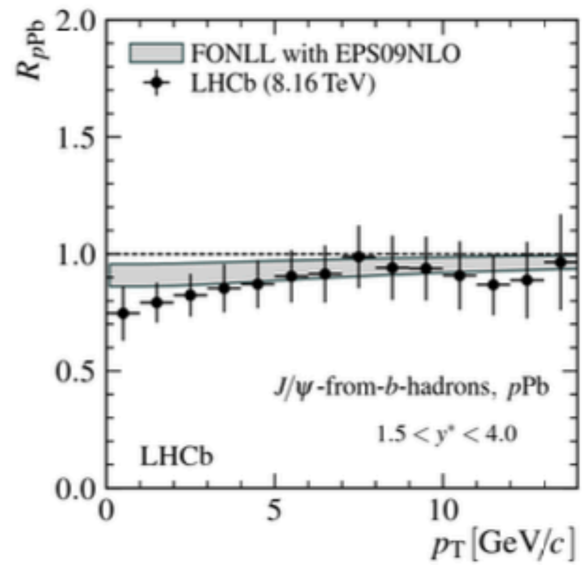


arXiv:1706.07122

non-prompt

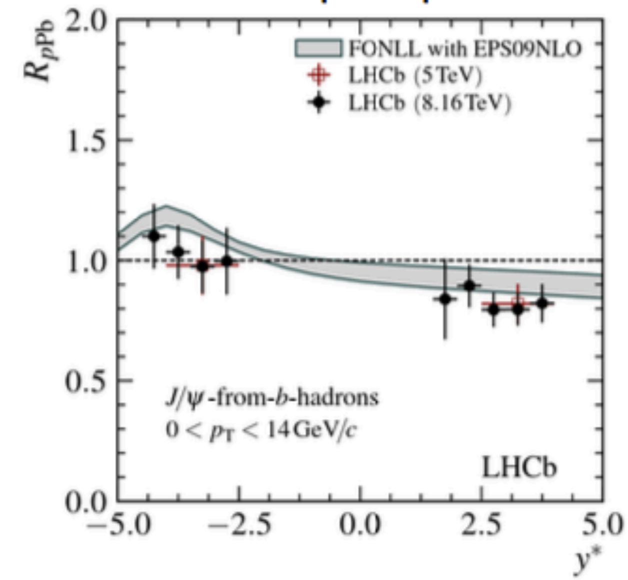

# Antiproton production in fixed-target *p*He collisions

LHCb-CONF-2017-002

- Measurement motivated by the need to understand energy dependence of $\bar{p}$ component from cosmic rays in space
- Theoretical uncertainties are limited by precise knowledge of cross section for basic processes in the interstellar medium, like those arising from *p*He collisions

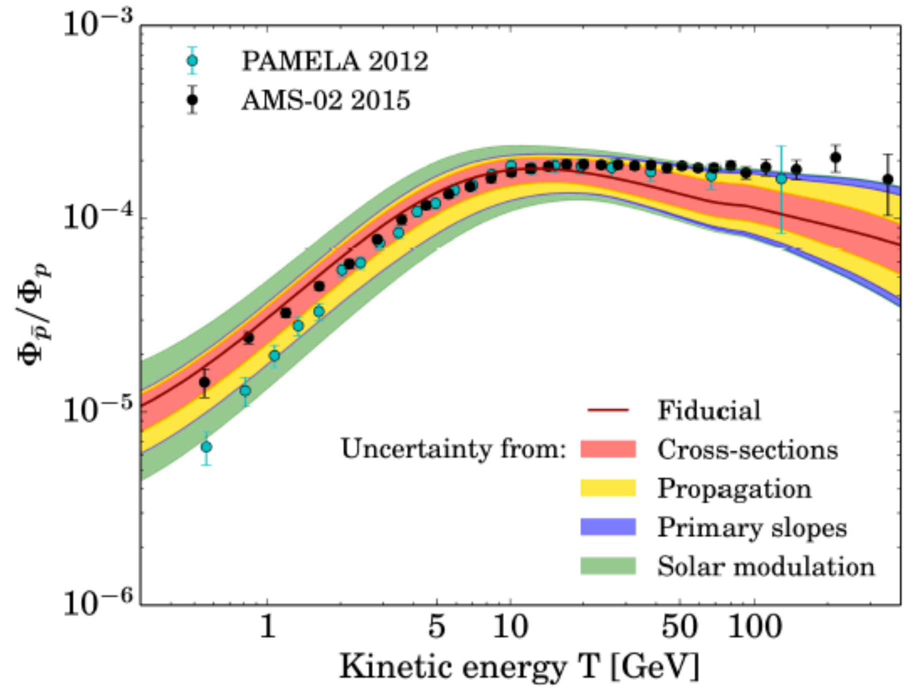


- LHCb can inject gas into the beam pipe for relevant cross-section measurements in the sector

# Antiproton production in fixed-target *p*He collisions

LHCb-CONF-2017-002

- The data sample used in this analysis was collected in May 2016 with 6.5 TeV protons
- One difficult aspect to measure absolute cross sections with SMOG is the determination of luminosity
- A method has been developed to exploit elastic $pe^-$ interactions
  - well known cross section
  - look for single $e^-$ tracks in the detector

# Antiproton production in fixed-target *p*He collisions

LHCb-CONF-2017-002

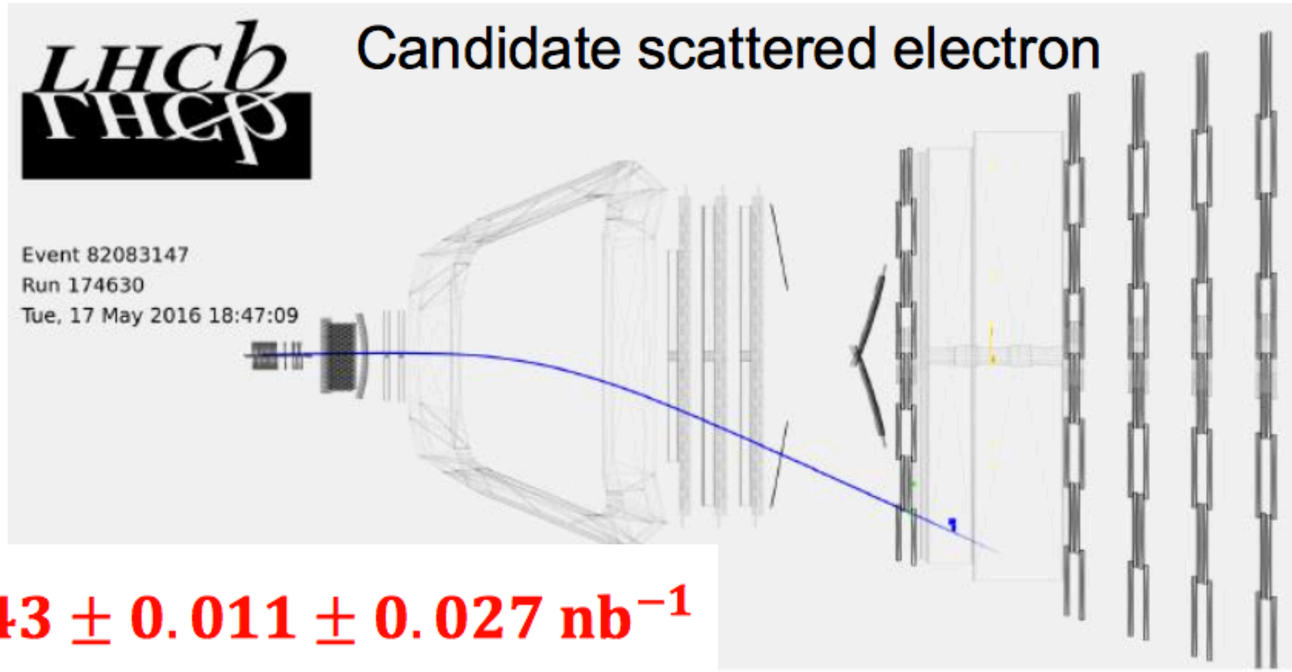


$$\mathcal{L} = 0.443 \pm 0.011 \pm 0.027\ \mathrm{nb}^{-1}$$

- Very good agreement between simulation and data

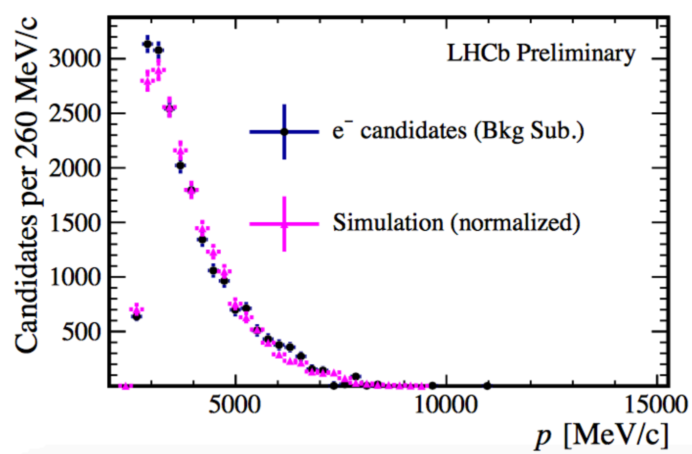


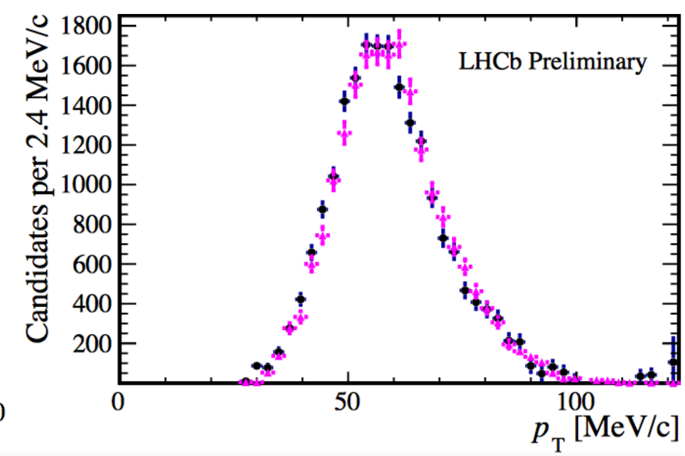

# Antiproton production in fixed-target *p*He collisions

**LHCb-CONF-2017-002**

- Antiproton cross section measured with 10% precision
  - The measurement is larger by 1.5 with respect to EPOS LHC
- Theoretical interpretation ongoing
- Additional production measurements are also important
  - antiprotons from $\Lambda$
  - anti-deuterium
  - anti-He
- Rich programme to develop!

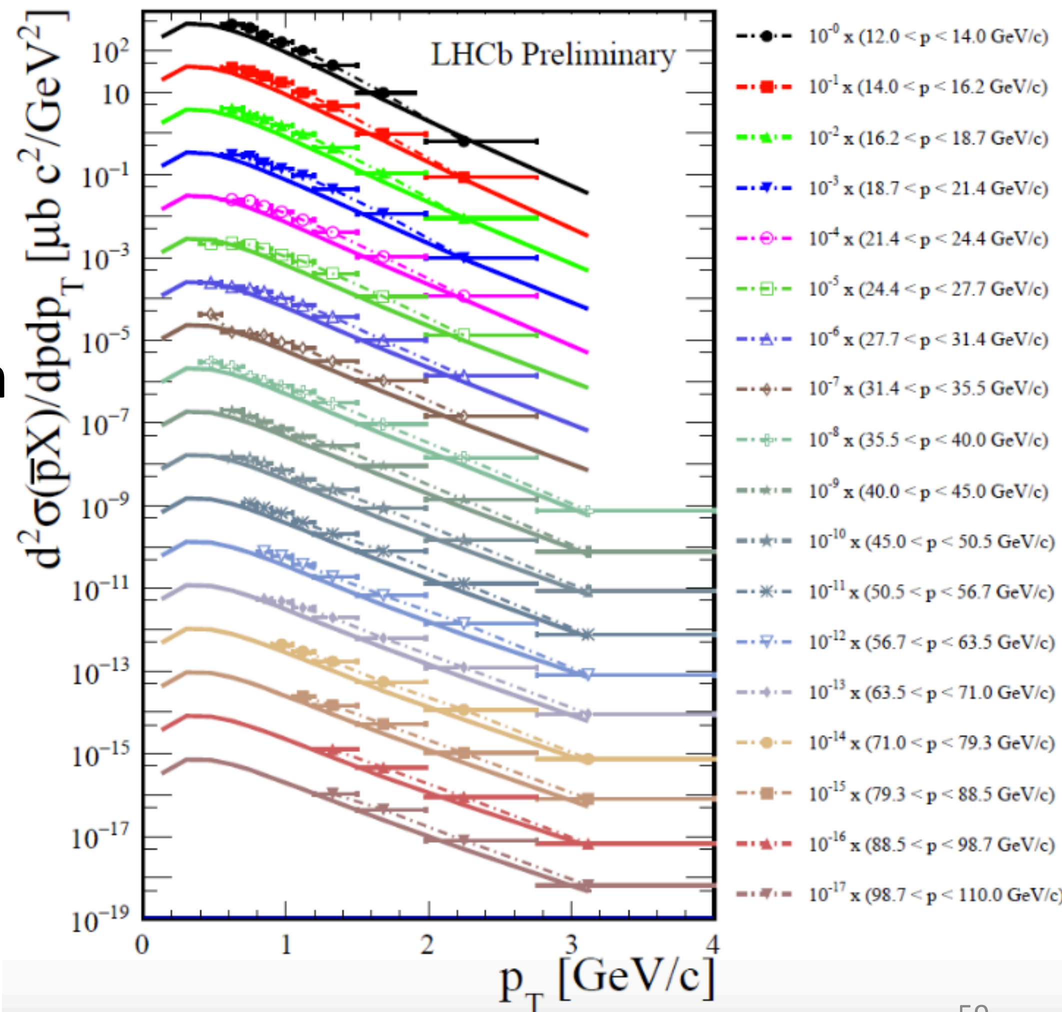

# LHCb Upgrade(s)

# LHCb going to upgrade at the end of 2018. Why?

- Main limitation that prevents exploiting higher luminosity with the present detector is the Level-0 (hardware) trigger
  - Level-0 output rate < 1 MHz (readout rate) requires raising thresholds
- This is particularly problematic for hadronic final states

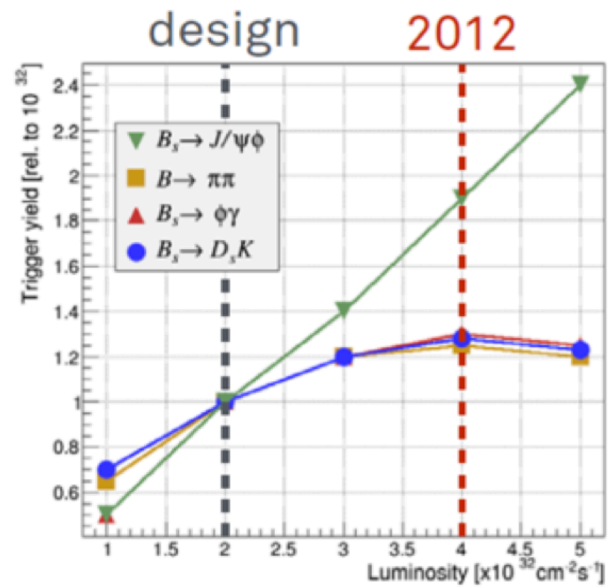


| | LHC Run | Period of data taking | Maximum $\mathcal{L}$ [cm$^{-2}$s$^{-1}$] | Cumulative $\int \mathcal{L}\,dt$ [fb$^{-1}$] |
|---|---|---|---|---|
| Current detector | 1 & 2 | 2010–2012, 2015–2018 | $4 \times 10^{32}$ | 8 |
| Phase-I Upgrade | 3 & 4 | 2021–2023, 2026–2029 | $2 \times 10^{33}$ | 50 |

## LHCb upgrade for Run-3

- running at $2 \times 10^{33}$ cm$^{-2}$s$^{-1}$ with full software trigger, running at 40 MHz and record 20 kHz

# New upgrade in Run-5?

- Expression of Interest submitted by the LHCb collaboration to the LHCC to propose a new upgrade to be in operation for the Run-5 of the LHC https://cds.cern.ch/record/2244311
- A series of yearly workshops in place
  - see e.g. https://agenda.infn.it/conferenceDisplay.py?ovw=True&confId=12253 for the latest one

| | LHC Run | Period of data taking | Maximum $\mathcal{L}$ $[\mathrm{cm}^{-2}\mathrm{s}^{-1}]$ | Cumulative $\int \mathcal{L}\, dt$ $[\mathrm{fb}^{-1}]$ |
|---|---|---|---|---|
| Current detector | 1 & 2 | 2010–2012, 2015–2018 | $4 \times 10^{32}$ | 8 |
| Phase-I Upgrade | 3 & 4 | 2021–2023, 2026–2029 | $2 \times 10^{33}$ | 50 |
| Phase-II Upgrade | 5 → | 2031–2033, 2035 → | $2 \times 10^{34}$ | 300 |

- The purpose is to raise the instantaneous luminosity by a further factor 10 with respect to the forthcoming upgrade → very challenging, needs major refactoring of the detector

# There's obviously much more...

- The LHCb collaboration published 384 publications since the start of the data taking, mostly with LHC Run-1 data
  - An another 15+ years of life are expected
- Only a few examples of relevant measurements shown today
  - e.g. completely skipped Charm physics and a plethora of other important measurements in various sectors
- Upgrade in Run-3 well on track and thoughts developing for a third life of the experiment in Run-5
- Exciting competition a few years ahead when Belle 2 will start taking a significant amount of data
  - and ongoing competition in some areas of the flavour sector (especially when dimuons are involved) with ATLAS and CMS

**Thanks for the invitation and for your attention!**

**Stop here**

# Vertex detector (VELO)

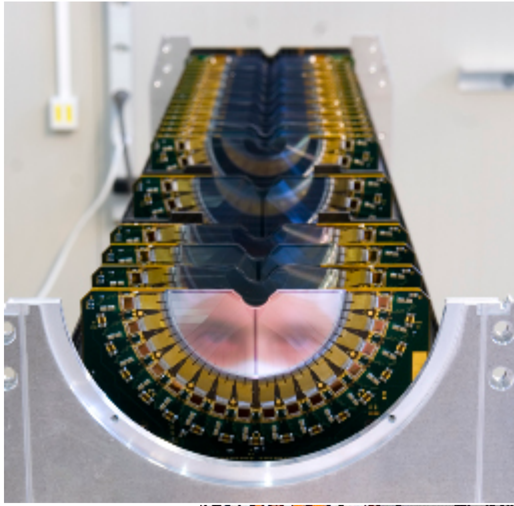

- 84 silicon micro strip sensors
  - 44 mm radius
  - R or ϕ geometry

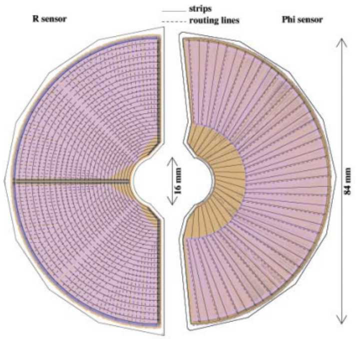


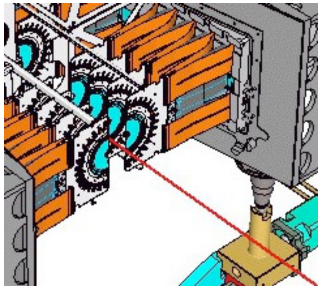

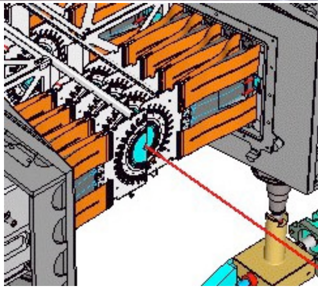

- Open and closes for each fill
  - Centred around the current beam position
    - It does not move during a fill
  - Mechanically reproducible to ~5 μm
- The silicon sensors come as close as 8mm to the LHC beam

# VELO performance

- The VELO allows for a very precise measurement of the track trajectories close to the interaction point, which is crucial to separate decays of beauty and charm hadrons from the background
- Impact parameter (distance of a track to a primary vertex) resolution is essential
  - Very good resolution
    - ~**20 µm at high $p_T$**
      - This means over 2 GeV
  - Primary vertex resolution excellent
    - ~16 µm in x,y, ~76 µm in z (20 tracks)

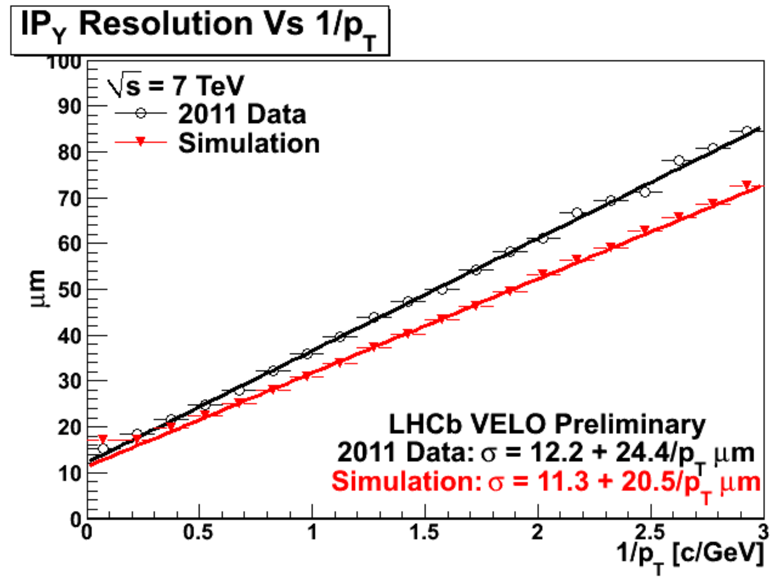

# Tracking system

- One station (TT) before the magnet
  - Si strips, 4 layers
- Dipole magnet
  - ∫Bdl = ~4 Tm ; polarity switched regularly
- 3 stations after the magnet
  - Si strips in centre (IT), straw tubes outside (OT)
  - 4 layers per station x-u-v-x, (5 degree stereo angle)
- Tracking efficiency over 96%
  - For tracks traversing the whole detector, over 5 GeV/c momentum
- The tracking system provides a measurement of momentum of charged particles with a relative uncertainty that varies from 0.5% at low momentum to 1.0% at 200 GeV/c

# Cherenkov detectors

- One distinctive feature of LHCb, when compared to the ATLAS and CMS detectors, is its particle identification capability for charged hadrons
- This is mainly achieved by means of two ring-imaging Cherenkov ("RICH") detectors placed on either side of the tracking stations
  - Once particle momenta are measured, the two RICH detectors enable the identification of protons, kaons and pions to be obtained
- Particle identification from 2 to ~100 GeV/c
  - 2 RICH, 3 radiators
  - Readout by HPD
    - High efficiency
    - Very low noise
    - 10-20 replaced each year
- Particle ID performance
  - ~95% efficiency for 5% contamination
    - Averaged over B daughter tracks

# Calorimeters

- An electromagnetic calorimeter (ECAL), complemented with scintillating-pad and preshower detectors, provides energy and position of photons and electrons, and allow for their identification in conjunction with information from the tracking system
  - made of shashlik blocks: lead-scintillator stack
  - ~6000 channels, readout by PMT
  - ~10% / √E + 1%
- The electromagnetic calorimeter is followed by a hadronic calorimeter (HCAL) that also gives some information to identify hadrons
  - scintillating tiles in iron
  - ~1500 channels, same readout and electronics as ECAL
  - ~70% / √E + 9%
  - Mainly used for trigger
- PreShower and SPD
  - same geometry as ECAL
  - Scintillator tiles readout by MAPMT
  - Identify electron/photon, used in L0 trigger

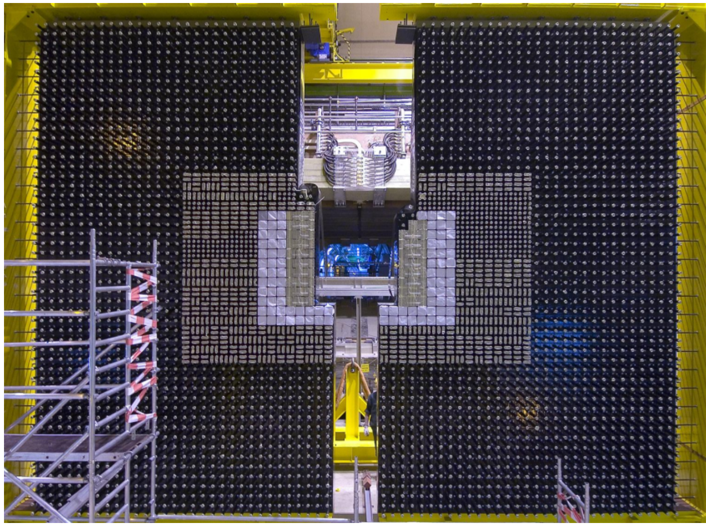

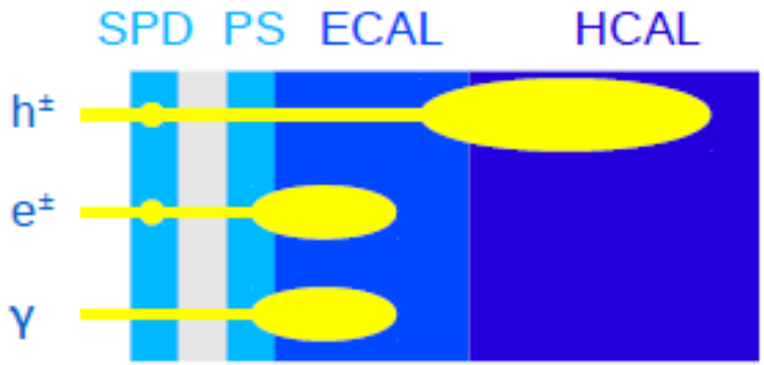

# Muon system

- Finally, muons are identified by a system composed of alternating layers of iron and multiwire proportional chambers
- 5 stations interleaved with iron walls
  – First station before the calorimeters
  – Projective geometry
    - Allows it to be used in the L0 trigger
  – Muon identification performance
    - ~97% efficiency for 3% mis-ID

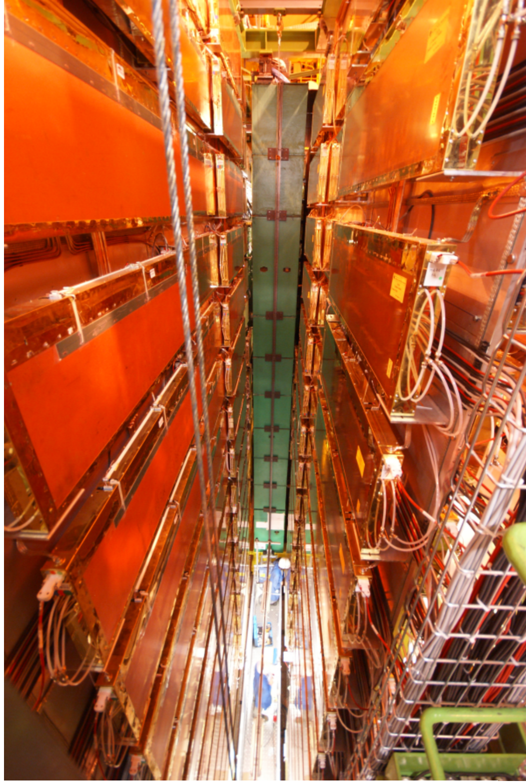

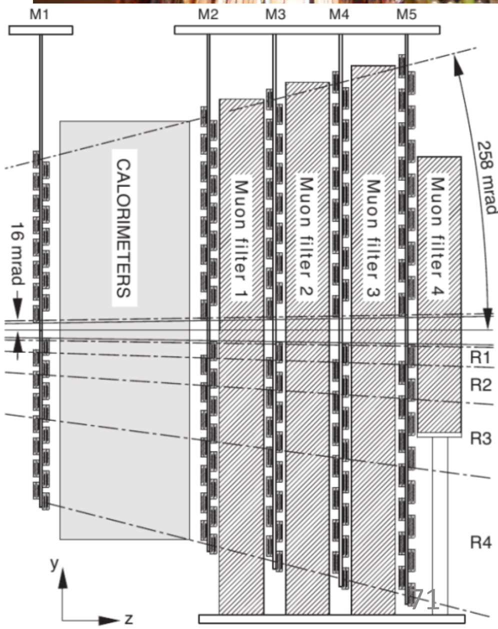

# Trigger in Run 1

- The online event selection is performed by a trigger which consists of a hardware stage, based on information from the calorimeter and muon systems, followed by a software stage, which applies full event reconstruction
- L0 hardware trigger, custom electronics
  - High $p_T$ local cluster in HCAL (3.6 GeV) or ECAL (2.6 GeV)
  - High $p_T$ muon (1.4 GeV) or di-muon
  - Accept rate limited to 1 MHz, latency < 4 μs
- HLT software trigger, 30000 copies on 1500 nodes
  - HLT1 mainly a topological trigger
    - At least one track with $p_T$ >1.6 GeV and impact parameter >100 μm
    - Accepts around 50 kHz
  - HLT2 selects by physics channel, inclusive or exclusive
    - Full track reconstruction but no particle-identification
  - 25% of the input events in Run 1 were **deferred**, i.e. stored on disk and processed during inter-fills
  - Total accept rate around 5 kHz

# Trigger evolution

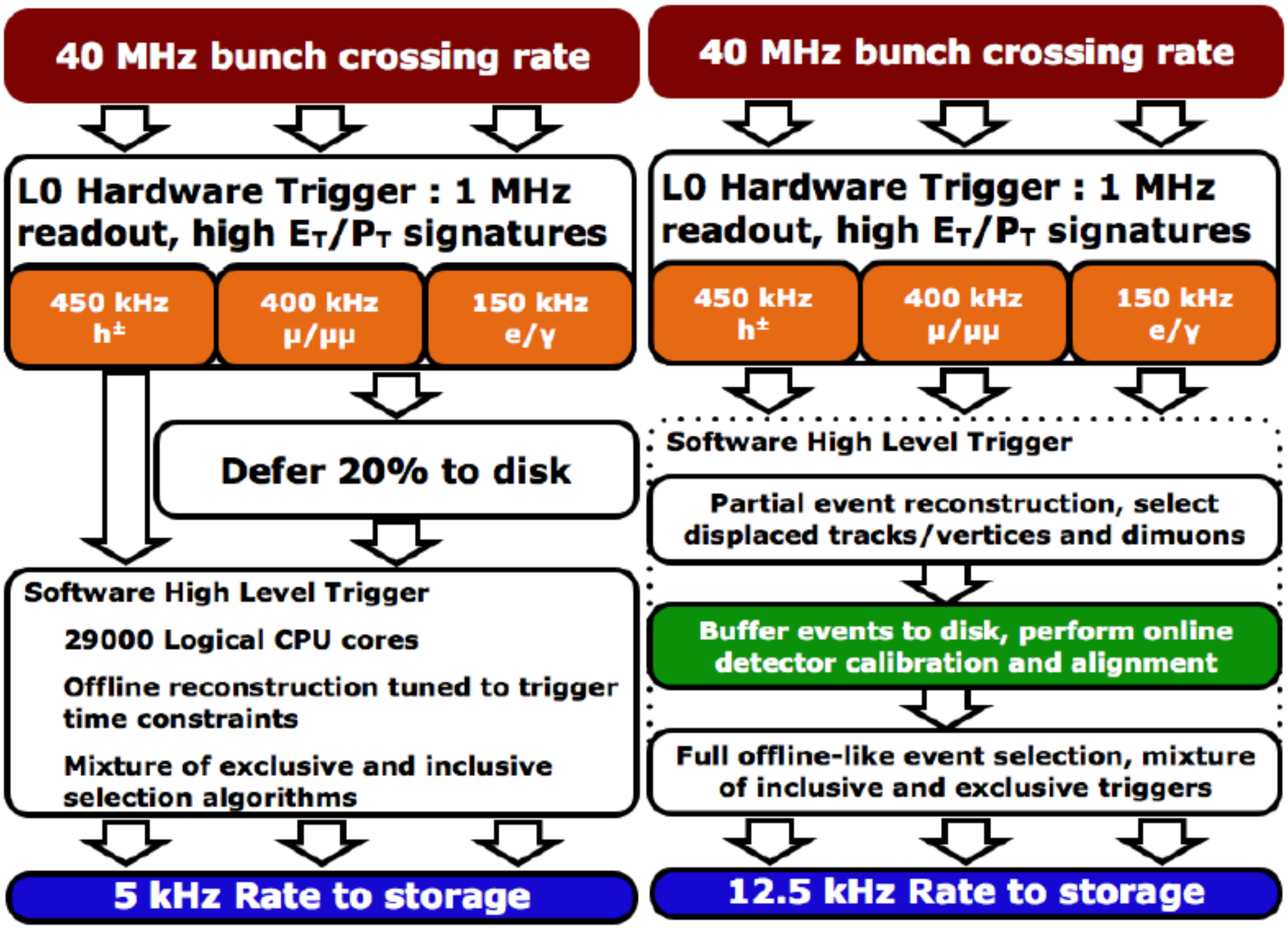


Run 1 Run 2

# LHC luminosity at the LHCb interaction point

- LHCb was designed for single collision crossings
  - Worries of ambiguities to assign the B to the proper primary vertex
    - Even intended to reject multiple interaction at level 0 trigger
  - Design luminosity 2x10 $^{32}$ cm$^{-2}$ s$^{-1}$ for ~2700 colliding bunches
- Realised later that higher collision rate was OK
  - In Run 1 and run 2 running at **4x10$^{32}$ cm$^{-2}$ s$^{-1}$** with only 1262 colliding bunches
    - 50 ns separation between bunches, 25 ns nominal and from 2015
    - This means 4 times more collisions per crossing than in the design
    - The average number of visible collisions per crossing is ~1.8
- The luminosity is kept constant thanks to the technique of "luminosity levelling"
    - Achieved by a dynamical adjustment of the transverse offset between the LHC beams during the fill
    - The beam separation is adjusted a few times per hour to maintain the luminosity constant → routine operation since 2011

# Sub-detectors to be upgraded

All subdetectors are read out at 40 MHz

RICH 1 redesigned; new photodetectors for RICH 1 and RICH 2

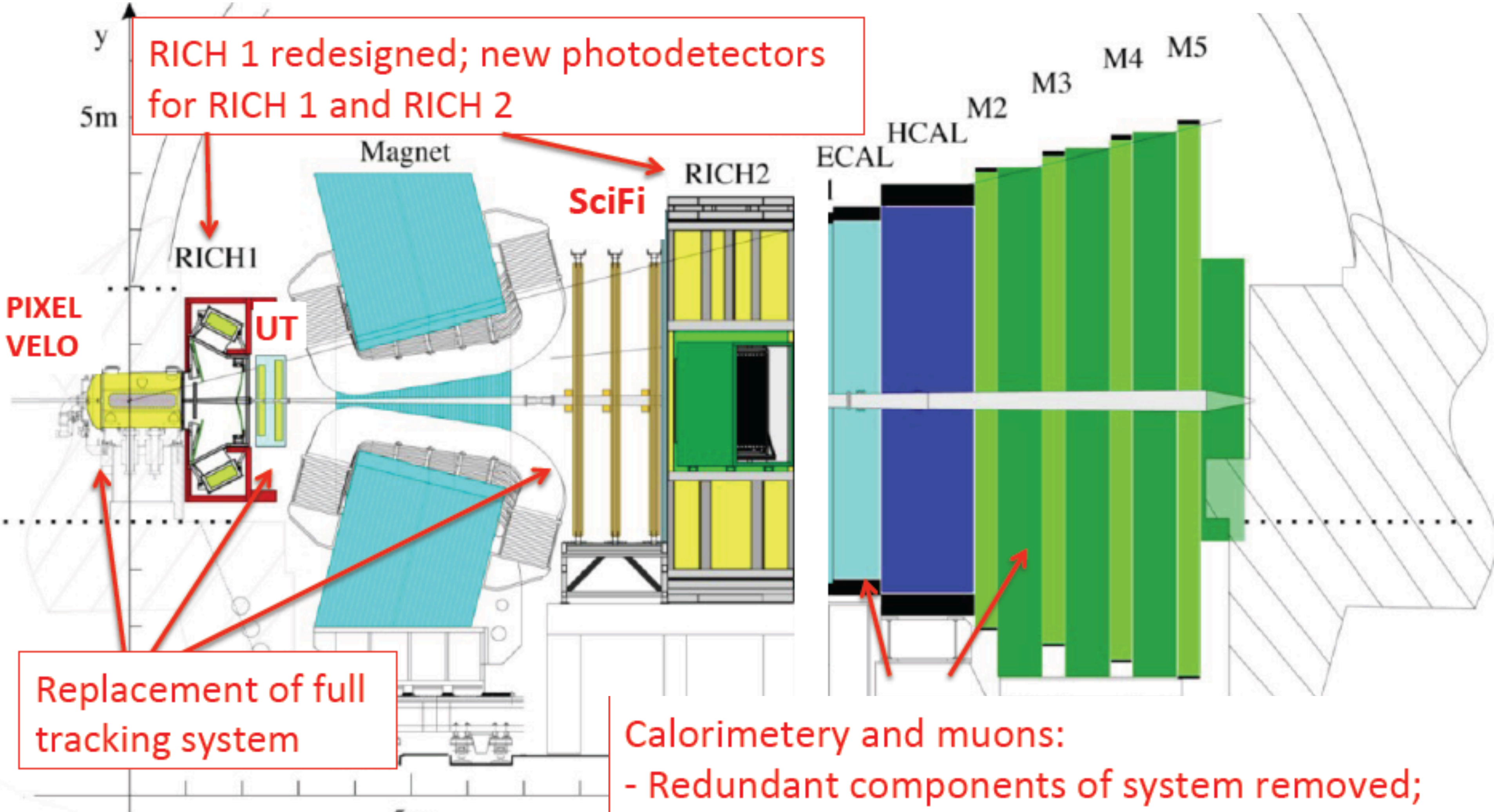


Replacement of full tracking system

Calorimetery and muons:
- Redundant components of system removed; new electronics added; more shielding included

# Upgrade of tracking detectors: VELO

- Pixel based vertex detector
  - 50x50 $\mu m^2$ pixels
- Good 3D pattern recognition
- Excellent resolution
- Main challenge
  - Radiation resistance

The layout is critical: 5 mm distance to the beam when closed!

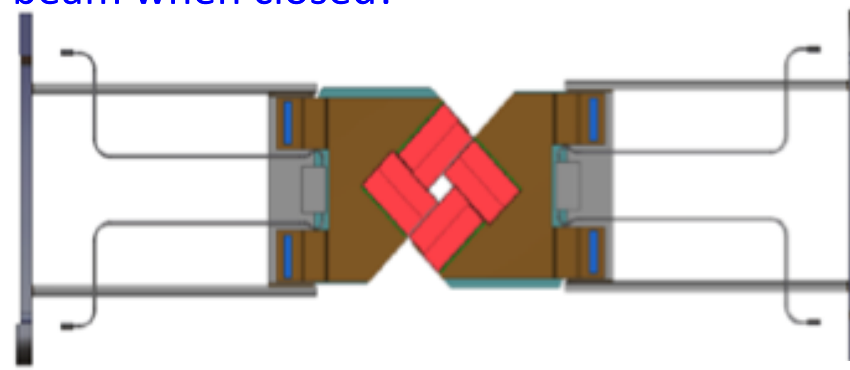

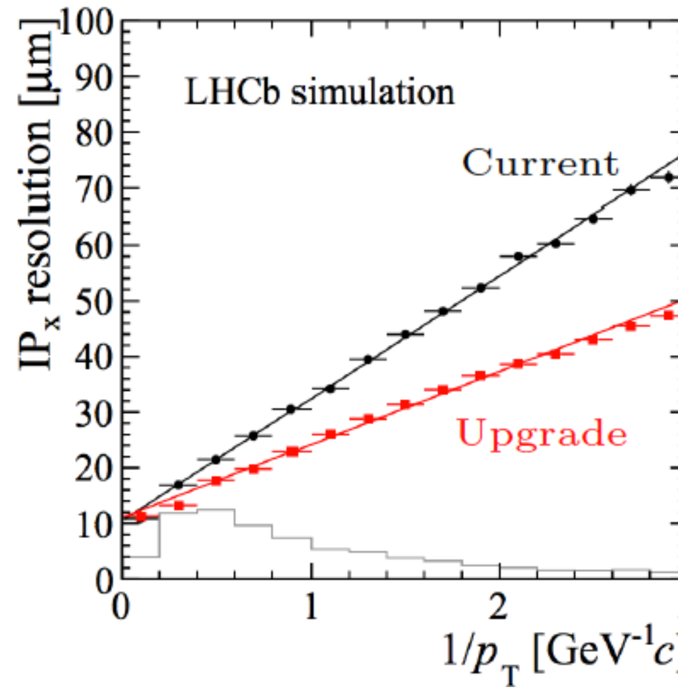


# Upgrade of tracking detectors: UT

- Silicon detector plane upstream the magnet
- Critical for tracking at trigger level
- Modules assembled in long staves
- Full acceptance and minimal material budget

# Upgrade of tracking detectors: Scintillating Fibre tracker

- Large scale tracking system based on mats of 2.5m long scintillating fibres of 250μm diameter, readout by SiPMs
- About 10000 km of scintillating fibres! Fibre quality control is an issue

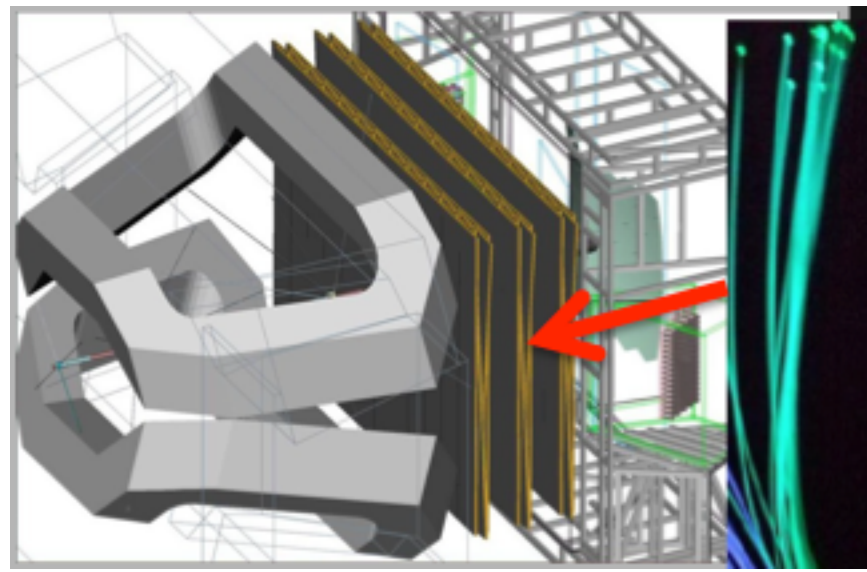

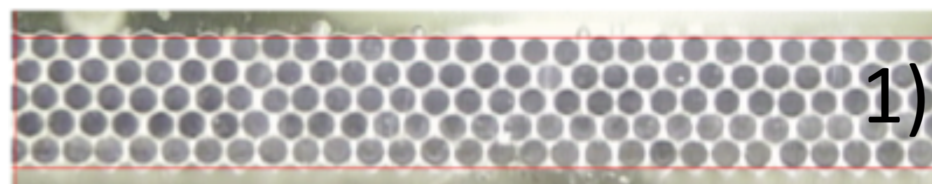


1. A good fibre mat and
2. a mat with a fibre with wrong diameter

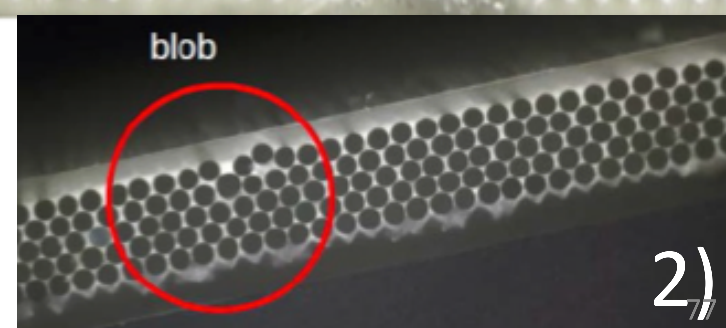

# Upgrade of PID detectors: RICH system

- Two main changes needed on RICH detectors
  - modify RICH1 optics to cope with increased occupancy
  - 40 MHz readout implies new photodetectors and new FE electronics

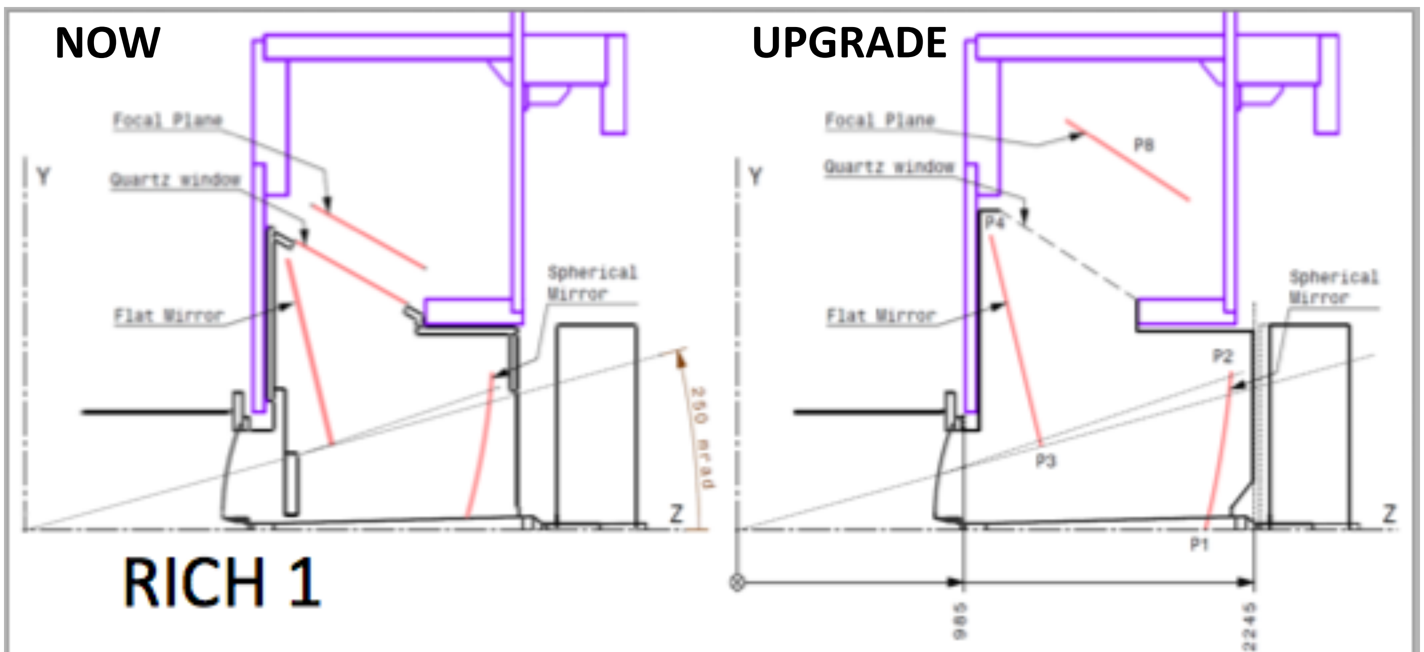

# Operator product expansion

**SM operators**

photon penguin

$$\mathcal{O}_7 = \frac{m_b}{e}\bar{s}\sigma^{\mu\nu}P_R b F_{\mu\nu}\,,$$

$$\mathcal{O}_8 = g_s\frac{m_b}{e^2}\bar{s}\sigma^{\mu\nu}P_R T^a b G^a_{\mu\nu}\,,$$

$$\mathcal{O}_9 = \bar{s}\gamma_\mu P_L b\,\bar{\ell}\gamma^\mu \ell\,,$$

$$\mathcal{O}_{10} = \bar{s}\gamma_\mu P_L b\,\bar{\ell}\gamma^\mu\gamma_5 \ell\,,$$

vector and axial-vector currents

**Beyond SM operators**

$$\mathcal{O}'_7 = \frac{m_b}{e}\bar{s}\sigma^{\mu\nu}P_L b F_{\mu\nu}\,,$$

$$\mathcal{O}'_8 = g_s\frac{m_b}{e^2}\bar{s}\sigma^{\mu\nu}P_L T^a b G^a_{\mu\nu}\,,$$

$$\mathcal{O}'_9 = \bar{s}\gamma_\mu P_R b\,\bar{\ell}\gamma^\mu \ell\,,$$

$$\mathcal{O}'_{10} = \bar{s}\gamma_\mu P_R b\,\bar{\ell}\gamma^\mu\gamma_5 \ell\,.$$

right handed currents (suppressed in SM)

# Bremsstrahlung recovery

- A recovery procedure is in place to improve the momentum reconstruction
  - Events are categorised depending on the number of recovered photon clusters
- Imperfect recovery due to
  - Energy threshold of the bremsstrahlung photon ($E_T$ > 75 MeV)
  - Calorimeter acceptance
  - Presence of energy deposits mistaken as bremsstrahlung photons

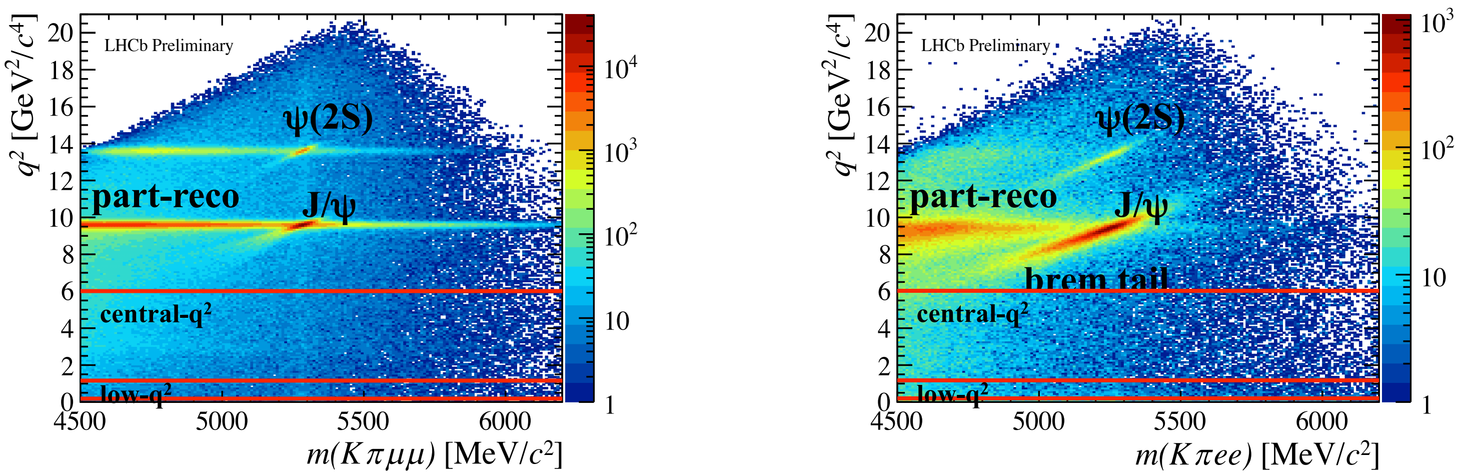


Incomplete recovery causes the reconstructed B mass to shift towards lower values and events to migrate in and out of the $q^2$ bins

# Tuning of simulation

- Particle identification
  - PID response of each particle species tuned using dedicated calibration samples
- Generator
  - Event multiplicity and $B^0$ kinematics matched to data using $B^0 \to K^{*0} J/\psi(\mu\mu)$ decay
- Trigger
  - Hardware and software trigger responses tuned using $B^0 \to K^{*0} J/\psi(ll)$ decays
- Data/MC differences
  - Residual discrepancies in variables entering the MVA reduced using $B^0 \to K^{*0} J/\psi(ll)$ decays
- After tuning, very good data/MC agreement in all key observables

# Fit procedure for muonic channel

- Simultaneous fit to resonant and non-resonant data

- Signal parameterisation
  - Hypatia function [NIM A, 764, 150 (2014)]
  - Free parameters: mass shift and width scale

- Background parameterisation
  - Combinatorial: exponential function
  - $\Lambda_b \to pK^- J/\psi(\mu\mu)$ background for $B^0 \to K^{*0} J/\psi$ modeled using simulation and data
  - $B_s \to K^{*0} J/\psi(\mu\mu)$ background for $B^0 \to K^{*0} J/\psi$ has identical signature but is shifted by $m_{Bs}$-$m_{B0}$

# Fit procedure for electron channel

- Simultaneous fit to resonant and non-resonant data split in trigger categories
  - bremsstrahlung fractions fixed from MC
- Signal
  - Crystal-Ball (Crystal-Ball and Gaussian)
  - Free parameters: mass shift and width scale
- Backgrounds
  - Combinatorial: exponential
  - $\Lambda_b \rightarrow pK^- J/\psi(ee)$ background for $B^0 \rightarrow K^{*0} J/\psi$ modelled using simulation and data, with yield constrained from muonic fit
  - $B_s \rightarrow K^{*0} J/\psi(ee)$ background for $B^0 \rightarrow K^{*0} J/\psi$ same signature as signal but shifted by $m_{Bs}$-$m_{B0}$, again constrained using muonic fit
  - Partially reconstructed decays background for $B^0 \rightarrow K^{*0} ee$ modelled using simulation and data

# Partially reconstructed backgrounds

- These are due to decays involving higher K resonances with one or more decay products in addition to a $K\pi$ pair that are not reconstructed
  - Mostly coming from $B \rightarrow K_1(1270)ee$ and $B \rightarrow K_2^*(1430)ee$

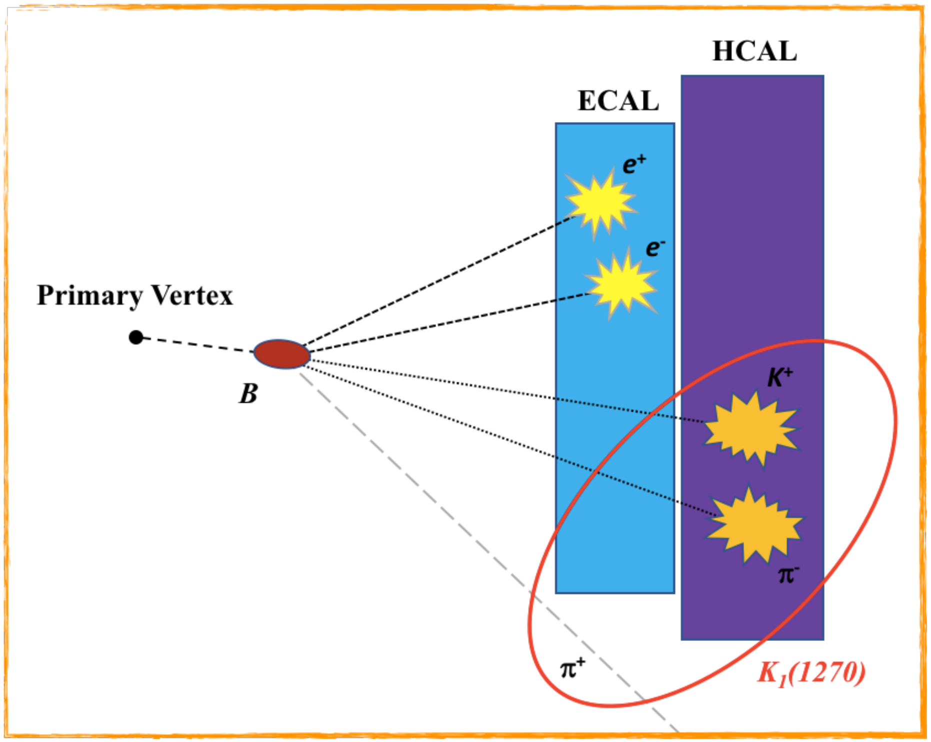

# Other cross checks

- BR($B^0 \rightarrow K^{*0} \mu\mu$) is determined and found to be in good agreement with previous LHCb publication
  - arXiv:1606.04731

- If corrections to simulations are not accounted for, the ratio of the efficiencies changes by less than 5%

- Further checks performed by measuring the following ratios

$$\mathcal{R}_{\psi(2S)} = \frac{\mathcal{B}(B^0 \rightarrow K^{*0}\psi(2S)(\rightarrow \mu^+\mu^-))}{\mathcal{B}(B^0 \rightarrow K^{*0}J/\psi(\rightarrow \mu^+\mu^-))} \Bigg/ \frac{\mathcal{B}(B^0 \rightarrow K^{*0}\psi(2S)(\rightarrow e^+e^-))}{\mathcal{B}(B^0 \rightarrow K^{*0}J/\psi(\rightarrow e^+e^-))}$$

$$r_\gamma = \frac{\mathcal{B}(B^0 \rightarrow K^{*0}\gamma(\rightarrow e^+e^-))}{\mathcal{B}(B^0 \rightarrow K^{*0}J/\psi(\rightarrow e^+e^-))}$$

which are found to be compatible with the expectations

# Cross check on bremsstrahlung recovery

- Relative population of bremsstrahlung categories compared between data and simulation using $B^0 \to K^{*0} J/\psi(ee)$ and $B^0 \to K^{*0}\gamma(ee)$ events

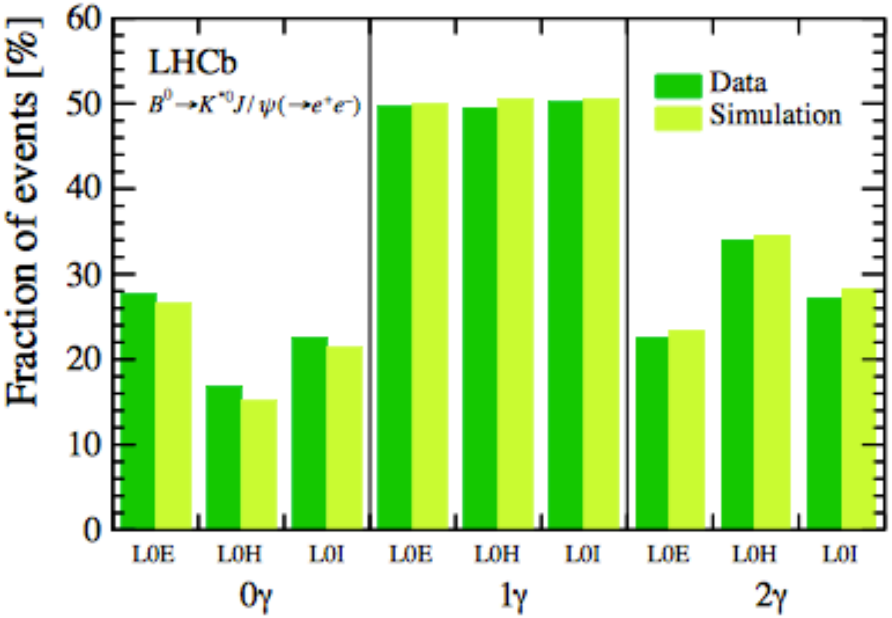


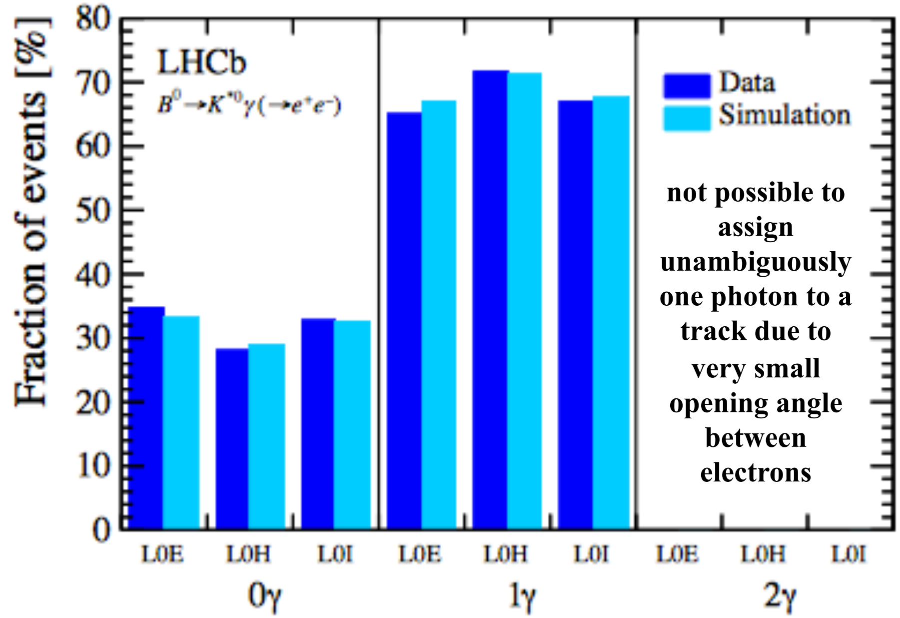


- Excellent agreement is observed

# Systematic uncertainties

- As $R_{K*}$ is determined as a double ratio, many experimental systematic effects cancel
- The measurement is statistically dominated (~15%)

| | low-$q^2$ | | | central-$q^2$ | | |
|---|---|---|---|---|---|---|
| **Trigger category** | L0E | L0H | L0I | L0E | L0H | L0I |
| **Corrections to simulation** | 2.5 | 4.8 | 3.9 | 2.2 | 4.2 | 3.4 |
| **Trigger** | 0.1 | 1.2 | 0.1 | 0.2 | 0.8 | 0.2 |
| **PID** | 0.2 | 0.4 | 0.3 | 0.2 | 1.0 | 0.5 |
| **Kinematic selection** | 2.1 | 2.1 | 2.1 | 2.1 | 2.1 | 2.1 |
| **Residual background** | – | – | – | 5.0 | 5.0 | 5.0 |
| **Mass fits** | 1.4 | 2.1 | 2.5 | 2.0 | 0.9 | 1.0 |
| **Bin migration** | 1.0 | 1.0 | 1.0 | 1.6 | 1.6 | 1.6 |
| $r_{J/\psi}$ **flatness** | 1.6 | 1.4 | 1.7 | 0.7 | 2.1 | 0.7 |
| **Total** | 4.0 | 6.1 | 5.5 | 6.4 | 7.5 | 6.7 |

- Total systematic uncertainty of 4-6% and 6-8% in the low- and central-$q^2$

# Systematic uncertainties

- Corrections to simulation: besides the uncertainty due to the size of the samples, an additional systematic is determined using different parameterisations of the corrections
- Kinematic selection: a systematic uncertainty for Data/MC differences in the description of the bremsstrahlung tail and the MVA classifier is determined by comparing simulation and background subtracted $B^0 \to K^{*0} J/\psi(ll)$ data
- Residual background: both data and simulation are used to assess a systematic uncertainty for residual background contamination due to $B^0 \to K^{*0} J/\psi(ee)$ events with a $K \leftrightarrow e$ or $\pi \leftrightarrow e$ swap

| | low-$q^2$ | | | central-$q^2$ | | |
|---|---|---|---|---|---|---|
| Trigger category | L0E | L0H | L0I | L0E | L0H | L0I |
| Corrections to simulation | 2.5 | 4.8 | 3.9 | 2.2 | 4.2 | 3.4 |
| Trigger | 0.1 | 1.2 | 0.1 | 0.2 | 0.8 | 0.2 |
| PID | 0.2 | 0.4 | 0.3 | 0.2 | 1.0 | 0.5 |
| Kinematic selection | 2.1 | 2.1 | 2.1 | 2.1 | 2.1 | 2.1 |
| Residual background | – | – | – | 5.0 | 5.0 | 5.0 |
| Mass fits | 1.4 | 2.1 | 2.5 | 2.0 | 0.9 | 1.0 |
| Bin migration | 1.0 | 1.0 | 1.0 | 1.6 | 1.6 | 1.6 |
| $r_{J/\psi}$ flatness | 1.6 | 1.4 | 1.7 | 0.7 | 2.1 | 0.7 |
| Total | 4.0 | 6.1 | 5.5 | 6.4 | 7.5 | 6.7 |

# Systematic uncertainties

- Mass fit: a systematic uncertainty is determined by running pseudo-experiments with different descriptions of the signal and background fit models
- Bin migration: the effect of the model dependence and description of the $q^2$ resolution in simulation are assigned as a systematic uncertainty
- $r_{J/\psi}$ flatness: the ratio is studied as a function of several properties of the event and decay products, and the observed residual deviations from unity are used to assign a systematic uncertainty

| | low-$q^2$ | | | central-$q^2$ | | |
|---|---|---|---|---|---|---|
| Trigger category | L0E | L0H | L0I | L0E | L0H | L0I |
| Corrections to simulation | 2.5 | 4.8 | 3.9 | 2.2 | 4.2 | 3.4 |
| Trigger | 0.1 | 1.2 | 0.1 | 0.2 | 0.8 | 0.2 |
| PID | 0.2 | 0.4 | 0.3 | 0.2 | 1.0 | 0.5 |
| Kinematic selection | 2.1 | 2.1 | 2.1 | 2.1 | 2.1 | 2.1 |
| Residual background | – | – | – | 5.0 | 5.0 | 5.0 |
| Mass fits | 1.4 | 2.1 | 2.5 | 2.0 | 0.9 | 1.0 |
| Bin migration | 1.0 | 1.0 | 1.0 | 1.6 | 1.6 | 1.6 |
| $r_{J/\psi}$ flatness | 1.6 | 1.4 | 1.7 | 0.7 | 2.1 | 0.7 |
| Total | 4.0 | 6.1 | 5.5 | 6.4 | 7.5 | 6.7 |

# Efficiency ratios between the nonresonant and resonant modes

| | $\varepsilon_{\ell^+\ell^-}/\varepsilon_{J/\psi(\ell^+\ell^-)}$ | |
|---|---|---|
| | **low-$q^2$** | **central-$q^2$** |
| $\mu^+\mu^-$ | $0.679 \pm 0.009$ | $0.584 \pm 0.006$ |
| $e^+e^-$ (L0E) | $0.539 \pm 0.013$ | $0.522 \pm 0.010$ |
| $e^+e^-$ (L0H) | $2.252 \pm 0.098$ | $1.627 \pm 0.066$ |
| $e^+e^-$ (L0I) | $0.789 \pm 0.029$ | $0.595 \pm 0.020$ |

# Measurement of sin(2β)

- *CP* violation due to interference between $B^0$-$\bar{B}^0$ mixing and $B^0 \rightarrow J/\psi K_S$ decay

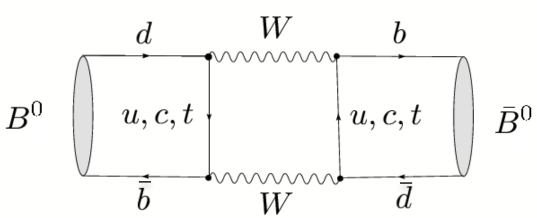


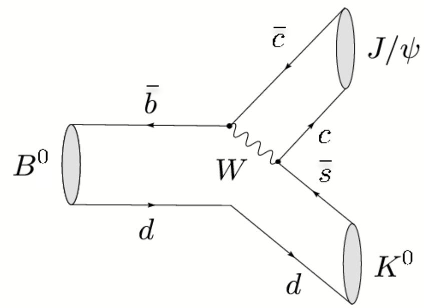


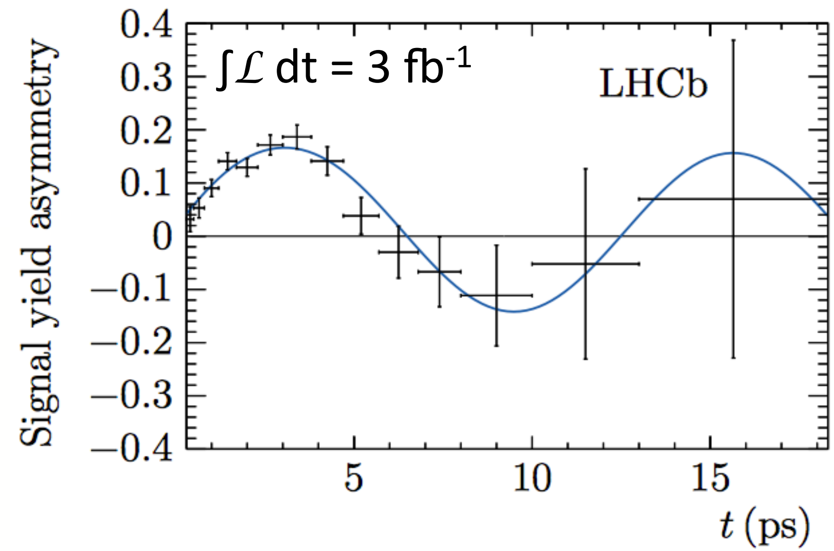


$$\mathcal{A}_{J/\psi K^0_S}(t) \equiv \frac{\Gamma(\overline{B}^0(t) \to J/\psi K^0_S) - \Gamma(B^0(t) \to J/\psi K^0_S)}{\Gamma(\overline{B}^0(t) \to J/\psi K^0_S) + \Gamma(B^0(t) \to J/\psi K^0_S)}$$

$$= S_{J/\psi K^0_S} \sin(\Delta m_d t) - C_{J/\psi K^0_S} \cos(\Delta m_d t).$$

$$C = -0.038 \pm 0.032 \pm 0.005$$

$$S = 0.731 \pm 0.035 \pm 0.020$$

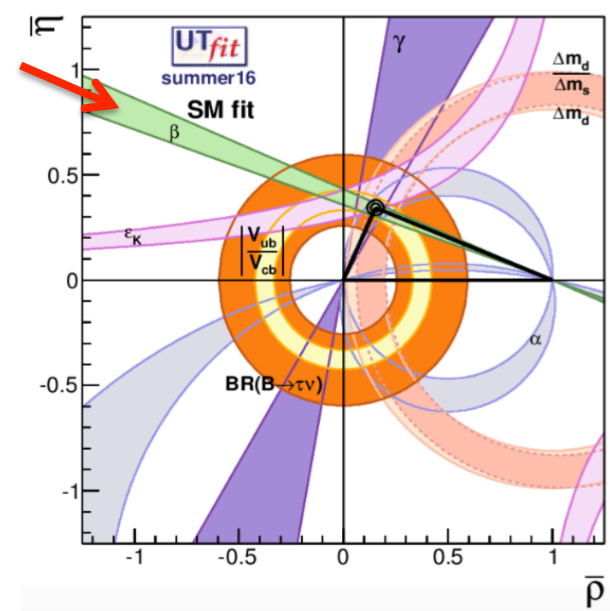


Phys. Rev. Lett. 115 031601 (2015)

# Measurement of $|V_{ub}|/|V_{cb}|$

- Measure $\mathfrak{B}(\Lambda_b \to p\mu\nu)$ relative to $\mathfrak{B}(\Lambda_b \to \Lambda_c\mu\nu)$

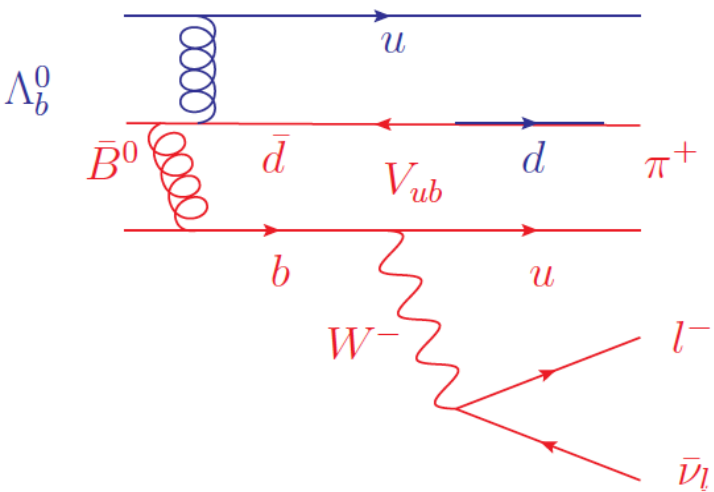


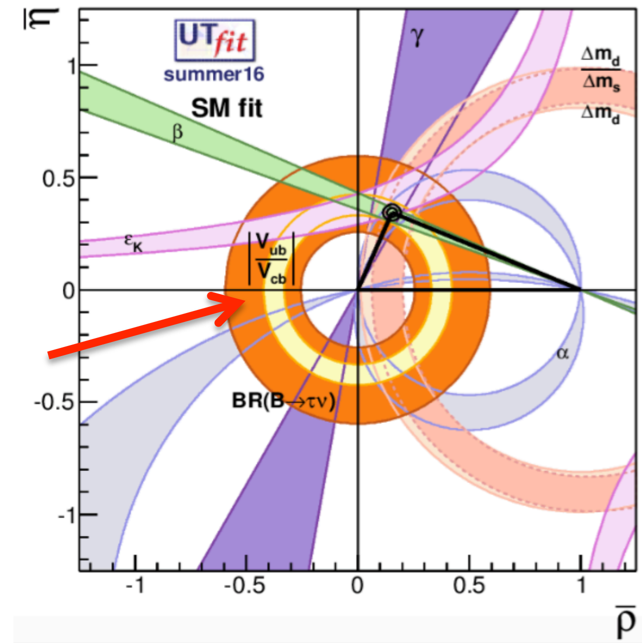


$$\frac{\mathcal{B}(\Lambda_b \to p\mu^-\overline{\nu}_\mu)_{q^2>15\,\mathrm{GeV}^2/c^4}}{\mathcal{B}(\Lambda_b \to \Lambda_c\mu\nu)_{q^2>7\,\mathrm{GeV}^2/c^4}} = \frac{N(\Lambda_b \to p\mu^-\overline{\nu}_\mu)}{N(\Lambda_b \to (\Lambda_c \to pK\pi)\mu^-\overline{\nu}_\mu)} \times \frac{\epsilon(\Lambda_b \to (\Lambda_c \to pK\pi)\mu^-\overline{\nu}_\mu)}{\epsilon(\Lambda_b \to p\mu^-\overline{\nu}_\mu)} \times \mathcal{B}(\Lambda_c \to pK\pi)$$

# Measurement of $|V_{ub}|/|V_{cb}|$

- Fit the corrected mas

$$M_{corr} = \sqrt{p_{\perp}^2 + M_{p\mu}^2} + p_{\perp}$$

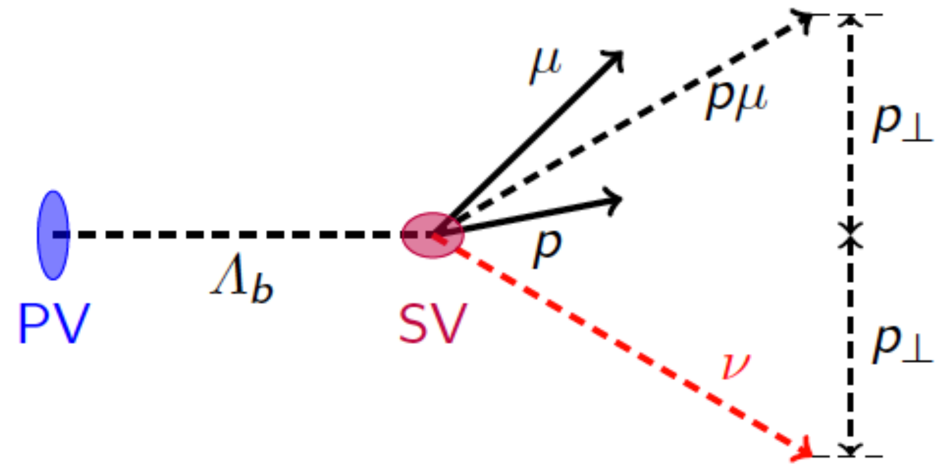


$$R_{exp} = \frac{\mathcal{B}(\Lambda_b^0 \to p\mu^-\overline{\nu}_\mu)_{q^2>15\,\mathrm{GeV}/c^2}}{\mathcal{B}(\Lambda_b^0 \to \Lambda_c^+\mu^-\overline{\nu}_\mu)_{q^2>7\,\mathrm{GeV}/c^2}} = (1.00 \pm 0.04 \pm 0.08) \times 10^{-2}$$

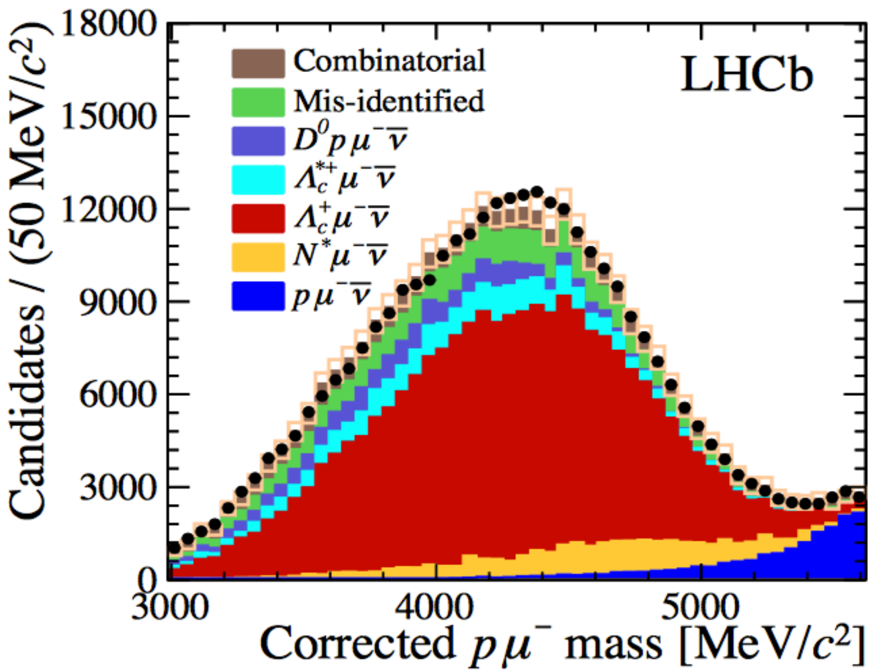


Nature Physics 10 (2015) 1038

$$R_{exp} = R_{theory}(|\mathrm{V_{ub}}|^2/|\mathrm{V_{cb}}|^2)$$

$$R_{theory} = 1.470 \pm 0.115(stat) \pm 0.104(syst)$$

$$\frac{|V_{ub}|}{|V_{cb}|} = 0.083 \pm 0.004 \pm 0.004$$

Signal $\Lambda_b \to p\mu\nu$ decays

$$N(\Lambda_b \to p\mu^-\overline{\nu}_\mu) = 17687 \pm 733$$

# Pentaquark in $\Lambda_b \rightarrow J/\psi pK$ decays

Amplitude analysis in 6 dimensions (decay angles and $m_{Kp}$)
2 $P_c$ states needed to describe the data

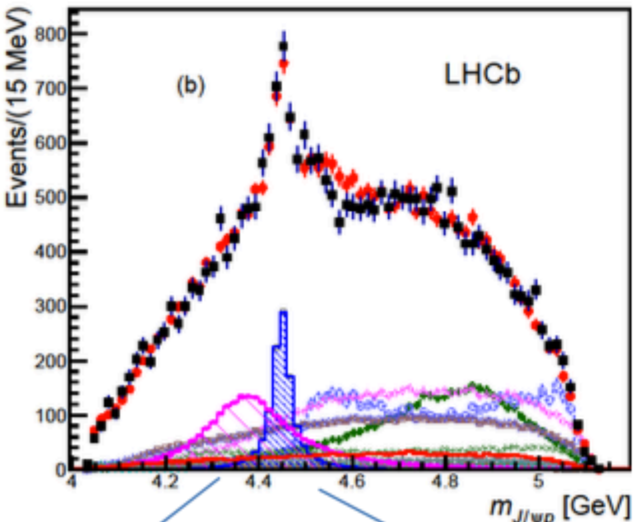


| $P_c(4380)$ | $P_c(4450)$ |
|---|---|
| 9 σ | 12 σ |
| $J^P = 3/2^-$ | $J^P = 5/2^+$ |

$J^P$ also compatible with $(3/2^+, 5/2^-)$ and $(5/2^+, 3/2^-)$

Minimal quark content: $c\bar{c}uud$

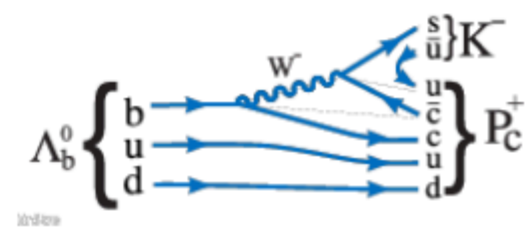


Argand diagrams:

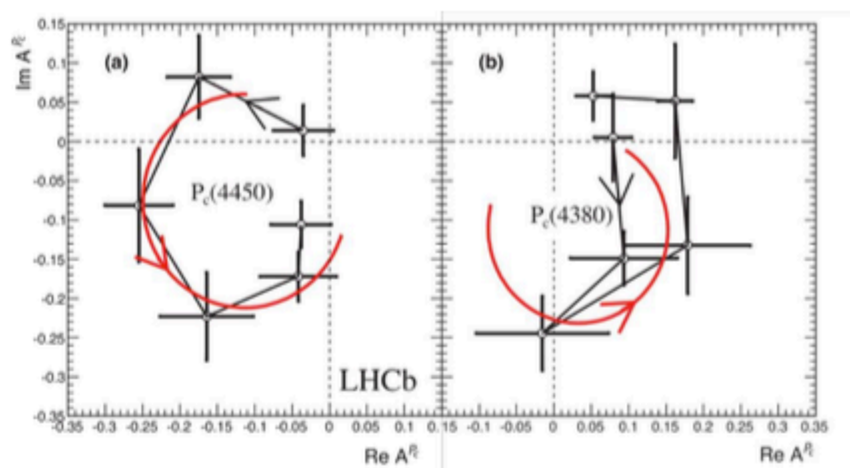


PRL 115 (2015) 072001

# Pentaquark in $\Lambda_b \to J/\psi p\pi$ decays

Search for these states in $\Lambda_b \to J/\psi p\pi$ decays in order to test hypothesis of threshold effects

Angular analysis indicates the need for exotic states at 3.3σ, but can't tell which (the two $P_c$ or $Z_c(4200)$).

Run 2 will help!

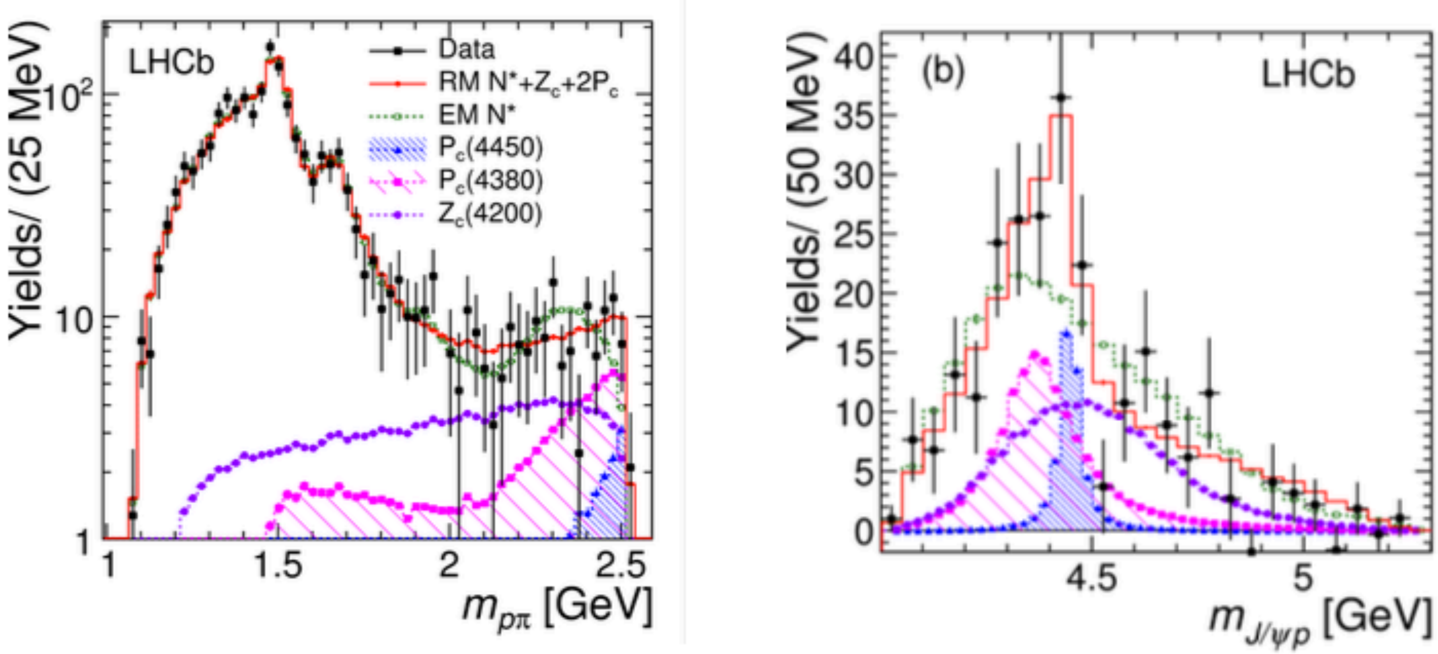


*PRL 117 (2016) 082003*

Other decays are also under study : $\Lambda_b \to \chi_{c(1,2)} pK$ *(arXiv:1704.07900)*, $\Xi_b \to J/\psi \Lambda K$ *(PLB 772 265)*, $B_{(s)} \to J/\psi pp$ *(JHEP 09(2013)006)* ,..

# Excited $\Omega_c$ states (?)

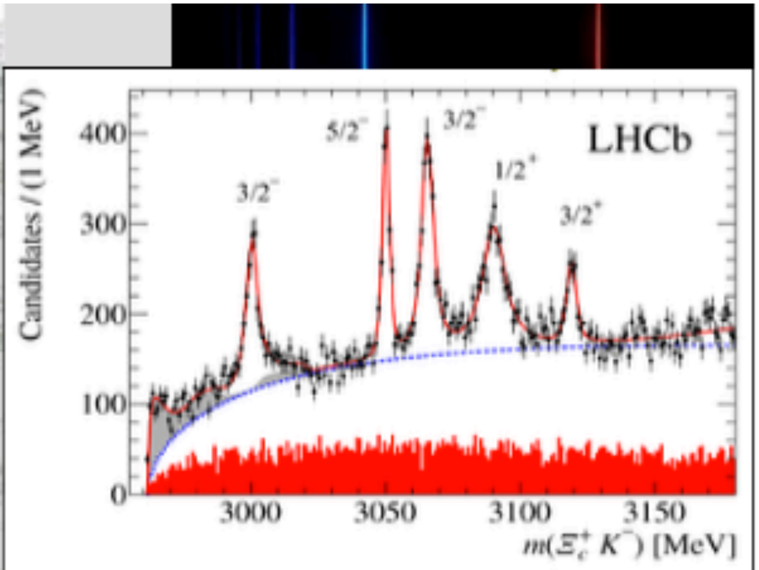


Table 8: Comparison of theoretical predictions for the masses of the $\Omega_c$ states.

| State $nL, J^P$ | our RQM | Roberts QM | Shah QM | Perez-Rubio lattice | Chen lattice | Agaev QCD SR | Experiment. PDG+LHCb |
|---|---|---|---|---|---|---|---|
| $1S, 1/2^+$ | 2698 | 2718 | 2695 | 2648(28) | 2695(28) | 2685(123) | 2695.2(1.7) |
| $2S, 1/2^+$ | 3088 | 3152 | 3100 | 3294(73) | | 3066(138) | $3090.2(^{7}_{8})$ |
| $1S, 3/2^+$ | 2768 | 2776 | 2767 | 2709(32) | 2781(25) | 2769(89) | 2765.9(2.0) |
| $2S, 3/2^+$ | 3123 | 3190 | 3126 | 3355(92) | | 3119(114) | $3119.1(^{1.0}_{1.1})$ |
| $1P, 1/2^-$ | 2966 | 2977 | 3028 | 2995(46) | 3015(45) | | |
| $1P, 1/2^-$ | 3055 | 2990 | 3011 | | | | |
| $1P, 3/2^-$ | 3054 | 2986 | 2976 | 3016(69) | | | $3065.6(^{6}_{7})$ |
| $1P, 3/2^-$ | 3029 | 2994 | 2993 | | | | $3000.4(^{4}_{6})$ |
| $1P, 5/2^-$ | 3051 | 3014 | 2947 | | | | $3050.2(^{4}_{5})$ |

- No theory consensus on quantum numbers:
  - Either all five P-wave states
    - Why two ½⁺ are narrow?
  - Or three P-wave state and two 2S states
    - Where are two ½⁺ states? One could go below threshold but other one must be here!

**Real puzzle: why all 5 states are so narrow?**

# Summary of Phase-II upgrade prospects

| Topics and observables | Experimental reach | Remarks |
|---|---|---|
| **EW Penguins** | | |
| Global tests in many $b \to s\mu^+\mu^-$ modes with full set of precision observables; lepton universality tests; $b \to dl^+l^-$ studies | *e.g.* 440k $B^0 \to K^*\mu^+\mu^-$ & 70k $\Lambda_b^0 \to \Lambda\mu^+\mu^-$; Phase-II $b \to d\mu^+\mu^-$ $\approx$ Run-1 $b \to s\mu^+\mu^-$ sensitivity. | Phase-II ECAL required for lepton universality tests. |
| **Photon polarisation** | | |
| $\mathcal{A}^\Delta$ in $B_s^0 \to \phi\gamma$; $B^0 \to K^* e^+e^-$; baryonic modes | Uncertainty on $\mathcal{A}^\Delta \approx 0.02$; $\sim 10k$ $\Lambda_b^0 \to \Lambda\gamma$, $\Xi_b \to \Xi\gamma$, $\Omega_b^- \to \Omega\gamma$ | Strongly dependent on performance of ECAL. |
| **$b \to cl^-\bar{\nu}_l$ lepton-universality tests** | | |
| Polarisation studies with $B \to D^{(*)}\tau^-\bar{\nu}_\tau$; $\tau^-/\mu^-$ ratios with $B_s^0$, $\Lambda_b^0$ and $B_c^+$ modes | *e.g.* 8M $B \to D^*\tau^-\bar{\nu}_\tau$, $\tau^- \to \mu^-\bar{\nu}_\mu\nu_\tau$ & $\sim 100k$ $\tau^- \to \pi^-\pi^+\pi^-(\pi^0)\nu_\tau$ | Additional sensitivity expected from low-$p$ tracking. |
| **$B_s^0, B^0 \to \mu^+\mu^-$** | | |
| $R \equiv \mathcal{B}(B^0 \to \mu^+\mu^-)/\mathcal{B}(B_s^0 \to \mu^+\mu^-)$; $\tau_{B_s^0 \to \mu^+\mu^-}$; $CP$ asymmetry | Uncertainty on $R \approx 20\%$ Uncertainty on $\tau_{B_s^0 \to \mu^+\mu^-} \approx 0.03\,\text{ps}$ | |
| **LFV $\tau$ decays** | | |
| $\tau^- \to \mu^+\mu^-\mu^-$, $\tau^- \to h^+\mu^-\mu^-$, $\tau^- \to \phi\mu^-$ | Sensitive to $\tau^- \to \mu^+\mu^-\mu^-$ at $10^{-9}$ | Phase-II ECAL valuable for background suppression. |
| **CKM tests** | | |
| $\gamma$ with $B^- \to DK^-$, $B_s^0 \to D_s^+K^-$ *etc.* | Uncertainty on $\gamma \approx 0.4°$ | Additional sensitivity expected |
| $\phi_s$ with $B_s^0 \to J/\psi K^+K^-$, $J/\psi\pi^+\pi^-$ | Uncertainty on $\phi_s \approx 3\,\text{mrad}$ | in $CP$ observables from Phase-II |
| $\phi_s^{s\bar{s}s}$ with $B_s^0 \to \phi\phi$ | Uncertainty on $\phi_s^{s\bar{s}s} \approx 8\,\text{mrad}$ | ECAL and low-$p$ tracking. |
| $\Delta\Gamma_d/\Gamma_d$ | Uncertainty on $\Delta\Gamma_d/\Gamma_d \sim 10^{-3}$ | Approach SM value. |
| Semileptonic asymmetries $a_{\text{sl}}^{d,s}$ | Uncertainties on $a_{\text{sl}}^{d,s} \sim 10^{-4}$ | Approach SM value for $a_{\text{sl}}^d$. |
| $\|V_{ub}\|/\|V_{cb}\|$ with $\Lambda_b^0$, $B_s^0$ and $B_c^+$ modes | *e.g.* 120k $B_c^+ \to D^0\mu^-\bar{\nu}_\mu$ | Significant gains achievable from thinning or removing RF-foil. |
| **Charm** | | |
| $CP$-violation studies with $D^0 \to h^+h^-$, $D^0 \to K_S^0\pi^+\pi^-$ and $D^0 \to K^\mp\pi^\pm\pi^+\pi^-$ | *e.g.* $4 \times 10^9$ $D^0 \to K^+K^-$; Uncertainty on $A_\Gamma \sim 10^{-5}$ | Access $CP$ violation at SM values. |
| **Strange** | | |
| Rare decay searches | Sensitive to $K_S^0 \to \mu^+\mu^-$ at $10^{-12}$ | Additional sensitivity possible with downstream trigger enhancements. |

# Key goals

- The Phase-II Upgrade will be capable of improving on a broad spectrum of important flavour-physics measurements
  - A comprehensive programme of measurements of $b \rightarrow sl^+l^-$ and $b \rightarrow dl^+l^-$ transitions, employing both muon and electron modes
  - Measurement of $\gamma$ with a precision of $0.4^o$
  - Measurement of $\phi_s$ with a precision of 3 mrad
  - Measurement of the ratio $B(B^0 \rightarrow \mu\mu)/B(B_s \rightarrow \mu\mu)$ with an uncertainty of about 10%, and the first precise measurements of relevant $B_s \rightarrow \mu\mu$ observables such as effective lifetime and *CP* violation
  - A wide-ranging set of lepton-universality tests in $b \rightarrow cl\nu$ decays, exploiting the full range of b-hadrons
  - *CP*-violation measurements in charm with $10^{-5}$ precision
- In addition, the Phase-II Upgrade will be capable of major discoveries in hadron spectroscopy, and pursuing a wide and unique programme of general physics measurements, complementary to those of ATLAS and CMS

# Challenges ahead

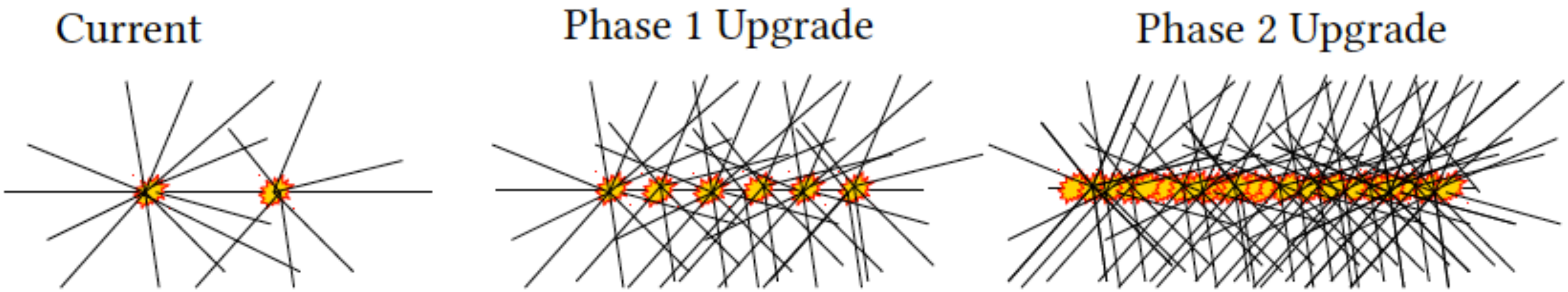


- The project is very challenging
  - otherwise we would have done it already...
- The mean number of interactions per event will be around 50
  - The increased particle multiplicity and rates will present significant problems for all detectors, notaby including increased radiation damage
- An essential attribute will be precise timing in the VELO detector, and also downstream of the magnet for both charged tracks and neutrals
  - A time resolution of a few tens of ps for charged tracks and photons will dramatically simplify pattern recognition and improve association of particles to the correct interaction vertex where they were produced
  - Furthermore, a high granularity tungsten sampling electromagnetic calorimeter will extend the experiment's capabilities in final states involving photons, $\pi^0$s and electrons

# Timing information

- In high pileup conditions, vertex reconstruction and assignment to a given decay becomes a limiting factor
  - Particles produced at same position can have very different production times
- Consider two beam bunches crossing at the interaction point

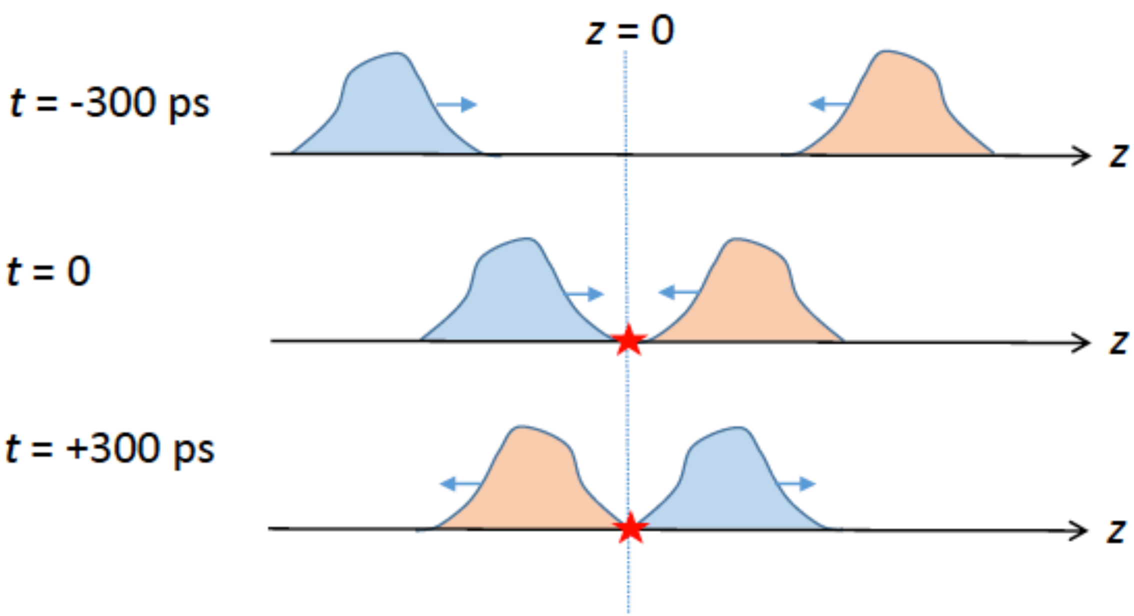


- In this cartoon, interactions at same *z* but separated by 300 ps
- If we would have precise enough time information for charged particles and neutral, the complexity of high-pileup events could be reduced to the present situation

# Challenges ahead

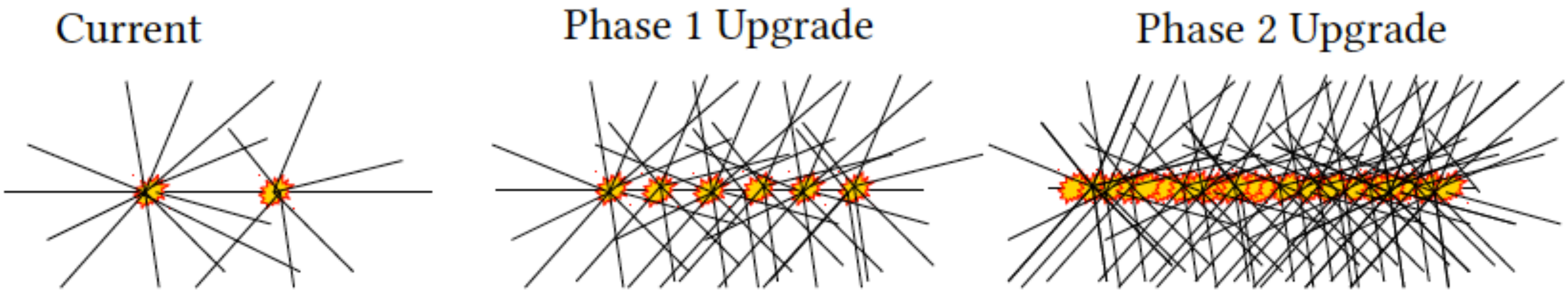


- By instrumenting the side walls of the dipole magnet, the tracking acceptance can be significantly increased for soft tracks, improving detector efficiency for high multiplicity decays

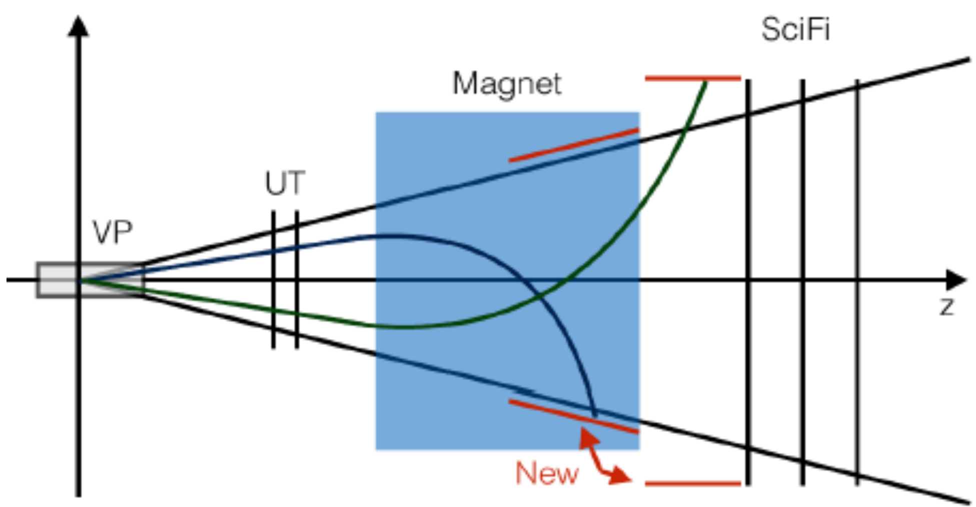

# Challenges ahead

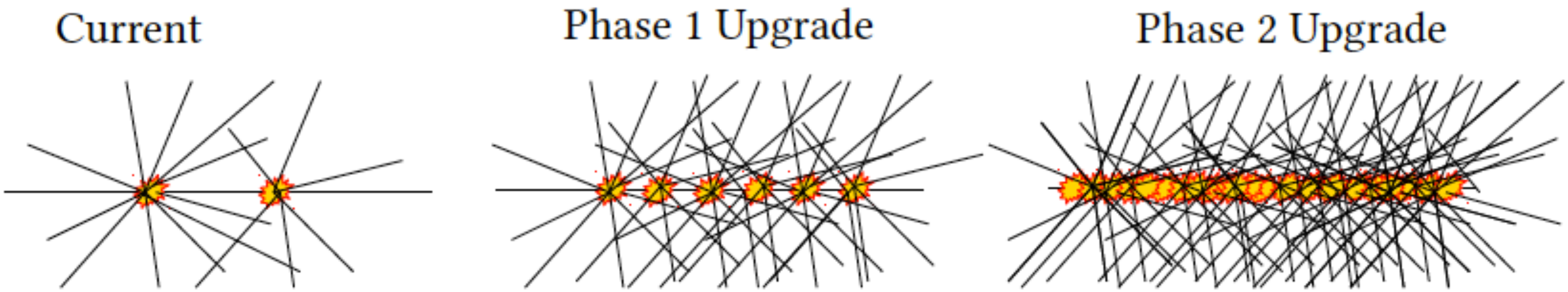


- Downstream fast-timing capabilities will allow improved rejection of combinatoric background and can also be used for improving particle identication at low momentum, along with improvements in the RICH system
- Initial steps of a limited number of these detector upgrade projects could already be installed for Run 4, allowing the Phase-I experiment to improve its physics reach even before the Phase-II upgrade takes place

# Matching the LHCb layout

1. Improve granularity and radiation hardness of detectors to cope with much higher number of interactions.

2. Add timing information to detectors to associate signals to a collision.

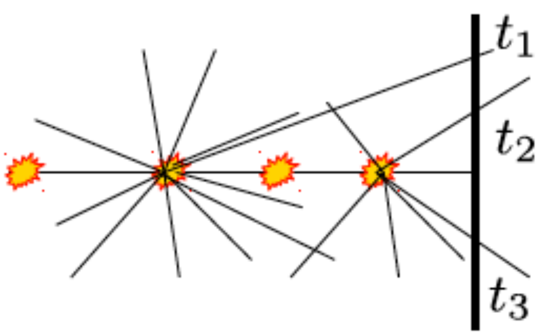


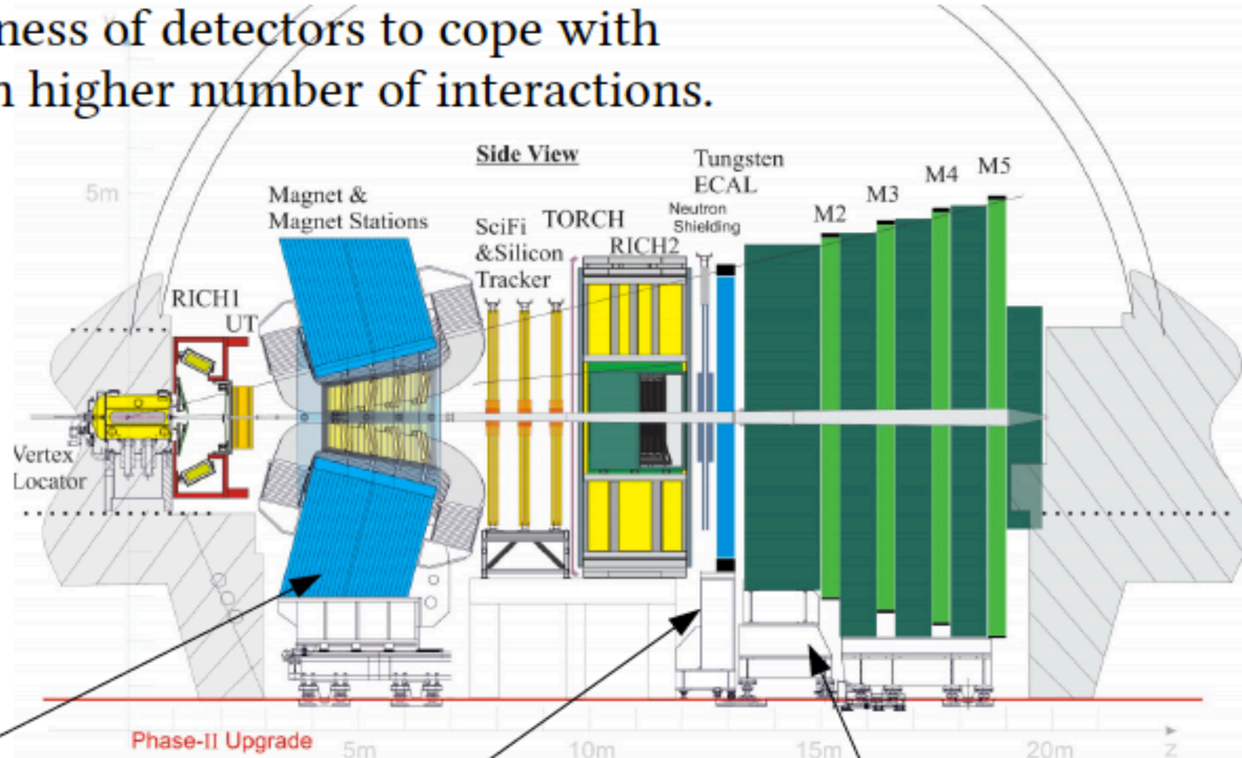


3. Improve low momentum tracking.

4. Highly improved electromagnetic calorimeter.

5. Better shielding for muons.